DOCKET NO. 72-1004
TAC NO. L23343

TN INC. RESPONSES TO NRC REQUEST FOR ADDITIONAL INFORMATION DATED JULY 3, 2002

Chapter 4 Thermal

Question 4-1

The staff has determined that there are potential errors in ANSYS® thermal models of the NUHOMS®-32PT Dry Shielded Canister (DSC). These potential errors primarily concern the calculation of effective conductivities of the materials in the basket. Attachment 1 provides a complete explanation of the potential errors discovered by the staff. The additional information requested below is needed by the staff to make a finding on the thermal performance of the NUHOMS®-32PT DSC.

1. *Revise the thermal model of the NUHOMS®-32PT DSC to take into account the orthortropic nature of the basket materials, including the helium, aluminum, and neutron poison materials. The thermal conductivity of the basket materials will not be the same across the aluminum and neutron poison plates (serial path) as it would be along the aluminum and neutron poison plates (parallel path).*

2. *If, after the revision to the thermal model as described above is complete, fuel cladding temperatures are above the applicable limits, provide an alternative path for certification of the NUHOMS®-32PT DSC.*

This information is needed to satisfy the provisions of 10 CFR 72.11 and 10 CFR 72.236(a) and (f).

Response – Question 4-1

The thermal model of the NUHOMS®-32PT DSC that was submitted to the staff for review (Reference 1), was based on the following assumptions:

Generally, good surface contact is expected between adjacent components within the basket structure. However to bound the heat conductance uncertainty between adjacent components, thermal gaps between the adjacent components had been included in the thermal model. To simplify the basket model, the XM-19 grid structure of the basket and its adjacent gaps ware modeled as a homogenous material. Similarly, the aluminum plates, poison plates, and the helium filled gaps between them were modeled as another homogenous material. The metal plates and the gaps were considered as parallel thermal resistances in each homogenized region. Effective conductivity values were calculated for each region based on the parallel thermal resistance theory. These effective conductivity values were used for both the series and parallel paths of the homogenized material. This assumption is reasonable, since the temperature gradients along the

basket plates (parallel) are much higher than the temperature gradients across (series) the plates.

The above methodology used in Reference 1 simplifies the basket model significantly. The results of this model are shown as **"Base Case"** in Table 1, which is the same as the 70°F ambient temperature storage case in the Amendment Application (Reference 1).

To demonstrate the accuracy of the above methodology, a detailed model of the NUHOMS®-32PT basket was developed in this analysis using ANSYS computer code. Each component of the basket (XM19, helium gaps, poison plate, and aluminum plate) was modeled discretely with SOLID70 elements. The gaps between adjacent components are also represented with SOLID70 elements with helium conductivity. The gap size between the XM-19 grid and the other basket components is 0.0075". The gap size between aluminum and poison plates is 0.00375". The gap size between the aluminum rail and the DSC shell is 0.08". These sizes of the gaps are the same as those used to calculate the effective conductivity values in Reference 1. Geometry of the detailed model is shown in Figures 1 to 5.

The normal, steady state case, 70°F ambient temperature storage case of Reference 1 (Base Case described above) shows the smallest margin to the fuel cladding temperature limit. The boundary conditions and the thermal material properties of that case are applied without any changes to the detailed model in this analysis. Since the components are modeled separately, it is not required to use any effective conductivity values in this detailed model.

Radiation heat transfer in the helium gaps between the components is not considered in the detailed model, which adds conservatism to the detailed model. The results of the detailed model are shown as **"Case 1"** in Table 1.

Table 1

Comparison of NUHOMS®-32PT DSC Basket and Fuel Cladding Temperatures for 70°F Ambient Storage Conditions

Case	Description	T_fuel-inner, max (°F)	T_fuel-outer, max (°F)	T_Aluminum plate, max (°F)	T_grid XM19, max / min (°F)	T_rail, max / min (°F)
Base Case	Simplified model (ref. 1). Homogenized basket components and gaps with isotropic properties.	613	525	597	597 / 290	369 / 287
Case 1	Detailed model. Basket components and gaps modeled as individual plates. No homogenized basket component materials.	611	518	596	596 / 291	367 / 287

The results from Table 1 show that the maximum component temperatures are changed by at most 2°F when the detailed model is used instead of the simplified model. It demonstrates that using the effective conductivity values for parallel basket plates in the simplified model has negligible impact on the results and therefore is a reasonable assumption.

To expedite the staff's review, Transnuclear decided to revise the thermal model of the NUHOMS®-32PT basket described in Reference 1 with the detailed model (Case 1) described above and redo the thermal analysis.

In subsequent discussions, the NRC staff asked Transnuclear to respond to two additional questions on this model. The two questions are:

1. *Perform nodalization study from a 6x6 to a 14x14 mesh grid with the NUHOMS®-32PT fuel homogenized model to demonstrate convergence.*

2. *Demonstrate that the 15x15 assembly is not the limiting fuel assembly.*

In response to Question 1 above, Transnuclear performed a nodalization study for the homogenized fuel region where the mesh grid was changed from 6x6 to 12x12, 14x14 and 16x16. The results show that convergence is achieved with a 14x14 mesh size and the model is mesh independent at the 14x14 mesh grid. Therefore, the thermal analysis was revised for all the normal, off-normal and accident cases using a 14x14 mesh grid for the homogenized fuel region. The results of this study are provided in the revised SAR Section M.4.4.1.2 included with this submittal.

In response to Question 2 above, to determine the limiting fuel assembly for fuel effective thermal conductivity calculation, Transnuclear recalculated fuel effective thermal conductivities for all the fuel assembly types included in this application. The analysis determined that Westinghouse (WE) 14x14 fuel assembly type resulted in the lowest (limiting) effective thermal conductivity for both the helium filled and vacuum cases. The methodology and the results of this analysis are provided in the revised SAR Section M.4.8. The thermal analysis included in the revised Chapter M.4 now use the limiting fuel effective thermal conductivity based on WE 14x14 fuel type.

Reference:

1. Revision 3 of Application for Amendment No. 5 to the NUHOMS® Certificate of Compliance No. 1004 (TAC NO. L23343) dated June 3, 2002.

Figure 1 – Detailed Model of NUHOMS®-32PT

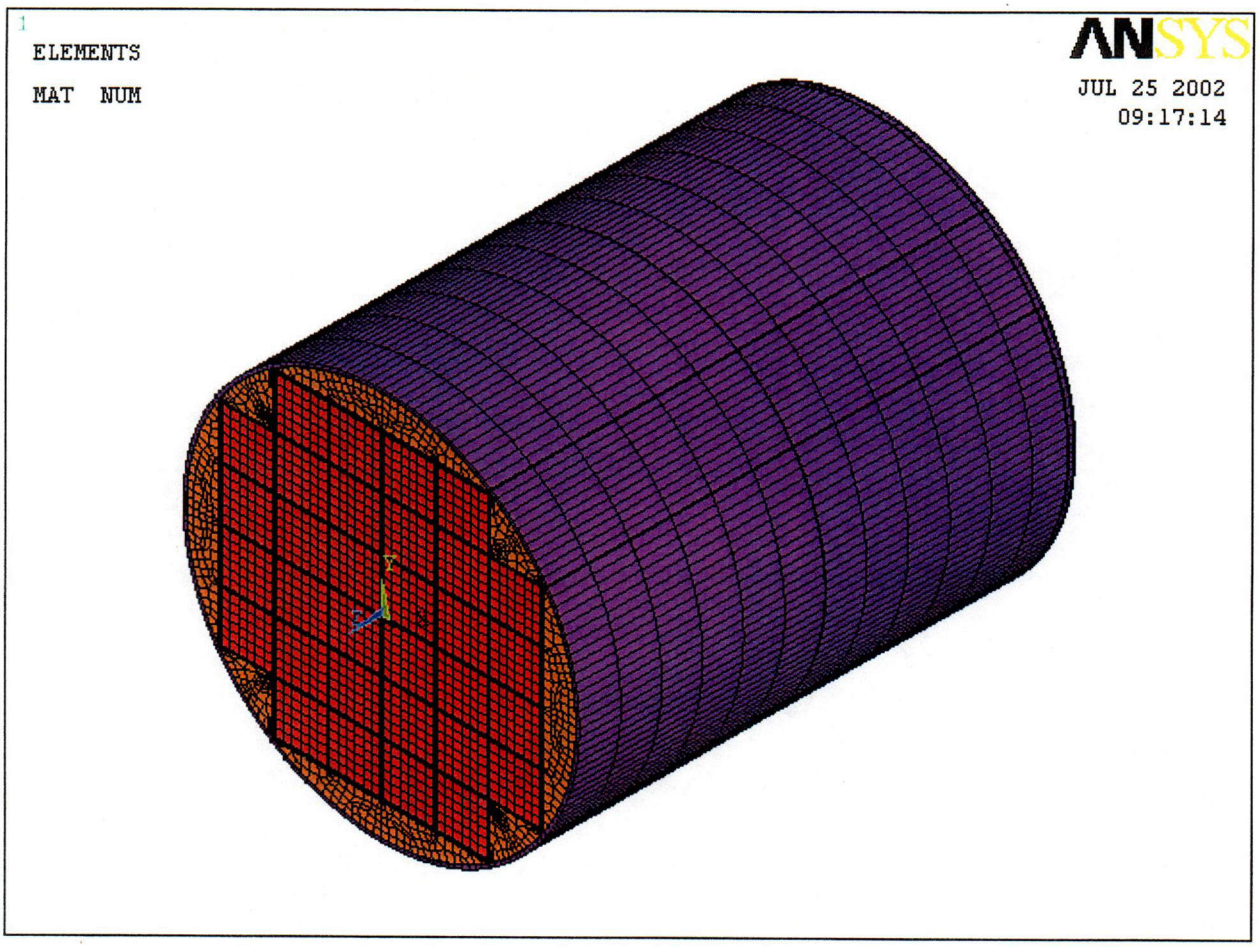

C01

Figure 2 – Detailed Model of NUHOMS®-32PT – Cross Section

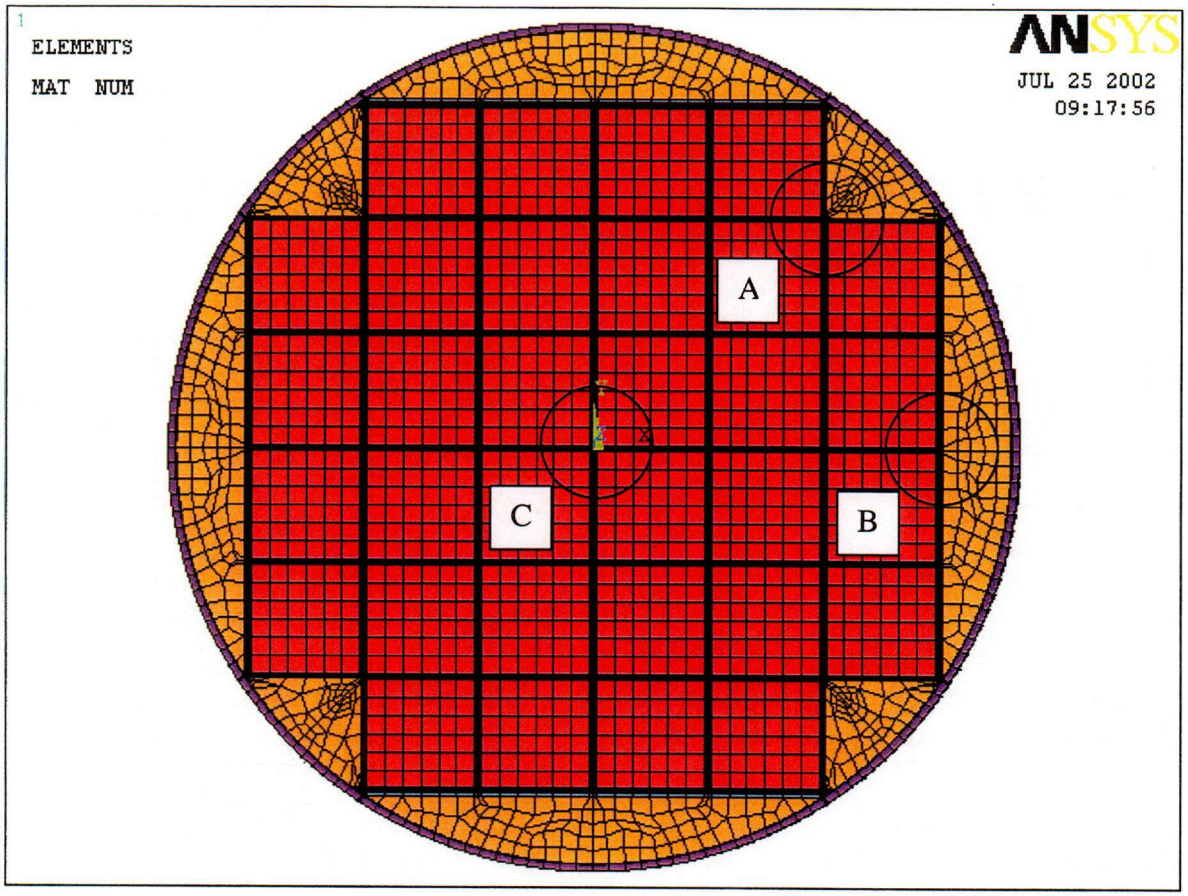

C02

Figure 3 - Detailed Model of NUHOMS®-32PT – Detail A

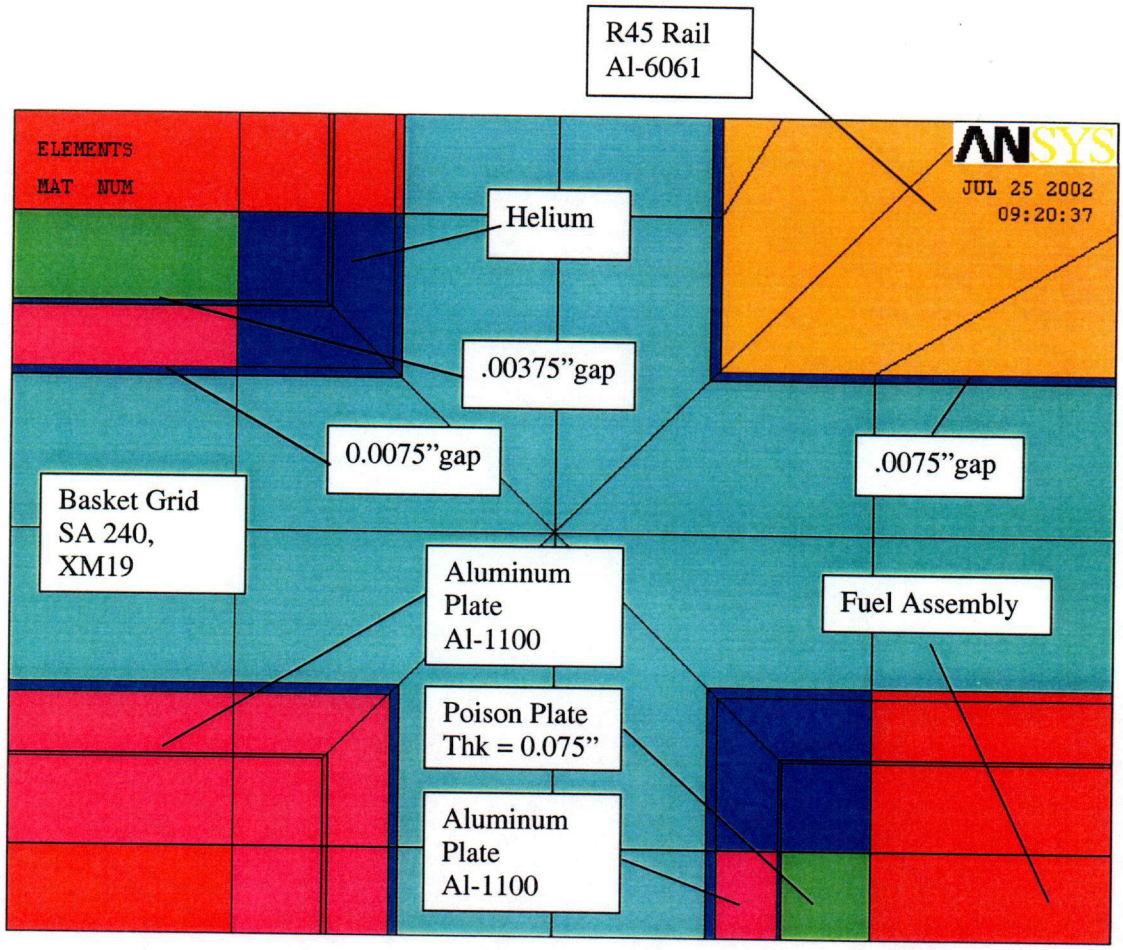

C03

Figure 4 - Detailed Model of NUHOMS®-32PT – Detail B

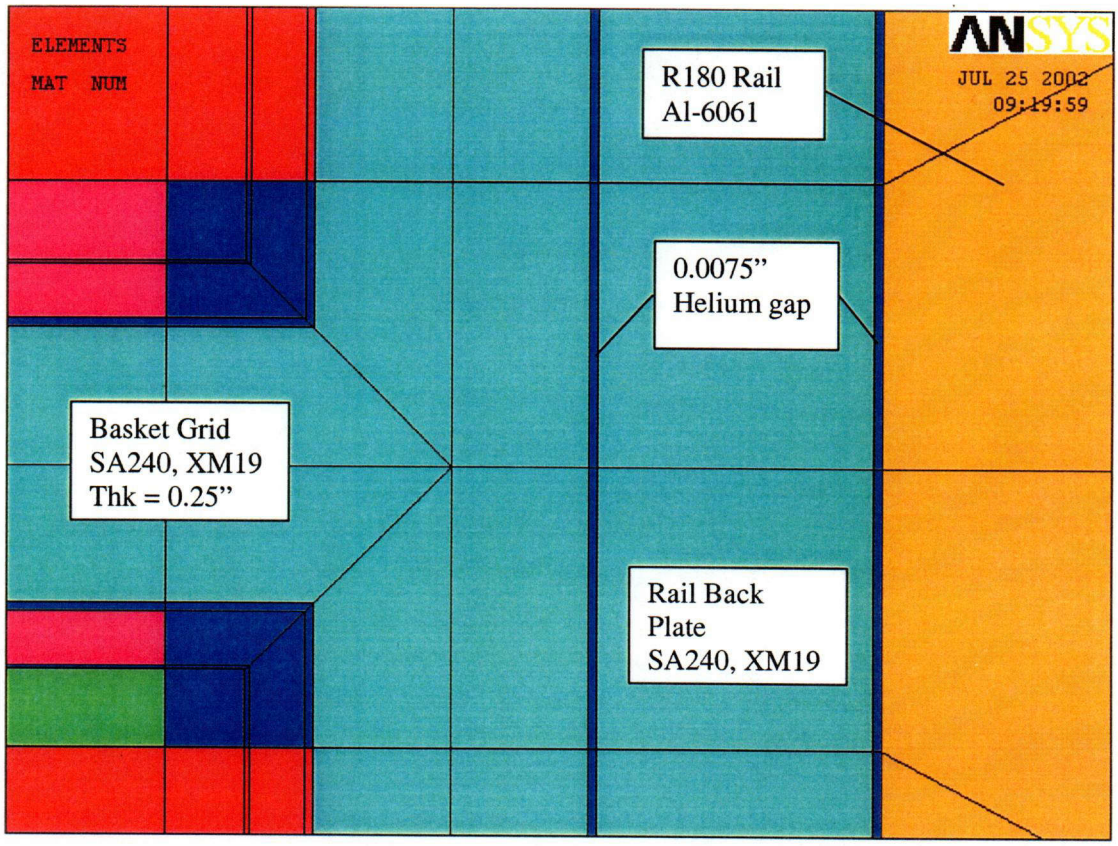

C04

Figure 5 - Detailed Model of NUHOMS®-32PT – Detail C

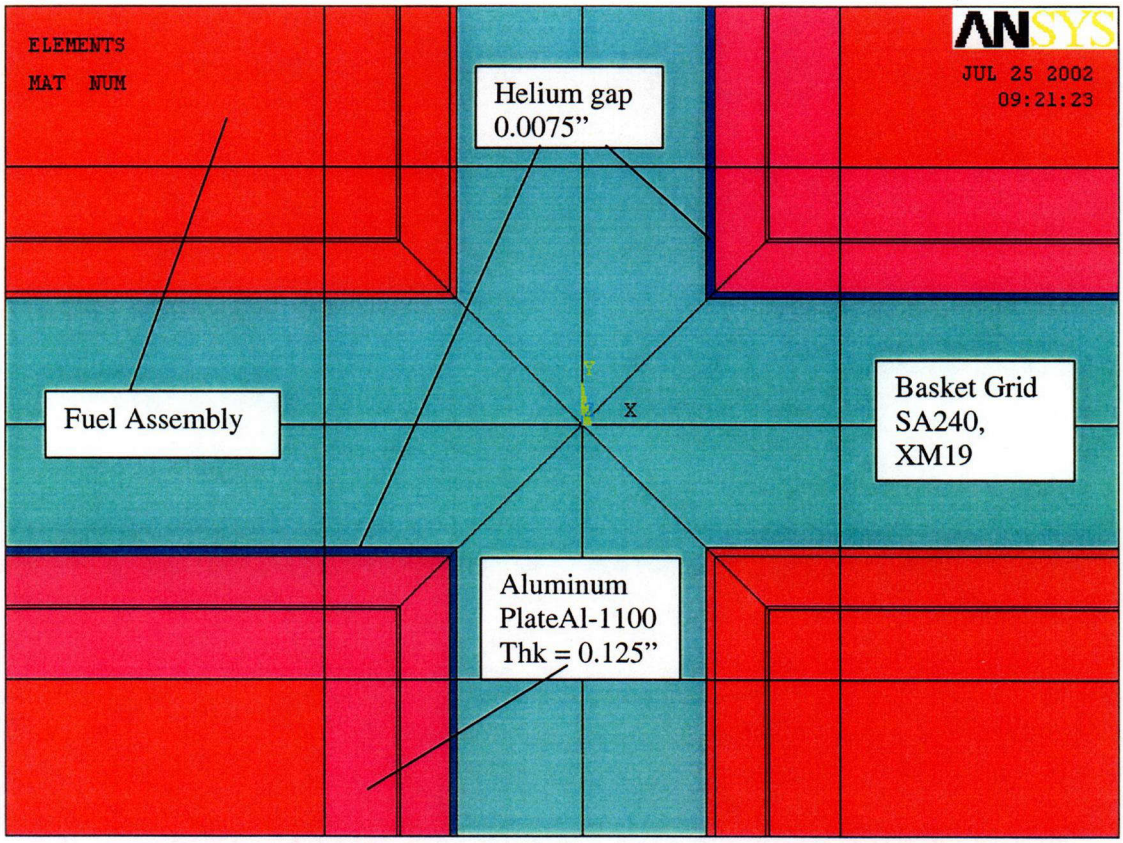

C05

ENCLOSURE 4 to NUH03-03-04

Calculation NUH32PT.0408, Revision 0

ATTACHMENT A

Description, Justification, and Evaluation of COC Amendment Changes

ATTACHMENT A

DESCRIPTION, JUSTIFICATION AND EVALUATION OF AMENDMENT CHANGES

1.0 INTRODUCTION

The purpose of this amendment application is to add a new Dry Shielded Canister (DSC), designated the NUHOMS®-32PT DSC, to the authorized contents of the Standardized NUHOMS® System. This is a transportable canister designed to accommodate 32 PWR fuel assemblies with or without Burnable Poison Rod Assemblies (BPRAs). It is designed for use with the existing NUHOMS® Horizontal Storage Module (HSM) and NUHOMS® transfer Cask (TC). No change to the HSM or TC design is required to accommodate the new canister.

This section of the application provides (1) a brief description of the changes, (2) justification for the change, and (3) a safety evaluation for this change.

Revision 1 of this Amendment is being submitted to provided a comprehensive response to the NRC Request for Additional Information (RAI); TAC NO. 23343.

Revision 4 of this Amendment is being submitted to reflect TN's response to the NRC Request for Additional Information (RAI) No. 2 dated July 3, 2002; and two additional questions raised in a subsequent teleconference with the NRC.

TN has revised the thermal model of the NUHOMS®-32PT DSC basket with a detailed model which simulates each basket component discretely. In addition, the analysis included in Appendix M has been revised based on the results of the bounding fuel assembly and the fuel region nodalization study. The analysis shows that the NUHOMS®-32PT DSC meets the acceptance criteria of ISG-11, Revision 2.

2.0 BRIEF DESCRIPTION OF THE CHANGE

2.1 Significant Changes to NUHOMS® CoC 72-1004, Amendment 4

The changes listed below are relative to CoC Amendment 4:

- Revise "Limit/Specification" and "Action" sections of Specification 1.2.1, "Fuel Specification", to add reference to Tables 1-1e, 1-1f, and 1-1g. Table 1-1e ,1-1f and 1-1g specify the applicable parameters for each type of PWR fuel allowed to be stored in the NUHOMS®-32PT DSC.

- Revise the "Bases" section of Specification 1.2.1, "Fuel Specification", to provide the supporting basis for storage of PWR fuel with or without BPRAs in the NUHOMS®-32PT DSC.

- Add Table 1-1e to identify the acceptable parameters for each type of intact PWR fuel assembly class allowed to be stored in the NUHOMS®-32PT DSC.

- Add Table 1-1f to specify PWR fuel assembly design characteristics for storage into NUHOMS®-32PT DSC.

- Add Table 1-1g to specify the initial enrichment for which each fuel assembly class is qualified and the required number of PRAs. The required PRA locations are per Figures 1-5 or 1-6 or 1-7.

- Add Table 1-1h to specify the minimum B10 content of the poison plates.

- Add Fuel Qualification Tables 1-2d, 1-2e, 1-2f, 1-2g, and 1-2h for the 32PT DSC (PWR Fuel without BPRAs).

- Add Fuel Qualification Tables 1-2i, 1-2j, 1-2k, 1-2l, and 1-2m for the 32PT DSC (PWR Fuel with BPRAs).

- Add Figures 1-2, 1-3, and 1-4 to specify the three heat load zoning configurations analyzed for the 32PT DSC. *Revise Figures 1-5, 1-6, and 1-7 to show the locations of the PRAs only.*

- Revise the title and "Applicability" section of Specification 1.2.3a to extend the applicability of this specification to 32PT DSC.

- Revise the title ,"Applicability" and the "Bases" sections of Specification 1.2.4a to extend the applicability of this specification to 32PT DSC.

- Revise the "Limit/Specification" section of Specification 1.2.7, "HSM Dose Rates", to reflect the limiting doses rates due to the addition of 32PT DSC. Revise the "Bases" section to include a reference to Appendix M where the shielding analysis for 32PT system is presented.

- Revise the "Bases" section of Specification 1.2.11, "Transfer Cask Dose Rates" to include a reference to Appendix M where the shielding analysis for 32PT system is presented.

- Add a new Specification 1.2.15a to specify the minimum boron concentration required during loading of the NUHOMS®-32PT system.

- *Restore* Specification 1.2.17, "Vacuum Drying Duration Limit" *back to reflect the limits for 61BT DSC only.*

- *Add a new Specification 1.2.17a to specify the vacuum drying duration limit for the NUHOMS®-32PT DSC. Revision 4 reflects the revised duration requirements to meet ISG-11, Revision 2 criteria.*

- Update Table 1.3.1 for the additional sections added to the specification.

2.2 Changes to NUHOMS® FSAR, Revision 6

Attachment C of this submittal includes a new FSAR Appendix M which has been prepared in a format consistent with the Standard Review Plan for Dry Cask Storage (NUREG 1536). It provides a complete evaluation of the new basket and the revised design features of the DSC. It also documents the changes where applicable to the existing safety analyses provided in the FSAR.

The Appendix M pages updated due to the RAI responses are submitted with Revision 1 of the application.

Revision 4 of Appendix M implements changes to the SAR to reflect RAI No. 2 responses and a complete revision of the thermal analysis based on the selection of the bounding assembly WE 14x14 and the fuel region nodalization study.

3.0 JUSTIFICATION OF CHANGE

The NUHOMS®-32PT System design has been developed based on research and development efforts driven by the needs of the commercial nuclear power industry. TN *has clients who have committed to use* the NUHOMS®-32PT system at their facilities. To support the needs of these *clients*, fabrication of the new canisters is planned to begin in early 2002 to support initial use in mid 2003.

4.0 EVALUATION OF CHANGE

TN has evaluated the NUHOMS®-32PT system for structural, thermal, shielding and criticality adequacy and has concluded that the addition of the new DSC to the standardized NUHOMS® System has no significant effect on safety. This evaluation is documented in Appendix M of the FSAR (Attachment C).

ATTACHMENT B

Suggested Changes to Technical Specifications of CoC 1004 Amendment 4

Technical Specifications included *as Changed Pages in Revision 4 of Amendment No. 5 to CoC 1004*:

- Section 1.2.1 *(Figures 1-5*, 1-6*, and 1-7* Only)*
- Section 1.2.17
- *Section 1.2.17a*
- Section 1.3.1

** These figures are schematics which are provided to show PRA locations only (Revision 4 deleted chevrons from these figures).*

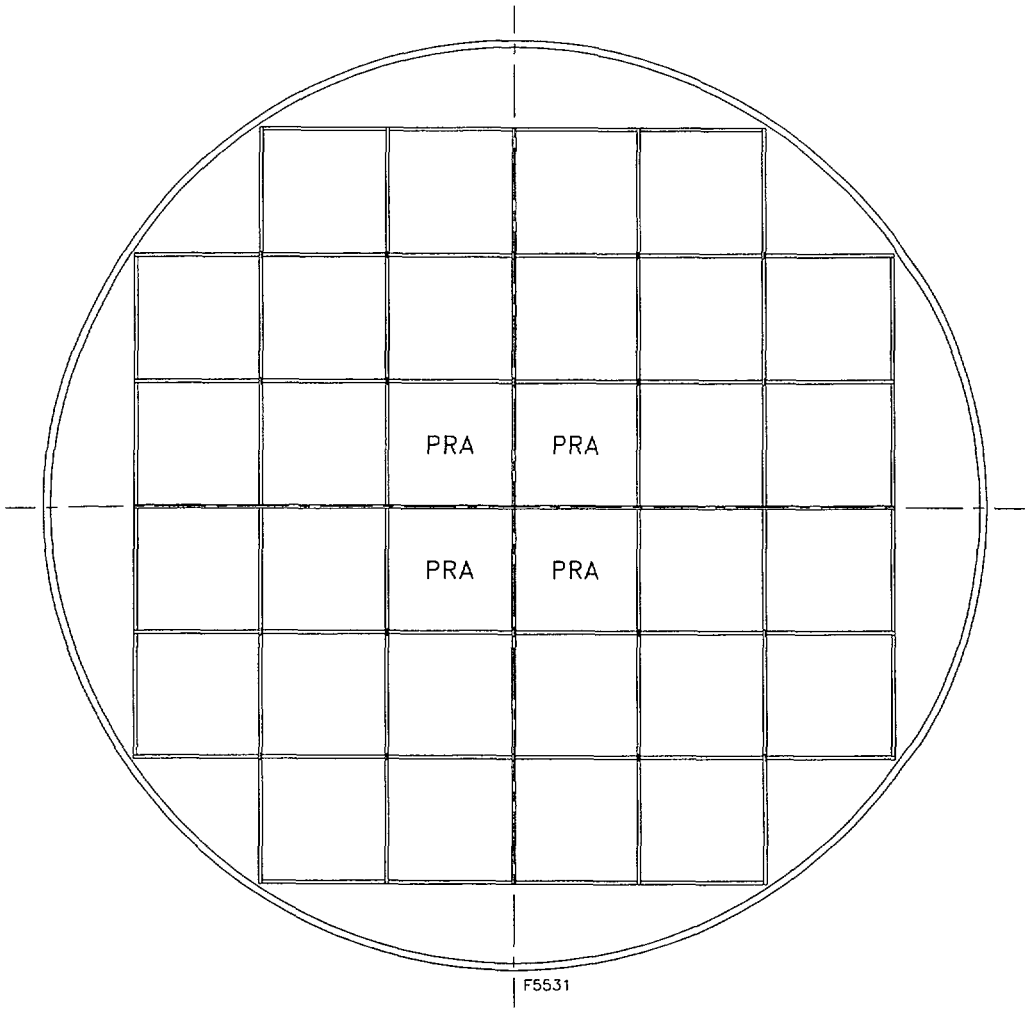

Figure 1-5
Required PRA Locations for Configurations with Four PRAs

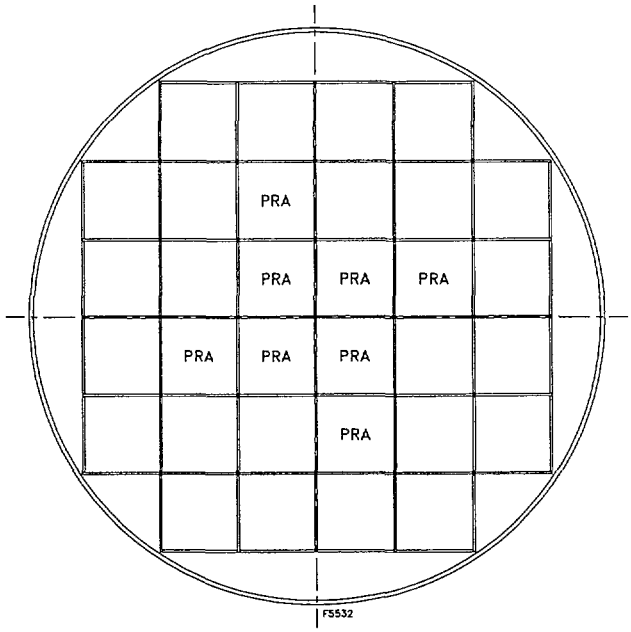

Or

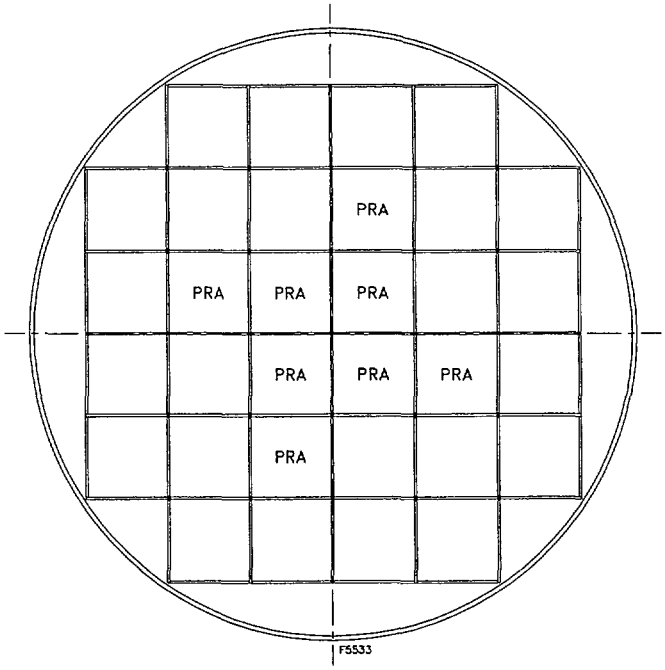

Figure 1-6
Required PRA Locations for Configurations with Eight PRAs

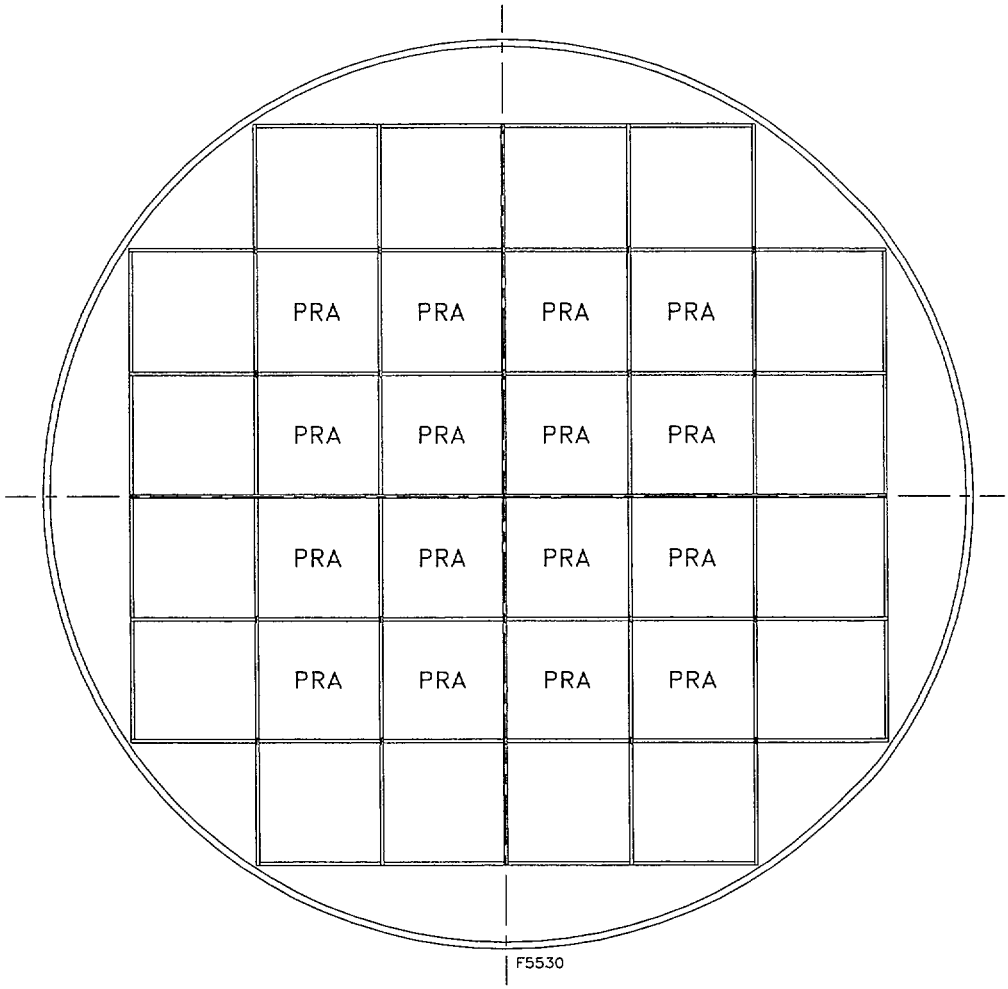

Figure 1-7
Required PRA Locations for Configurations with Sixteen PRAs

1.2.17 61BT DSC Vacuum Drying Duration Limit

Limit/Specifications:

1. Time limit for duration of Vacuum Drying is 96 hrs after completion of 61BT DSC draining.

Applicability: This specification is applicable to a 61BT DSC with greater than 17.6 kw heat load.

Objective: To ensure that 61BT DSC basket structure does not exceed 800^0 F.

Action:

1. If the DSC vacuum drying pressure limit of Technical Specification 1.2.2 cannot be achieved at 72 hours for 61BT DSC, the DSC must be backfilled with 0.1 atm or greater helium pressure within 24 hours.

2. Determine the cause of failure to achieve the vacuum drying pressure limit as defined in Technical Specification 1.2.2.

3. Initiate vacuum drying after actions in Step 2 are completed or unload the DSC within 30 days.

Surveillance: No maintenance or tests are required during the normal storage. Monitoring of the time duration during the vacuum drying operation is required.

Bases: The time limits of 96 hours for the 61BT DSC were selected to ensure that the temperature of the DSC basket structure is within the design limits during vacuum drying.

1.2.17a *32PT DSC Vacuum Drying Duration Limit*

Limit/Specifications:

1. *The limit for duration of Vacuum Drying is 31 hrs for a 32PT DSC with a heat load greater than 8.4 kW and up to 24 kW after initiation of vacuum drying.*
2. *The limit for duration of Vacuum Drying is 36 hrs for a 32PT DSC with a heat load of up to 8.4 kW after initiation of vacuum drying.*

Applicability: *This specification is applicable to a 32PT DSC with heat load as described above.*

Objective: *To ensure the fuel cladding temperature in the 32PT DSC does not exceed 752°F during drying and also to meet the thermal cycling limit of 117°F during drying, helium backfilling and transfer operations.*

Action:

1. *If the DSC vacuum drying pressure limit of Technical Specification 1.2.2 cannot be achieved at the specified time limits after initiation of vacuum drying, the DSC must be backfilled with 0.1 atm or greater helium pressure within 2 hours.*
2. *Determine the cause of failure to achieve the vacuum drying pressure limit as defined in Technical Specification 1.2.2.*
3. *Initiate vacuum drying after actions in Step 2 are completed or unload the DSC within 30 days.*

Surveillance: *No maintenance or tests are required during the normal storage. Monitoring of the time duration during the vacuum drying operation is required.*

Bases: *The time limits for the 32PT DSC were selected to ensure that the maximum cladding temperature is within the acceptable limit of 752°F during vacuum drying. These time limits also ensure that the cladding temperature meets the thermal cycling criteria of 117°F during drying, helium backfilling and transfer operations*

Table 1.3.1

Summary of Surveillance and Monitoring Requirements

Surveillance or Monitoring	Period	Reference Section
1. Fuel Specification	PL	1.2.1
2. DSC Vacuum Pressure During Drying	L	1.2.2
3. DSC Helium Backfill Pressure	L	1.2.3 or 1.2.3a
4. DSC Helium Leak Rate of Inner Seal Weld	L	1.2.4 or 1.2.4a
5. DSC Dye Penetrant Test of Closure Welds	L	1.2.5
6. Deleted	-	-
7. HSM Dose Rates	L	1.2.7
8. HSM Maximum Air Exit Temperature	24 hrs	1.2.8
9. TC Alignment with HSM	S	1.2.9
10. DSC Handling Height Outside Spent Fuel Pool Building	AN	1.2.10
11. Transfer Cask Dose Rates	L	1.2.11
12. Maximum DSC Surface Contamination	L	1.2.12
13. TC/DSC Lifting Heights as a Function of Low Temperature and Location	L	1.2.13
13. TC/DSC Lifting Heights as a Function of Low Temperature and Location	L	1.2.13

Legend

PL Prior to loading
L During loading and prior to movement to HSM pad
24 hrs Time following DSC insertion into HSM
S Prior to movement of DSC to or from HSM
AN As necessary
D Daily (24 hour frequency)

14. TC/DSC Transfer Operations at High Ambient Temperatures	L	1.2.14
15. Boron Concentration in DSC Cavity Water (24-P Designs Only)	PL	1.2.15
15a Boron Concentration in DSC Cavity Water (32PT Designs Only)	*PL*	*1.2.15a*
16. Provision of TC Seismic Restraint Inside the Spent Fuel Pool Building as a Function of Horizontal Acceleration and Loaded Cask Weight	PL	1.2.16
17. Visual Inspection of HSM Air Inlets and Outlets	D	1.3.1
18. HSM Thermal Performance	D	1.3.2
19 61BT DSC Vacuum Drying *Duration* Limits	L	1.2.17
20 32PT DSC Vacuum Drying Duration Limits	*L*	*1.2.17a*

Legend

PL Prior to loading
L During loading and prior to movement to HSM pad
24 hrs Time following DSC insertion into HSM
S Prior to movement of DSC to or from HSM
AN As necessary
D Daily (24 hour frequency)

ATTACHMENT C

List of Changed Appendix M Pages

- *M.2-2*
- *M.2-12*
- *M.2-13*
- *M.2-41 through M.2-43*
- *M.3.1-2*
- *M.3.1-2a (New Page)*
- *M.3.1-7*
- *M.4 (Entire Section)*

M.2.1 Spent Fuel To Be Stored

There are four design configurations for the NUHOMS®-32PT DSC, two 100-ton configurations, one long and one short canister; and two 125-ton configurations, one long and one short canister. The main difference between the 100-ton and 125-ton configuration designs are the thicknesses of shield plugs and DSC cover plates. The long 100-ton configuration is designated the 32PT-L100 and the short 100-ton configuration is designated the 32PT-S100. Likewise the long 125-ton configuration is designated the 32PT-L125 and the short 125-ton configuration the 32PT-S125. The basket layout for these two configurations is identical except for the length of the components. Each of the DSC configurations is designed to store 32 intact standard PWR fuel assemblies. The 32PT-L100 and 32PT-L125 are also designed to store 32 intact standard PWR fuel assemblies with or without BPRAs. The NUHOMS®-32PT DSCs can store intact PWR fuel assemblies and BPRAs with the characteristics described in Table M.2-1. The NUHOMS®-32PT DSC may store PWR fuel assemblies arranged in any of three alternate heat zoning configurations with a maximum decay heat of 1.2kW per assembly and a maximum heat load of 24 kW per canister. The heat load zoning configurations are shown in Figure M.2-1 through Figure M.2-3. The NUHOMS®-32PT DSC is inerted and backfilled with helium at the time of loading. The maximum fuel assembly weight with a BPRA is 1682 lbs. which is the same as the NUHOMS®-24P DSC design.

The maximum fuel cladding temperature limit of 400°C (752°F) is applicable to normal conditions of storage and all short term operations from spent fuel pool to ISFSI pad including vacuum drying and helium backfilling of the NUHOMS®-32PT DSC per Interim Staff Guidance (ISG) No. 11, Revision 2 [2.7]. In addition, ISG-11 does not permit thermal cycling of the fuel cladding with temperature differences greater than 65°C (117°F) during DSC drying, backfilling and transfer operations.

The maximum fuel cladding temperature limit of 570°C (1058°F) is applicable to accidents or off-normal thermal transients [2.7].

Calculations were performed to determine the fuel assembly type which was most limiting for each of the analyses including shielding, criticality, heat load and confinement. These evaluations are performed in Chapter M.5, M.6, M.4 and M.7. The fuel assembly types considered are listed in Table M.2-2. It was determined that the B&W 15x15 is the enveloping fuel design for the shielding source term calculation because of its total assembly weight and highest initial heavy metal loading. For criticality safety, the B&W 15x15 assembly is the most reactive assembly type for a given enrichment. This assembly is used to determine the most reactive configuration in the DSC. Using this most reactive configuration, criticality analysis for all other fuel assembly classes is performed to determine the maximum enrichment allowed as a function of number of Poison Rod Assemblies (PRAs). For thermal analysis, the WE 14x14 fuel assembly is limiting, since it results in the lowest fuel conductivity. The confinement analyses is based on B&W 15x15 fuel assembly, since it results in the smaller free volume inside the DSC cavity more than a 14x14 fuel assembly.

All four NUHOMS®-32PT DSC design configurations have the same minimum boron content for the poison neutron plates. The minimum boron-10 content for the poison plates is 0.0070

M.2.5 Summary of NUHOMS®-32PT DSC Design Criteria

The additional principal design criteria for the NUHOMS®-32PT DSC are presented in Table M.2-19. The NUHOMS®-32PT DSC is designed to store 32 intact standard PWR fuel assemblies with or without BPRAs with assembly average burnup, initial enrichment and cooling time as described in Table M.2-1. The maximum total heat generation rate of the stored fuel is limited to 1.2 kW per fuel assembly and 24 kW per NUHOMS®-32PT DSC in order to keep the maximum fuel cladding temperature below the limit [2.7]necessary to ensure cladding integrity. The fuel cladding integrity is assured by the NUHOMS®-32PT DSC and basket design which limits fuel cladding temperature and maintains a nonoxidizing environment in the cask cavity as described in Section M.4.

The NUHOMS®-32PT DSC (shell and closure) is designed and fabricated as a Class 1 component in accordance with the rules of the ASME Boiler and Pressure Vessel Code, Section III, Subsection NB, and the alternative provisions to the ASME Code as described in Table M.3.1-1.

The NUHOMS®-32PT DSC is designed to maintain a subcritical configuration during loading, handling, storage and accident conditions. A combination of fixed neutron absorbers, soluble boron in the pool and favorable geometry are employed to maintain the upper subcritical limit of 0.9411. The fixed neutron absorbers are in the form of borated metallic plates and PRAs which are inserted in the guide tubes of certain assemblies in the basket. The basket is designed and fabricated in accordance with the rules of the ASME Boiler and Pressure Vessel Code, Section III, Subsection NG, Article NG-3200 and the alternative provisions to the ASME Code as described in Table M.3.1-1.

The NUHOMS®-32PT DSC design, fabrication and testing are covered by TN's Quality Assurance Program, which conforms to the criteria in Subpart G of 10CFR72.

The NUHOMS®-32PT DSC is designed to withstand the effects of severe environmental conditions and natural phenomena such as earthquakes, tornadoes, lightning and floods. Section M.11 describes the NUHOMS®-32PT DSC behavior under these accident conditions.

M.2.6 References

2.1 NUREG-1536, "Standard Review Plan for Dry Cask Storage Systems," 1997.

2.2 American Society of Mechanical Engineers, ASME Boiler And Pressure Vessel Code, Section III, Division 1 - Subsections NB, NG and NF, 1998 edition including 2000 Addenda.

2.3 Young, W.C., "Roark's Formulas for Stress and Strain," 6th Edition, McGraw-Hill Book Company, New York, 1989.

2.4 ANSI N14.5-1997, "Leakage Tests on Packages for Shipment," February 1998.

2.5 Deleted.

2.6 Deleted.

2.7 Interim Staff Guidance No. 11, Revision 2, "Cladding Considerations for the Transportation and storage of Spent Fuel", dated July 30, 2002.

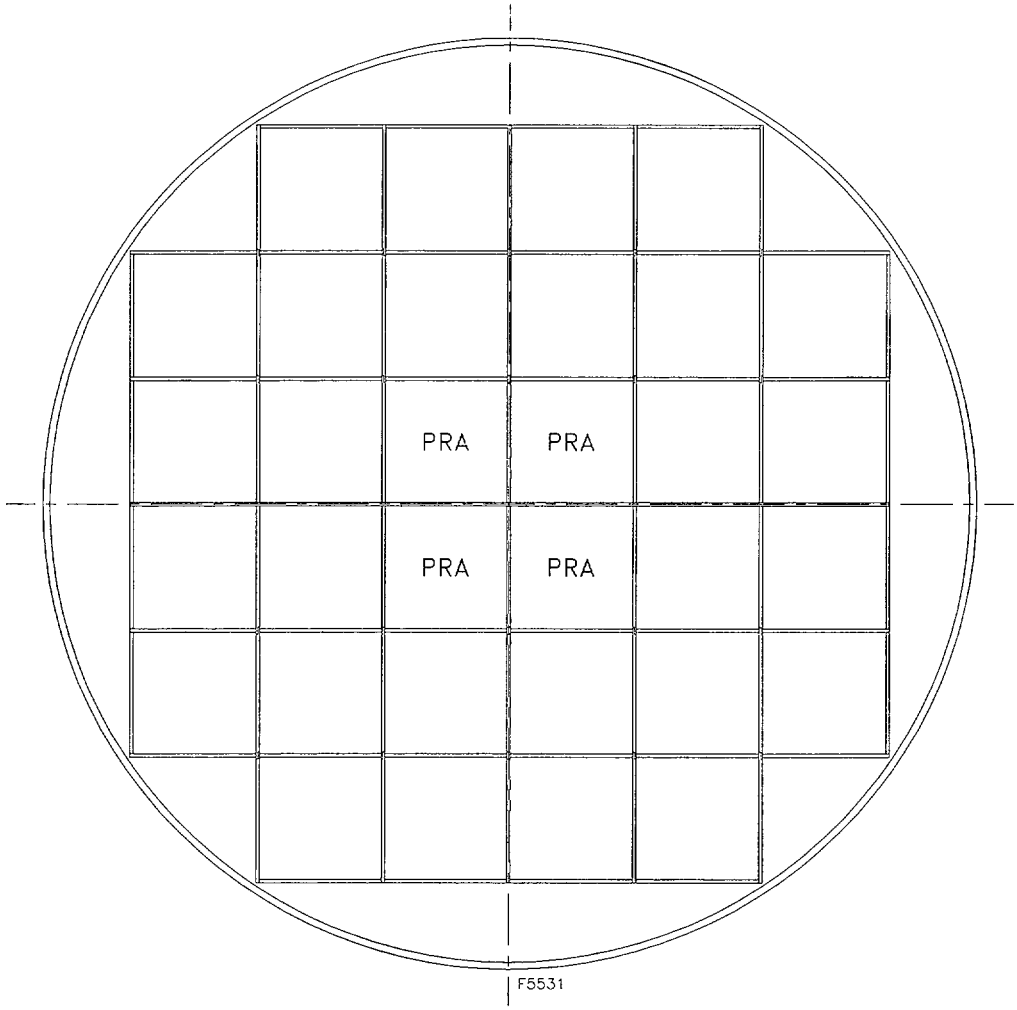

Figure M.2-4
Required PRA Locations for Configurations with Four PRAs

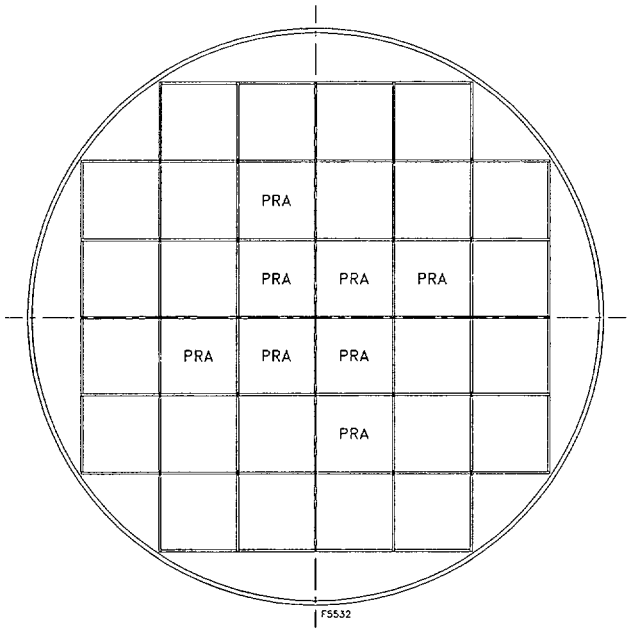

OR

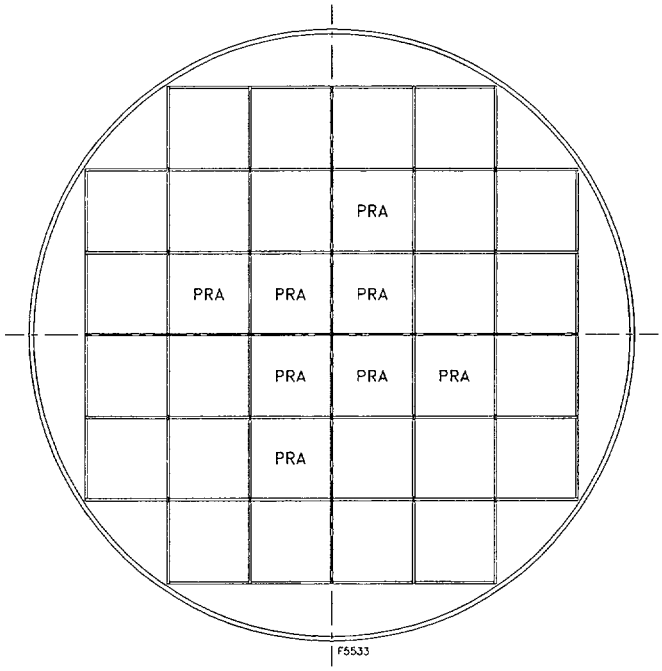

Figure M.2-5
Required PRA Locations for Configurations with Eight PRAs

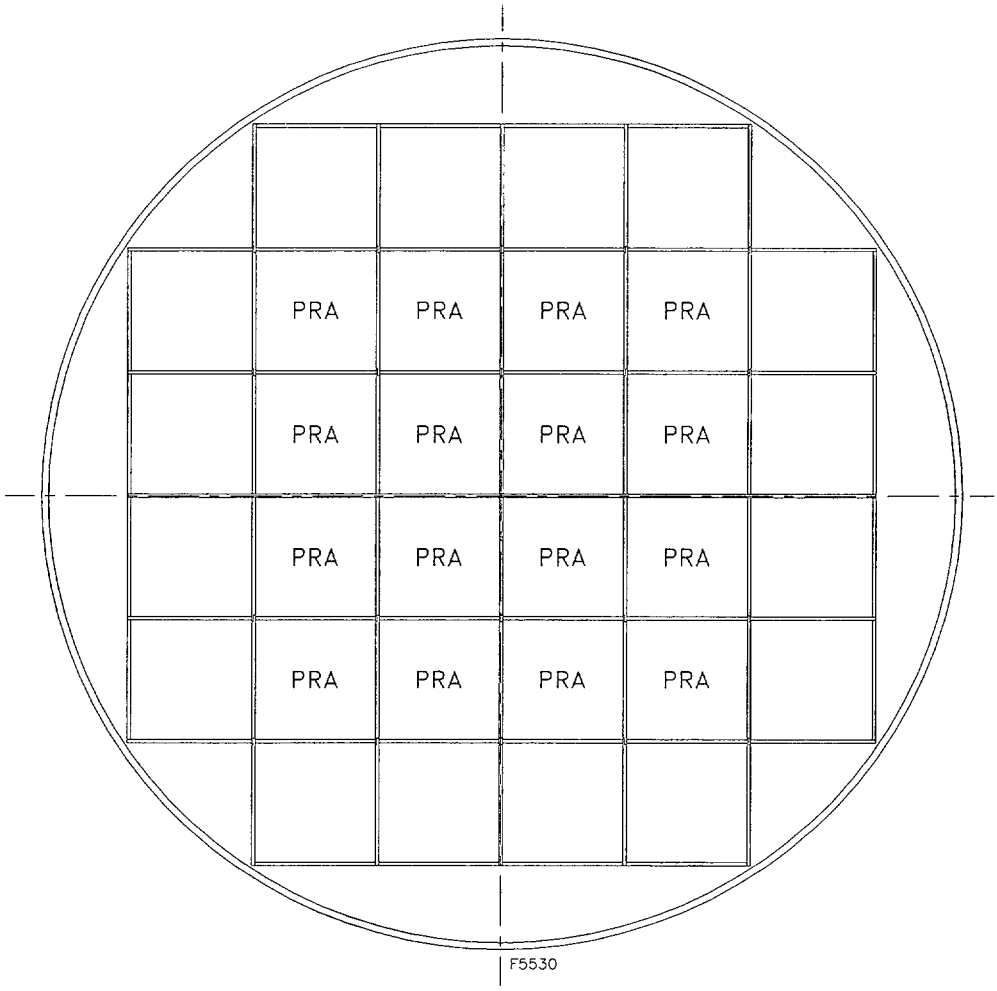

Figure M.2-6
Required PRA Locations for Configurations with Sixteen PRAs

The NUHOMS®-32PT basket is a welded assembly of stainless steel plates or tubes that make up a fuel support assembly grid designed to accommodate up to 32 PWR fuel assemblies. The basket structure consists of the fuel support structure, the transition rails, aluminum heat transfer material, and neutron absorbing material.

The 32PT basket assembly is shown on drawings NUH-32PT-1003, -1004 and -1006. These drawings are provided in Section M.1.5.

- The fuel support structure is fabricated from high strength (Type XM-19) stainless steel and contains 32 square fuel compartments in a box arrangement.
- The transition rails provide the transition between the "rectangular" fuel support grid and the cylindrical internal diameter of the DSC shell. There are two sizes of transition rails. The large rails are referred to as the R90 transition rails. The smaller transition rails are referred to as the R45 transition rails.

Note on the Revised Thermal Analysis in Chapter M.4.: The NUHOMS®-32PT basket configuration with welded steel transition rails and the corresponding thermal analysis have been deleted. Accordingly, the structural analysis for the basket with welded steel rail option as presented in this Chapter M.3 will be deleted following approval of this application.

Revised thermal analysis profiles for the basket components (with solid aluminum rail design configuration) are presented in Chapter M.4. These results have been reconciled with the temperature profiles (corresponding to the steel rails configuration) used in the Chapter M.3 stress analysis. The following is a summary of this reconciliation.

Blocked Vent: Maximum temperatures and temperature gradients corresponding to the revised thermal analysis results documented in Chapter M.4 are lower for all basket components than the temperatures and temperature gradients used in the stress analysis. Therefore, the revised thermal results have no impact on the existing stress evaluations for the blocked vent condition.

Vacuum Drying: The maximum temperatures corresponding to the revised thermal analysis results documented in Chapter M.4 are lower for all basket components than the maximum temperatures used in the stress analysis. The temperature gradients for the solid aluminum rail components are also lower. Therefore, the revised thermal results have no impact on the existing stress evaluations of the solid aluminum rail components. The temperature gradient across the XM-19 steel grid component increases, causing an increase in the stress of about 1.0 ksi. The maximum thermal stress intensity in the grid component is small (4.33 ksi, from Table M.3.4-2). Considering that the only other load for this condition is deadweight (0.06 ksi, from Table M.3.6-5), the margin to allowable (84.6 ksi, from Table M.3.3-3, at 800°F) remains very large (4.33+1.1+0.06=5.39 ksi versus 84.6 ksi). Therefore, the impact of the revised thermal results is negligible.

Storage and Transfer Conditions: The maximum temperatures corresponding to the revised thermal analysis results documented in Chapter M.4 are lower for all basket components than the maximum temperatures used in the stress analysis. The temperature gradients for the solid

aluminum rail components are also lower. Therefore, the revised thermal results have no impact on the existing stress evaluations of the solid aluminum rail components. The temperature gradient across the XM-19 steel grid component increases, causing a maximum (envelope of all transfer/storage cases) stress increase of 1.55 ksi. The maximum thermal stress intensity in the grid component is small (4.95 ksi, from Table M.3.4-2). The controlling stress intensity (which includes the thermal stress) for the grid component is 18.3 ksi (from Table M.3.6-6). Considering the incremental stress, the revised stress intensity is 19.85 ksi versus 84.6 ksi allowable. Therefore, considering the large margin available, the impact of the revised thermal results is negligible.

Accident Transfer Case (117°F ambient, loss of sunshade, loss of neutron shield): The maximum temperature for the accident transfer case has increased. As shown in Table M.4-14, the revised maximum temperature for the steel grid is 852°F. The structural evaluation used allowable for the steel grid at 800°F. An exception to the material temperature limits of ASME Section II, Part D for the XM-19 grid plate material is added to Table M.3.1-2. This is a post-drop accident condition, where the only primary loads on the basket are due to deadweight and the expected reduction in material strength is small (less than 1 ksi by extrapolation, from Table M.3.3-3). Therefore, this case is not a concern considering that the deadweight stress is small.

The shell assembly temperatures used in the structural analysis are bounded by the revised thermal results and, thus, there is no impact on the shell assembly. The calculated pressures due to the increased temperatures for the postulated post-drop accident transfer case (117°F ambient, loss of sunshade, loss of neutron shield) bound the pressures used in the structural evaluations.

Therefore, the revised thermal analysis results presented in Chapter M.4 have negligible impact on the DSC structural analysis results as presented in this Chapter for the solid aluminum rail design.

Two material/fabrication designs are evaluated for the transition rails:

- Solid Aluminum Rails: The transition rails are solid sections of 6061 aluminum alloy. The large (R90) rails include an XM-19 "cover plate" between the fuel support grid and the aluminum body. The structural evaluation of the rails uses properties for annealed aluminum (no credit is taken for enhanced properties obtained by heat treatment).

- Welded Steel Transition Rails: The steel transition rails are welded steel structures fabricated with 3/8" thick Type 304 stainless steel. To enhance heat transfer through the rails, aluminum plates are connected to the transition rail structure. No credit is taken for these aluminum plates in the structural evaluation of the steel transition rails.

- The fuel support grid structure contains aluminum alloy 1100 plates as heat transfer material and neutron absorbing plates. No credit is taken for the structural capacity of the aluminum heat transfer plates or neutron absorbing materials in the structural evaluation of the support grid structure.

Table M.3.1-2
Alternatives to the ASME Code Exceptions for the NUHOMS®-32PT DSC Basket Assembly

Reference ASME Code Section/Article	Code Requirement	Alternatives, Exception, Justification & Compensatory Measures
NG-1100	Requirements for Code Stamping of Components	The NUHOMS®-32PT DSC baskets are designed & fabricated in accordance with the ASME Code, Section III, Subsection NG as described in the SAR, but Code Stamping is not required. As Code Stamping is not required, the fabricator is not required to hold an ASME N or NPT stamp or be ASME Certified.
NG-2000	Use of ASME Material	The poison material and aluminum plates are not used for structural analysis, but to provide criticality control and heat transfer. They are not ASME Code Class 1 material. Material properties in the ASME Code for Type 6061 aluminum are limited to 400°F to preclude the potential for annealing out the hardening properties. Annealed properties (as published by the Aluminum Association and the American Society of Metals) are conservatively assumed for the solid aluminum rails for use above the Code temperature limits.
NG-2130	Material must be supplied by ASME approved material suppliers.	All materials designated as ASME on the SAR drawings are obtained from ASME approved Material Organization with ASME CMTR's. Material is certified to meet all ASME Code criteria, but is not eligible for certification or Code Stamping if a non-ASME fabricator is used. As the fabricator is not required to be ASME certified, material certification to NG-2130 is not possible. Material traceability & certification are maintained in accordance with TNW's NRC approved QA program.
NG-4121	Material Certification by Certificate Holder	
NG-8000	Requirements for nameplates, stamping & reports per NCA-8000	The NUHOMS®-32PT DSC nameplate provides the information required by 10CFR71, 49CFR173 and 10CFR72 as appropriate. Code stamping is not required for the NUHOMS®-32PT DSC. In lieu of Code stamping, QA Data packages are prepared in accordance with the requirements of 10CFR71, 10CFR72 and TNW's approved QA program.
NCA	All	Not compliant with NCA as no Code stamp is used. TNW Quality Assurance requirements, which are based on 10CFR72 Subpart G, are used in lieu of NCA-4000. Fabrication oversight is performed by TNW and utility personnel in lieu of an Authorized Nuclear Inspector.
NG-3000/ Section II, Part D, Table 2A	Maximum temperature limit for XM-19 plate material is 800°F	Not compliant with ASME Section II Part D Table 2A material temperature limit for XM-19 steel for the postulated transfer accident case (117°F, loss of sunshade, loss of neutron shield). This is a post-drop accident scenario, where the calculated maximum steady state temperature is 852°F, the expected reduction in material strength is small (less than 1 ksi by extrapolation), and the only primary stresses in the basket grid are deadweight stresses. The recovery actions following the postulated drop accident are as described in Section 8.2.5 of the FSAR.

M.4 Thermal Evaluation

M.4.1 Discussion

The NUHOMS®-32PT system is designed to passively reject decay heat during storage and transfer for normal, off-normal and accident conditions while maintaining temperatures and pressures within specified regulatory limits. Objectives of the thermal analyses performed for this evaluation include: (1) determination of maximum and minimum temperatures with respect to material limits to ensure components perform their intended safety functions, (2) determination of temperature distributions for the NUHOMS®-32PT DSC components to support the calculation of thermal stresses for the structural components, (3) determination of maximum internal pressures for the normal, off-normal and accident conditions, (4) determination of the maximum fuel cladding temperature, and (5) confirmation that this temperature will remain sufficiently low to prevent unacceptable degradation of the fuel during storage.

The methodology used to calculate the effective fuel conductivity and to predict the fuel and basket temperature distribution in the NUHOMS®-32PT DSC has been benchmarked [4.25] against experimental data obtained for the TN-24 cask [4.26]. The results of the benchmarking study show that with the cask in a horizontal configuration, the TN methodology predicted fuel cladding temperatures which are 77°F higher than the test data.

In the specific case of the TN-24 cask, with the cask backfilled with helium and in a horizontal configuration, the maximum fuel cladding temperature noted in the PNL Test Report [4.26] was 419°F. The use of TN-24 test data is appropriate for validating the thermal model which is intended for use at higher temperature levels based on the following justification:

- For a thermal model that captures the basic thermo physical processes (i.e., conduction, convection, and radiation) present, the primary areas of uncertainty will be the modeling of the geometry and the thermal properties used for each component. Once the correct geometry and thermal properties are captured, the effect of higher temperature levels on the fundamental heat transfer processes involved is well understood and documented. Thus, simply changing the temperature level for a simulation will not necessarily increase the uncertainty level for the thermal model.

- Changes to the thermal conductivity of the metallic components with temperature are well understood and documented for temperature levels well in excess of 700°F. As such, the effect is easily captured through the use of temperature dependant properties.

- Radiation heat transfer is a function of view factor, surface area, and emissivity. View factors and surface area do not change with increased temperature level. As such, a thermal model that incorporates radiation exchange and which has been validated at a lower temperature is typically conservative (i.e., yield higher temperatures) for application at a higher temperature level.

- Any impact on temperatures due to the potential changes in the thermal parameters between the TN-24 temperature regime and the NUHOMS®-32PT DSC temperature regime is fully bounded by the conservatism demonstrated in the results of the benchmark analysis.

Therefore, a thermal model that has been properly constructed and predicts conservatively high temperatures in comparison with the TN-24 test data can be fully expected to yield accurate results at the higher temperature levels similar of the NUHOMS®-32PT DSC design.

Several thermal design criteria are established for the thermal analysis of the 32PT DSC basket as discussed below.

- Maximum temperatures of the confinement structural components must not adversely affect the confinement function,

- Maximum fuel cladding temperature limit of 400°C (752°F) is applicable to normal conditions of storage and all short term operations including vacuum drying and helium backfilling of the 32PT DSC per Interim Staff Guidance (ISG) No. 11, Revision 2 [4.24]. In addition, ISG-11 does not permit thermal cycling of the fuel cladding with temperature differences greater than 65°C (117°F) during drying and backfilling operations,

- Maximum fuel cladding temperature limit of 570°C (1058°F) is applicable to accidents or off-normal thermal transients [4.24],

- The maximum DSC cavity internal pressures during normal, off-normal and accident conditions must be below the design pressures of 15 psig, 20 psig and 105 psig, respectively, and

- Figure M.4-1, Figure M.4-2, and Figure M.4-3 show the heat load zoning configurations used in the NUHOMS®-32PT DSC design. The maximum total heat load per DSC is 24 kW or 22.4 kW depending on the specific heat load zoning configuration.

The analyses consider the effect of the decay heat flux varying axially along a fuel assembly. The axial heat flux profile for a PWR fuel assembly is shown in Figure M.4-4 and is based on [4.3].

A description of the detailed analyses performed for normal storage and transfer conditions is provided in Section M.4.4, off-normal conditions in Section M.4.5, accident conditions in Section M.4.6, and loading/unloading conditions in Section M.4.7. The thermal evaluation concludes that with a design basis heat load of up to 24 kW per DSC, all design criteria are satisfied.

The effective thermal conductivity of the fuel assemblies used in the 32PT DSC thermal analysis is based on the conservative assumption of radiation and conduction heat transfer only where any convection heat transfer is neglected. In addition, the fuel assembly with the lowest effective thermal conductivity at the maximum heat load, WE 14x14, is selected as the basis for the thermal analysis . Section M.4.8 presents the calculations that determined WE 14x14 to be the fuel assembly with the lowest effective thermal conductivity in a helium or vacuum environment.

The thermal analysis model conservatively neglects convection heat transfer in the basket regions.

The basket design used for the NUHOMS®-32PT DSC is similar to the basket design of the TN-32 cask [Docket 72-1021]. Both designs use a tube and support rail type of basket which is significantly different than the spacer disc and guide sleeve type of basket design used for the NUHOMS®-24P DSCs.

M.4.2 Summary of Thermal Properties of Materials

The analyses use interpolated values where appropriate for intermediate temperatures. The interpolation assumes a linear relationship between the reported values. The use of linear interpolation between temperature values in the tables for determining intermediate value of property is justified by the near-linear behavior as a function of temperature for the range of interest.

The emissivity of stainless steel is 0.587 [4.7]. For additional conservatism an emissivity of 0.46 for stainless steel is used for the basket steel plates in the analysis. The emissivity values assumed in the analysis for the aluminum sheets (Type 1100) and aluminum based neutron poison plates is 0.85 which is achieved by either anodizing or other processes. The emissivity of the oxidized Zircalloy surface is 0.8 [4.14]. Emissivity for the aluminum rail material (Type 6061) is not required for the analysis because radiation between the rails and the DSC shell is conservatively neglected in the analysis.

The tables below provide the thermal properties of materials used in the analysis of the NUHOMS®-32PT DSC.

1. PWR Fuel with Helium Backfill

The effective thermal conductivity is the lowest calculated value for the various PWR fuel assembly types that may be stored in this DSC and corresponds to the WE 14x14 PWR assembly. Section M.4.8 presents the calculations that determined WE 14x14 to be the fuel assembly with the lowest effective thermal conductivity in both helium and vacuum environment.

Temperature (°F)	K (Btu/min-in-°F)	ρ (lb_m/in^3)	T (°F)	C_p (Btu/lb_m-°F)
Fuel in Helium, Transverse [Section M.4.8]				
138	2.894E-04	0.1166	80	0.0592
233	3.317E-04		260	0.0654
328	3.968E-04		692	0.0725
423	4.744E-04		1502	0.0778
519	5.668E-04			
616	6.715E-04			
714	7.879E-04			
812	9.208E-04			

Temperature (°F)	K (Btu/min-in-°F)	ρ (lb_m/in^3)	T (°F)	C_p (Btu/lb_m-°F)
Fuel in Helium, Axial [Section M.4.8]				
200	7.949E-04	0.1166	See values above	
300	8.387E-04			
400	8.824E-04			
500	9.189E-04			
600	9.554E-04			
800	1.036E-03			

2. PWR Fuel in Vacuum

Temperature (°F)	K (Btu/min-in-°F)	ρ (lb_m/in^3)	T (°F)	C_p (Btu/lb_m-°F)
Fuel in a Vacuum [Section M.4.8]				
215	9.484E-05	0.1166	80	0.0592
288	1.246E-04		260	0.0654
367	1.633E-04		692	0.0725
452	2.119E-04		1502	0.0778
540	2.701E-04			
632	3.373E-04			
726	4.125E-04			
822	4.949E-04			

3. Zircalloy

Temperature (°F)	K (Btu/min-in-°F) [4.14]	ρ (lbm/in^3) [4.28]	C_p (Btu/lb_m-°F) [4.14]	
200	0.0109	0.237	80	0.067
300	0.0115		260	0.072
400	0.0121		692	0.079
500	0.0126		1502	0.090
600	0.0131		-	
800	0.0142			

4. UO_2 Fuel Pellet

Temperature (°F)	K (Btu/min-in-°F [4.14]	ρ (lbm/in^3) [4.28]	C_p (Btu/lb_m-°F) [4.14]	
200	5.537E-3	0.396	32	0.056
300	5.038E-3		212	0.063
400	4.622E-3		392	0.068
500	4.270E-3		752	0.072
600	3.968E-3		2192	0.079
700	3.707E-3			
800	3.478E-3			

5. SA-240, Type 304 Stainless Steel [4.4]

Temperature (°F)	K (Btu/min-in-°F)	ρ (lbm/in^3)	C_p (Btu/lb$_m$-°F)
70	0.0119	0.284	0.116
100	0.0121		0.117
150	0.0125		0.119
200	0.0129		0.121
250	0.0133		0.124
300	0.0136		0.125
350	0.0140		0.127
400	0.0144		0.128
500	0.0151		-
600	0.0157		-
700	0.0164		-
800	0.0169		-

6. SA-240 Type XM-19 (22Cr-13Ni-5Mn) [4.4]

Temperature (°F)	K (Btu/min-in-°F)	ρ (lb$_m$/in^3)	C_p (Btu/lb$_m$-°F)
70	8.89e-3	0.284	0.113
100	9.17e-3		0.116
150	9.58e-3		0.119
200	9.86e-3		0.120
300	0.0107		0.125
400	0.0114		0.127
500	0.0122		0.130
600	0.0129		0.133
700	0.0138		0.135
800	0.0144		0.137
900	0.0150		0.137

7. Aluminum, Type 1100 [4.4]

Temperature (°F)	K (Btu/min-in-°F)	ρ (lb_m/in^3)	C_p (Btu/lb_m-°F)
70	0.185		0.214
100	0.183		0.216
150	0.181		0.219
200	0.178		0.222
250	0.177	0.098	0.224
300	0.175		0.227
350	0.174		0.229
400	0.173		0.232
774	0.173(*)		0.232*

* For aluminum Type 1100 and aluminum based neutron poison material, the calculated maximum temperatures do not exceed 774°F during blocked vent conditions. The assumption of constant conductivity value at 400°F for temperatures up to 774°F is justified since, for pure aluminum, the conductivity change is approximately 2% for range of 400°F – 774°F [4.19]. Therefore, this small change would have a negligible impact on thermal results.

8. Aluminum, Type 6061 (used for transition rails only) [4.4]

Temperature (°F)	K (Btu/min-in-°F)	ρ (lb_m/in^3)	C_p (Btu/lb_m-°F)
70	0.133		0.213
100	0.135		0.215
150	0.136		0.218
200	0.138		0.221
250	0.139	0.098	0.223
300	0.140		0.226
350	0.141		0.228
400	0.142		0.230
633	0.142(*)		0.230(*)

(*) Assumed values.

9. Aluminum Based Neutron Poison (from Section M.4.3)

Temperature (°F)	K (Btu/min-in-°F)	ρ (lb_m/in^3)**	C_p (Btu/lb_m-°F)**
68	0.120		0.214
212	0.144		0.222
482	0.148	0.098	0.232
572	0.148		0.232
774	0.148(*)		0.232(*)

(*) Assumed values.

(**) Assumed to be the same as aluminum.

10. Air [4.5]

Temperature (°F)	K (Btu/min-in-°F)	ρ (lb_m/in^3)	C_p (Btu/lb_m-°F)
71	2.075E-5	4.323e-5	0.240
107	2.199E-5	4.051e-5	0.241
206	2.528E-5	3.443e-5	0.242
314	2.869E-5	2.963e-5	0.243
404	3.139E-5	2.656e-5	0.245
512	3.447E-5	2.361e-5	0.248
602	3.693E-5	2.159e-5	0.251
692	3.929E-5	1.991e-5	0.253
764	4.114E-5	1.875e-5	0.256
800	4.203E-5	1.823e-5	0.257

11. Helium [4.6]

Temperature (°F)	K (Btu/min-in-°F)	ρ (lb_m/in^3)	C_p (Btu/lb_m-°F)
200	1.361E-4	4.81e-6	1.240
300	1.493E-4	4.18e-6	
400	1.635E-4	3.69e-6	
500	1.793E-4	3.31e-6	
600	1.949E-4	2.99e-6	
700	2.094E-4	2.74e-6	
800	2.232E-4	2.52e-6	

M.4.3 Specifications for Components

The thermal conductivity of the neutron poison plates must be verified by testing. The neutron poison plates must have the following minimum thermal conductivity.

Temperature (°F)	Thermal Conductivity (Btu/min-in-°F)
68	0.120
212	0.144
482	0.148
572	0.148
774	0.148

M.4.4 Thermal Evaluation for Normal Conditions of Storage (NCS) and Transfer (NCT)

M.4.4.1 NUHOMS®-32PT DSC Thermal Models

The NUHOMS®-32PT DSC finite element models are developed using the ANSYS computer code [4.9]. ANSYS is a comprehensive thermal, structural and fluid flow analysis package. It is a finite element analysis code capable of solving steady state and transient thermal analysis problems in one, two or three dimensions. Heat transfer via a combination of conduction, radiation and convection can be modeled by ANSYS. Solid entities are modeled by SOLID70 Elements for 3-D models and PLANE55 elements for 2-D models.

M.4.4.1.1 NUHOMS®-32PT DSC Basket and Payload Model

The three-dimensional model (Figure M.4-5) represents the NUHOMS®-32PT DSC with all aluminum transition rails, and includes the geometry and material properties of the basket components, the basket rails, and DSC shell. The cross-section view is shown in Figure M.4-6. Each component of the basket (XM-19 grid, poison plates, aluminum plates, and aluminum transition rails) is modeled individually with SOLID70 elements. The gaps between adjacent basket components are also represented with SOLID70 elements with helium or air conductivity as appropriate. The material properties from Section M.4.2 are used for the fuel region. Within the model, heat is transferred via conduction through fuel regions, the poison plates, steel of the basket and the gas gaps between the poison plate and steel members. Generally, good surface contact is expected between adjacent components within the basket structure. However, to bound the heat conductance uncertainty between adjacent components owing to imperfect contact between the neutron poison material, aluminum and the basket grid structure, uniform gaps along the entire surfaces are assumed. This is a conservative assumption because, although there will be imperfect contact between the adjacent plates, they will be in contact with each other at most of the locations. Therefore, thermal resistance to heat flow from the fuel assembly out to the DSC surface is lower with the actual imperfect contact as compared with the modeled uniform gaps along the entire surfaces. The gaps used in the thermal analysis of the 32PT DSC are summarized in the table below and shown in the figure below.

Gap Number	Gap Location	Gap Size, Inches
1	DSC Shell and Transition Rails	0.08
2	Basket grid structural plates and adjacent rails, or aluminum or composite material poison plates	0.0075
3	Aluminum and composite material poison plates	0.00375
4	Between any two pieces of aluminum rails in axial direction	0.125
5	Aluminum block and XM-19 plate for R-90 rail	0.0075

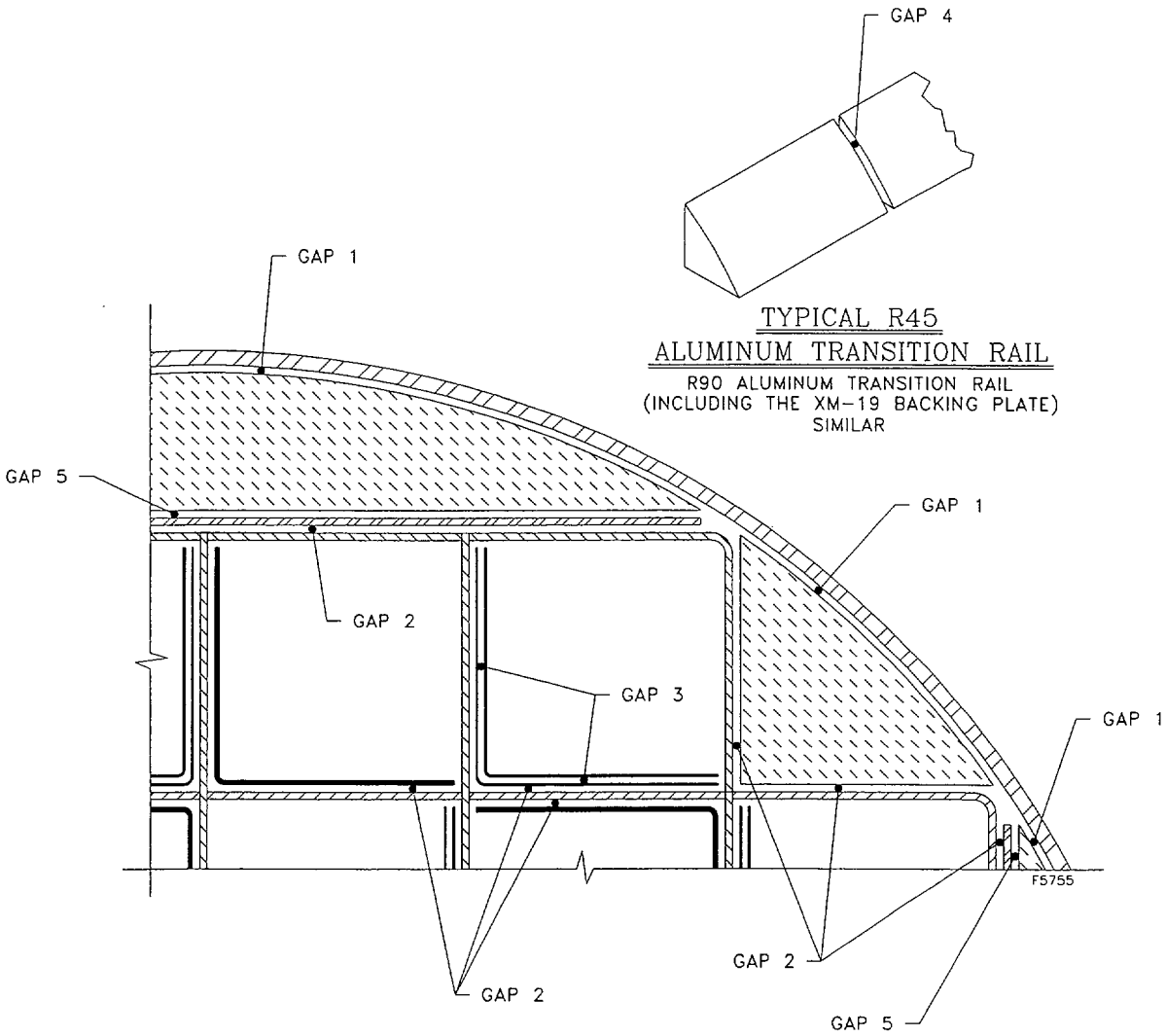

All heat transfer across the gaps is by gaseous conduction. Other modes of heat transfer i.e radiation and convection across the gaps are conservatively neglected. Heat is transferred through the basket support rails via conduction.

Each aluminum rail may be fabricated as a single piece or in separate segments (3 maximum). Rails consisting of three segments are assumed for thermal analyses. An axial gap of 0.125 in. is considered between any two pieces of aluminum rail. The elements representing the XM-19 grid structure include an adjustment to the conductivity to account for gaps between the basket components.

The 3-D model is extended to approximately half the length of the DSC cavity, or 83.8 in. to model the bottom half of the canister. A symmetry boundary is applied on the axial top of the model. The heat generations are applied over the active fuel, starting from 8.625 in. from the bottom of the fuel regions and extending all the way to the top of the model. The placement of the active fuel and the model size results in slight overprediction of temperatures since the symmetry boundary at (167/2-8.625)=74.875 in. from the beginning of active fuel is located well beyond half of the active fuel, or 141.8/2=70.9 in., where peak temperatures would be expected. Active length of B&W 15x15 assembly is shorter than that of WE 14x14 assembly. Therefore using the active length of B&W assembly results in higher heat generating rates in the model, which is conservative. In addition, active fuel of WE 14x14 assembly begins about 4" from the bottom of fuel assembly. Shifting the active fuel length to 8.625" from the bottom, shifts the active fuel length away from regions of dropping DSC shell temperature in the model. This is conservative, since being away from the regions of dropping DSC shell temperatures causes higher fuel cladding temperature. Longer DSC cavity configurations (32PT-L100 and 32PT-L125) provide larger radial surface areas for heat dissipation and are therefore bounded by the shorter cavity (32PT-S100 and 32PT-S125) DSC configurations.

M.4.4.1.2 Mesh Sensitivity Study

The 32PT DSC model described above is based on a 14x14 mesh for the cross section of each fuel assembly. A sensitivity study was performed with fuel mesh sizes of 12x12 and 16x16. The results show that convergence is achieved with a 14x14 mesh and the maximum fuel cladding temperature change is less than 1°F with a 16x16 mesh. Hence the 14x14 mesh size model is mesh insensitive.

M.4.4.1.3 Boundary Conditions for the DSC Basket Model

For the DSC shell near the end (where the shield plug is located), a linear decrease in the temperature to the end is assumed. The temperatures at the end of the cylindrical shell are assumed to be 90% (based on degrees Rankine) of the temperature in the active fuel region. This assumption is reasonable for the normal and off-normal storage and transfer cases because the heat generating region is 8.675" from the bottom cover plate. The DSC shell temperature drop from the active fuel region to the bottom cover plate is expected to be exponential because the metal on the end of the fuel assembly should thermally behave as a fin. An exponential drop would result in lower temperatures and thus more axial heat transfer. Therefore, the linear decrease is considered reasonable.

To determine the sensitivity of the 32PT DSC thermal model to the variation in the assumed boundary conditions at the axial periphery of the model (the cold end of the DSC), two alternate configurations are evaluated. Alternate No. 1 assumes the same DSC shell temperature profile as described above, but extended it to the entire DSC length. No change was made to the manner in which the DSC end was modeled (a linear temperature distribution between T_{top}, T_{side} and T_{bottom}

was modeled). Alternate No. 2 is similar to Alternate No. 1 but applied adiabatic boundary condition at the DSC end. The results show that the variations in the boundary conditions (at the cold end of the DSC) have a negligible impact on the heat transfer within the hottest region of the DSC and on the maximum fuel cladding temperature.

M.4.4.1.4 Heat Generation for the the DSC Basket Model

Heat generation is calculated based on the dimensions of the fuel and basket. The heat is assumed to be distributed evenly radially through the 8.7 in. square nominal fuel cell opening. Axial variations are accounted for in ANSYS by using the peaking factors in Figure M.4-4 along the active length of the PWR fuel assembly. Heat generation rates with the corresponding peaking factors are applied according to the decay heat load zoning configurations 1 through 3 given in Figure M.4-1, Figure M.4-2, and Figure M.4-3.

The equation below shows a typical calculation for peak heat generation (for 1.2 kW heat load) based on these peaking factors.

$$\dddot{q} = \frac{1.2kW \cdot 1.108 \cdot 3414 \frac{Btu/hr}{kW} \cdot \frac{1hr}{60\min}}{(8.7in)^2 \cdot 141.8in} = 7.049e-3 \frac{Btu}{\min \cdot in^3}$$

A peaking factor is applied to the base heat generation rate based on axial location of each element within 12 zones of the active fuel region (a half-length model). The volumetric heat generation multiplied by the average peaking factor of each zone is then used in the ANSYS models.

An example of the ANSYS input file routine, which applies the decay heat load for outer fuel assemblies is shown in Section M.4.11.1.

The normal conditions of storage are used for the determination of the maximum fuel cladding temperature, basket component temperatures, NUHOMS®-32PT DSC internal pressure and thermal stresses. The 10CFR Part 71.71(c) insolation averaged over a 24-hour period is used as steady state boundary condition.

M.4.4.1.5 Thermal Model of DSC in Horizontal Storage Module

The methodology used to calculate the HSM concrete and DSC shell temperatures with 32PT DSC is the same as that used for the NUHOMS®-24P DSC design described in FSAR Section 8.1.3. The axial location of the cross-section is the mid-section of the HSM, which also corresponds to the mid-section of the DSC at the approximate center of the active fuel.

There are two inlet and two outlet vents at each of the two sidewalls of the HSM. The location of these vents is designed such that it results in nearly uniform natural circulation flow patterns around the heat-generating region of a fuel assembly. The methodology given in Section 8.1.3 is used to calculate bulk air temperatures within the HSM. Note that bulk air temperatures are based on the conservative assumption of 100% of the heat removal from the DSC surface by convection ignoring any heat removal by radiation to the heat shield and concrete. These conservative assumptions

provide reasonable assurance that the selected cross-section of the HSM/DSC results in hottest temperatures.

To determine the temperature distribution on the surface of the DSC during storage, a two-dimensional ANSYS model of the cross section of the HSM with loaded DSC is used to represent the NUHOMS®-32PT system (Figure M.4-7). Solid entities are modeled in ANSYS by PLANE55 two-dimensional thermal elements. Radiation within the HSM is modeled in ANSYS by MATRIX50 super elements.

The decay heat from the payload is modeled as a uniform heat flux on the inner surface of the DSC shell. Heat from the DSC surface dissipates via natural convection to the air within the HSM and via radiation to the HSM heat shield and walls. Heat dissipates from the HSM heat shield via radiation to walls and then via conduction through the walls of the HSM, via convection to the HSM air and via convection and radiation from the HSM outer surfaces to the ambient environment.

There are two length configurations for the NUHOMS®-32PT DSC: Short (186.2 inches long) and Long (192.2 inches). The NUHOMS® HSM can accommodate DSCs with lengths from 186.05 to 195.92 inches. The shorter HSM and shorter 32PT DSC is used to calculate the maximum HSM concrete temperatures. This configuration is conservative in calculating HSM concrete temperatures because it has higher thermal resistance to the air flow compared to the configuration with the longer HSM and longer 32PT DSC.

M.4.4.1.6 Transfer Cask (TC) Thermal Model

To determine the temperature distribution on the surface of the DSC during transfer operations, a two-dimensional model of the cross-section of the TC with a loaded 32PT DSC was created using ANSYS.

The 32PT DSC is qualified for transfer in the OS197/OS197H transfer cask. The geometry of the transfer cask used in the thermal analysis is identical for both OS197 and OS197H casks.

The ANSYS model shown in Figure M.4-8 represents a two-dimensional slice of the OS197 cask at the axial centerline. The following dimensions from Appendix E are used for the model:

- The inner diameter of the inner liner is 68",
- The thickness of the inner liner is 0.5" and it is made of stainless steel (SA-240, Type 304),
- The thickness of the lead is 3.56",
- The air gap between lead and structural shell is assumed to be 0.03125",
- The thickness of the structural shell portion is 1.5". This shell is made of stainless steel (SA-240, type 304) material,
- The neutron shield is water, with 24 stainless steel stiffeners which connect the structural shell to the neutron shield panel. Each stiffener consists 0.12" thick plate and is made up of two side plates 4.25" long oriented at 45° that connect the structural shell to the neutron shield panel, and,

a top side 1.00" long welded to the neutron shield panel. The thickness of the neutron shield region is 3". The stiffener material is SA-240, type 304,

- The neutron shield panel is constructed of SA-240, Type 304 material and is 0.1875" thick, and
- DSC shell thickness is 0.5".

The material properties are taken from Section 8.1 with the exception of the calculation of the effective conductivity of water within the neutron shield, which is calculated in Section M.4.9.

The neutron shield region of the cask model is broken into 24 angular segments 7.5 degrees each.

For each angular segment, the bounding k_{eff} value (as calculated in Section M.4.9) is applied to the ANSYS model.

Radiation is modeled by overlaying surface elements and using the /AUX12 processor to compute view factors to the environment with SURF151 elements in ANSYS. The emissivity of the outer surface is 0.587 for unfinished steel [4.7]. An absorptivity of the outer surface is 0.587. Radiation is also modeled between the DSC shell surface and the cask inner surface with unfinished steel emissivities of 0.587 [4.7] using the /AUX12 processor in ANSYS.

The DSC shell is offset in the model to provide a realistic approximation of the horizontal orientation gap thicknesses at the top and bottom of the DSC. The DSC-cask air gap thicknesses are assumed to be 0.702" at the top and 0.108" at the bottom based on a nominal cask inner diameter of 68" and a nominal shell outer diameter of 67.19". The DSC rests on two cask rails that are located 18.5° from vertical downward below the DSC. A thickness of 0.12" is used for the cask rails. The gap at the bottom closes from 0.12" to 0.105".

Insolation is applied to the top half of the model. The insolation considered is 123 Btu/hr-ft^2, which is consistent with the maximum insolation used for storage in the HSM. The absorptivity of 0.587 was applied to the outer cask surface.

The convection to the ambient is conservatively based on the average film temperature for convection coefficient evaluation in the ANSYS model.

The heat is applied to the model as a heat flux on the inner surface of the DSC using SURF151 elements in ANSYS. The heat transfer through the ends of the DSC is conservatively neglected in calculating the heat flux. The heat flux is calculated based on DSC shell length as:

$$\ddot{q} = \frac{24kW \cdot 3414 \frac{\text{Btu}/\text{hr}}{\text{kW}}}{60\frac{\text{min}}{\text{hr}} \cdot (\pi \cdot 66\text{in} \cdot 186.2\text{in})} = 0.0354 \frac{\text{Btu}}{\text{min} \cdot \text{in}^2}$$

A second set of cases with 22.4 kW total heat load (and 0.0330 BTU/min.in^2) was run in order to support heat load zoning configuration #3.

An example of ANSYS input file routine that overlays surface effect elements on the top outside surface of the cask is included in Section M.4.11.2.

M.4.4.1.7 Boundary Conditions, Storage

Normal Conditions of Storage analyses of the NUHOMS®-32PT DSC within the HSM are carried out for the following ambient conditions:

- Maximum normal ambient temperature of 100°F with insolation,
- Minimum normal ambient temperature of 0°F without insolation, and
- Long-term average maximum ambient temperature of 70°F, with insolation.

The HSM thermal model described in Section M.4.4.1.5 provides the surface temperatures of the DSC shell. These temperatures are applied as boundary conditions to the DSC shell in the basket and payload models in Section M.4.4.1.1 which calculate the temperature distribution in the basket components and fuel.

M.4.4.1.8 Boundary Conditions, Transfer

In accordance with Section 8.1, analyses of the NUHOMS®-32PT DSC within the TC are performed for the following ambient conditions:

- Maximum normal ambient temperature of 100°F with insolation, and
- Minimum normal ambient temperature of 0°F without insolation.

The maximum calculated DSC temperatures using the TC thermal model described in Section M.4.4.1.6, are conservatively applied to the exterior surface of the DSC in the DSC/Basket/Payload finite element model in Section M.4.4.1.1.

M.4.4.2 Maximum Temperatures

M.4.4.2.1 Fuel Cladding

M.4.4.2.1.1 Long-Term Storage Temperatures

The maximum fuel cladding temperatures for long-term storage with 70°F ambient condition are evaluated for each of the three decay heat load zoning configurations and compared with the corresponding fuel cladding temperature limit for long-term storage in Table M.4-1.

The conservatisms in the cladding temperature limit method and conservative assumptions included in the calculation of maximum cladding temperatures are described below:

1) Credit for any convection in the DSC basket cavity is not taken.

2) Conservative gaps are assumed between basket component plates even though adjacent basket components are connected to each other by mechanical fasteners.

3) Credit for any radiation in the gaps between the adjacent basket components is not taken.

Based on these conservatisms, there is a higher margin in the calculated maximum cladding temperatures than those shown in Table M.4-1. Thus, there is reasonable assurance that the cladding will maintain its integrity during storage conditions.

M.4.4.2.1.2 Short-Term Event Temperatures

The short-term events are defined in Section M.4.1 for storage and transfer. The results are reported for heat load zoning configuration 1, 2, and 3 which yield the highest fuel cladding temperatures. The maximum fuel cladding temperatures for short-term normal conditions of storage and transfer are given in Table M.4-2.

M.4.4.2.1.3 DSC Basket Material Temperatures

The maximum and minimum temperatures of the basket assembly components for normal conditions of storage and transfer for heat load zoning configurations 1, 2 and 3 are listed in Table M.4-3, Table M.4-4, and Table M.4-5, respectively. The minimum component temperatures reported in these tables represent the minimum temperature for those components at the hottest radial cross section, not the minimum component temperature in the entire basket. The maximum basket temperature distributions for configuration 3 during normal conditions of storage and transfer are presented in Figure M.4-9 and Figure M.4-10, respectively. The temperature distribution from the bottom to the top of the DSC at the hottest cross-section is shown in Figure M.4-17 for 70°F ambient storage case.

M.4.4.3 Minimum Temperatures

Under the minimum temperature condition of 0°F ambient, the resulting DSC component temperatures will approach 0°F if no credit is taken for the decay heat load. Since the DSC materials, including confinement structures, continue to function at this temperature, the minimum temperature condition has no adverse effect on the performance of the NUHOMS®-32PT DSC.

M.4.4.4 Maximum Internal Pressures

M.4.4.4.1 Pressure Calculation

This section describes the pressure calculations used to determine maximum internal pressures during storage and transfer within the NUHOMS®-32PT DSC and basket when loaded with a payload of worst case B&W 15x15 fuel assemblies with a maximum burnup of 45 GWd/MTU. The limiting fuel assembly type considered in this evaluation is the B&W 15 x 15 assembly. The fission gasses produced by the WE 17x17 are slightly higher than those from the B&W 15x15, but the B&W 15x15 fuel assembly has the highest heavy metal and fuel assembly weight and therefore displaces the most free volume relative to all the other assembly types considered in Chapter M.2.

The calculations include the DSC free volume, the quantities of DSC backfill gas, fuel rod fill gas, and fission products and the average DSC cavity gas temperature. The 32PT-S100, 32PT-S125, 32PT-L100 and 32PT-L125 canister configurations are considered. The 32PT-L100 and 32PT-L125 DSC internal pressure evaluations also include the contribution due to BPRAs. The internal pressures are then calculated using:

$$P = \frac{nRT}{V}$$

where:

n = Total number of moles of gases,

R = Universal gas constant,

T = Gas temperature (°R),

V = Gas volume, and

P = Internal pressure.

M.4.4.4.2 Free Volume

M.4.4.4.2.1 DSC Cavity

The DSC Cavity free volumes are shown below:

Canister Type	32PT-S100	32PT-S125	32PT-L100	32PT-L125
Cavity Volume (in^3)	583,580	574,977	604,225	595,623
Basket Volume (in^3)	176,312	173,689	182,613	180,008
Fuel Volume (in^3)	181,126	181,126	185,518	185,518
Free Volume (in^3)	226,141	220,163	236,095	230,097

M.4.4.4.3 Quantity of Helium Fill Gas in DSC

The DSC free volume is assumed to be filled with 3.5 psig (18.2 psia) of helium. The maximum temperatures from the 70°F ambient storage case are used to estimate the number of moles of helium backfill.

The average long-term helium fill temperature for the worst case payload, 449°F (909°R) is used. Using the ideal gas law, the quantity of helium in each DSC is calculated and the results are presented in Table M.4-6.

M.4.4.4.4 Quantity of Fill Gas in Fuel Rod

The volume of the helium fill gas in a B&W 15x15 fuel pin at cold, unirradiated conditions is 1.326 in^3, and there are 208 fuel pins in an assembly. The maximum fill pressure is 415 psig (429.7 psia)

and the fill temperature is assumed to be room temperature (70°F or 530°R). The quantity of fuel rod fill gas in 32 fuel assemblies is:

$$n_{he} = \frac{(429.7\,psia)(6894.8\,Pa/psi)(32 \cdot 208 \cdot 1.326\,in^3)(1.6387x10^{-5}\,m^3/in^3)}{(8.314\,J/mol \cdot K)(530°R)(5/9\,K/°R)}$$

$$n_{he} = 175.0\,g-moles$$

Based on NUREG 1536 [4.10], the maximum fraction of the fuel pins that are assumed to rupture and release their fill and fission gas for normal, off-normal and accident events is 1, 10 and 100%, respectively. 100% of the fill gas in each ruptured rod is assumed to be released. The amount of helium fill gas released for each of these conditions is summarized below.

Case	Percentage of Rods Ruptured	Moles of Helium Fill Gas Released
Normal	1	1.75
Off-Normal	10	17.50
Accident	100	175.0

M.4.4.4.5 Quantity of Fission Product Gases in Fuel Rod

The B&W 15x15 fuel assembly used in the pressure calculations is assumed to be burned to 45,000 MWd/MTU, which is the highest burnup proposed for the NUHOMS®-32PT configuration. The maximum burnup creates a bounding case for the amount of fission gases produced in the fuel rod during reactor operation. The amounts of tritium, krypton-85 and xenon-131m at STP for each assembly are summarized below.

Isotope	Volume (liters/assy)	Volume (in^3/assy)
Tritium (H^3)	0.26	16
Kr^{85}	60.4	3,686
Xe^{131m}	547	33,380
Total	607.7	37,081

The total fission gas volume for a fuel assembly is equal to 607.7 liters (37,081 in^3). The total amount of fission gas products produced is calculated using 32°F as:

$$n_{fg} = \frac{(32)(14.7)(6894.8\,Pa/psi)(37{,}081\,in^3)(1.6387x10^{-5}\,m^3/in^3)}{(8.314\,J/mol \cdot K)(460°R + 32°F)(5/9\,K/°R)}$$

$$n_{fg} = 867\,g-moles$$

The amount of fission gas released into the DSC cavity for normal, off-normal and accident condition cases assuming a 30% gas release from the fuel pellets and a 1%, 10%, and 100% rod rupture percentage, respectively, is summarized below.

Case	Percentage of Rods Ruptured	Moles of Fission Gas Released
Normal	1	2.6
Off-Normal	10	26.0
Accident	100	260

M.4.4.4.6 Quantity of Gas in Control Components (BPRAs)

The 32PT-L100 and 32PT-L125 DSC configurations may include BPRAs. In the NUHOMS®-32PT DSC, a maximum of 16 BPRAs per DSC are allowed. These BPRAs have an initial helium fill of 14.7 psia, and if 100% of the boron is consumed, and 30% released into the DSC, a total of 53.8 *(16/24) = 35.9 g-moles of gas could be released to the DSC assuming 100% cladding rupture (the 53.8 g-moles is based on 24 BPRAs in the 24P DSC; from Appendix J, Section J.4).

The percentage of BPRA rods ruptured during normal, off-normal and accident conditions is assumed to be 1%, 10% and 100%, respectively, similar to the assumptions for the fuel rod rupturing. The maximum amount of gas released to the DSC cavity from the BPRAs for normal, off-normal and accident conditions is given below.

Case	Percentage of Rods Ruptured	Moles of Fission Gas Released per DSC from BPRAs
Normal	1	0.359
Off-Normal	10	3.59
Accident	100	35.9

The maximum average helium temperature for normal conditions of storage and transfer occurs when the 32PT DSC is in the TC with an ambient temperature of 100°F and maximum insolation. This case bounds the 100°F ambient case in the HSM. In addition the maximum pressure will occur with the 45,000 MWd/MTU burnup fuel so that lesser burnups will be enveloped by this calculation. The average helium temperature is 545°F (1005°R), however 550°F (1,010°R) is conservatively used. The maximum normal operating condition pressures are summarized in Table M.4-7.

M.4.4.5 Maximum Thermal Stresses

The maximum thermal stresses during normal conditions of storage and transfer are calculated in Section M.3.

M.4.4.6 Evaluation of Cask Performance for Normal Conditions

The NUHOMS®-32PT DSC shell and basket are evaluated for the calculated temperatures and pressures in Section M.3. The maximum fuel cladding temperatures are well below the allowable long-term fuel temperature limits and the short-term limit of 752°F (400°C). The maximum DSC internal pressure remains below 15.0 psig during normal conditions of storage and transfer. Based on the thermal analysis, it is concluded that the NUHOMS®-32PT DSC design meets all applicable normal condition thermal requirements.

M.4.5 Thermal Evaluation for Off-Normal Conditions

The NUHOMS®-32PT system components are evaluated for the extreme ambient temperatures of -40°F (winter) and 117°F (summer). Should these extreme temperatures ever occur, they would be expected to last for a very short duration of time. Nevertheless, these ambient temperatures are conservatively assumed to occur for a significant duration to result in a steady-state temperature distribution in the NUHOMS®-32PT system components.

The 117°F off-normal ambient temperature is considered extreme in a given 24-hour period. It is reasonable to consider a 24-hour average given the large thermal mass of the canister, HSM and transfer casks. The temperature of the fuel is not expected to vary with temperature cycles over 24-hour periods.

In order to calculate a conservative 24-hour average temperature given a maximum temperature, a minimum daily range must be specified. From Table 1 in Chapter 24 of [4.20], the minimum mean daily temperature range in the contiguous United States with a maximum summer ambient above 110°F is 27°F in Needles, California. For the 117°F ambient condition, [4.20] is used to derive a daily average for the steady-state condition with a mean range of 27°F. The mean range is defined as the difference between the average daily maximum and the average daily minimum during the warmest month of the year. The use of a mean range is appropriate since the HSM and DSC would take several days to heat up to steady-state conditions in such a scenario.

Reference [4.20] gives a method for calculating the temperature variations in a day, given a daily range in Chapter 26, Table 3. Percentages ranging between 0 and 100% of the mean range are given as a function of hour in the day. The temperature variation is calculated using this methodology for a maximum temperature of 117°F with daily range of 27°F. A sample calculation shows the expected temperature at 8 o'clock in the morning:

$$T_{amb} = 117 - 0.84 \cdot 27 = 94.3°F$$

The remaining calculated temperatures are presented in the table below.

Ambient Temperature Variation on 117°F Ambient Day.		
Time, hour	**% Daily Range**	**T, °F**
1	87	93.5
2	92	92.2
3	96	91.1
4	99	90.3
5	100	90.0
6	98	90.5
7	93	91.9
8	84	94.3
9	71	97.8
10	56	101.9
11	39	106.5
12	23	110.8
13	11	114.0
14	3	116.2
15	0	117.0
16	3	116.2
17	10	114.3
18	21	111.3
19	34	107.8
20	47	104.3
21	58	101.3
22	68	98.6
23	76	96.5
24	82	94.9

The corresponding average is 101.8°F. 107°F was used as the ambient air temperature in the stead-state analyses to be conservative for the maximum off-normal condition.

M.4.5.1 Off-Normal Maximum/Minimum Temperatures during Storage

The thermal performance of the NUHOMS®-32PT DSC within the HSM under the extreme minimum ambient temperatures of -40°F with no insolation and 117°F with maximum insolation are evaluated with heat load zoning configurations 1, 2 and 3.

M.4.5.1.1 Boundary Conditions, Storage

Off-normal conditions of storage analyses of the NUHOMS®-32PT DSC within the HSM includes:

- Maximum off-normal ambient temperature of 117°F with insolation, and
- Minimum off-normal ambient temperature of -40° F without insolation.

The HSM thermal model described above provide the surface temperatures that are applied to the DSC, basket and payload model.

M.4.5.2 Off-Normal Maximum/Minimum Temperatures during Transfer

The thermal performance of the NUHOMS®-32PT DSC during transfer under the extreme minimum ambient temperature of 0°F with no insolation and 117°F with maximum insolation, and decay heat load configurations 1, 2 and 3 are examined. For transfer operations when ambient temperatures exceed 100°F up to 117°F, a solar shield is used.

M.4.5.2.1 Boundary Conditions, Transfer

In accordance with Section M.4.4.1.6, analyses of a 32PT DSC within the TC are performed for the following ambient conditions:

- Maximum normal ambient temperature of 117°F with solar shield in place, and
- Minimum off-normal extreme ambient temperature of 0°F without insolation.

These analyses determine maximum DSC surface temperatures. The maximum calculated DSC temperatures are applied to the exterior surface of the DSC in the DSC/basket/payload finite element model.

M.4.5.3 Off-Normal Maximum and Minimum Temperatures During Storage/Transfer

According to the NUHOMS® CoC 1004, Technical Specification 1.2.4, "TC/DSC Transfer Operations at High Ambient Temperatures" for transfer operations, when ambient temperatures exceed 100°F up to 125°F, a solar shield shall be used to provide protection against direct solar radiation.

The thermal performance of the DSC during transfer operations when the DSC is in the transfer cask without the sunshade at an ambient temperature of 100°F is limiting and bounds the maximum off-normal 117°F transfer case with sunshade. This is demonstrated by results provided in Table M.4-8 and Table M.4-2.

A comparison of the thermal analysis results for 32PT-DSC during transfer operations for the cases of 100°F ambient temperature without sunshade and 117°F ambient temperature with sunshade shows that the maximum fuel cladding temperatures are 720°F (Table M.4-2) and 715°F (Table M.4-8), respectively.

M.4.5.3.1 Fuel Cladding

The results are reported in Table M.4-8 for heat load zoning configurations 1, 2 and 3 which yield the highest fuel cladding temperatures.

M.4.5.3.2 DSC Basket Materials

The maximum and minimum temperatures of the basket assembly for off-normal conditions of storage and transfer for heat load zoning configurations 1, 2 and 3 are listed in Table M.4-9, Table M.4-10, and Table M.4-11, respectively. The minimum temperatures reported for each component

are not the minimum absolute component temperature in the entire basket. The minimum component temperatures reported in these tables represent the minimum temperature for those components at the hottest radial cross section. The bounding basket temperature distributions for heat load zoning configuration 3 off-normal conditions of storage and transfer are presented in Figure M.4-11 and Figure M.4-12, respectively.

M.4.5.4 Off-Normal Maximum Internal Pressure During Storage/Transfer

The off-normal condition maximum pressure calculation also considers the DSC in the TC at 100°F ambient. This case bounds the case in which the DSC is in the HSM with 117°F ambient and the 117°F TC case with the sunshade in place. The average helium temperature is 545°F (1005°R), however, 550°F (1010°R) is conservatively used. Per NUREG 1536, the percentage of fuel rods ruptured for off-normal cases is 10%.

A summary of the maximum off-normal operating pressures for the various 32PT DSC configurations are presented in Table M.4-12.

M.4.5.5 Maximum Thermal Stresses

The maximum thermal stresses during off-normal conditions of storage and transfer for the NUHOMS®-32PT DSC are calculated in Section M.3.

M.4.5.6 Evaluation of Cask Performance for Off-Normal Conditions

The NUHOMS®-32PT DSC shell and basket are evaluated for calculated temperatures and pressures in Section M.3. The maximum fuel cladding temperatures are well below the allowable fuel temperature limit of 752°F (400°C) for transfer and 1058°F (570°C) for storage conditions. The maximum DSC internal pressures remain below 20.0 psig during off-normal conditions of storage and transfer. The pressures and temperatures associated with off-normal conditions in the NUHOMS®-32PT DSC design meet all applicable off-normal thermal requirements.

M.4.6 Thermal Evaluation for Accident Conditions

Since the NUHOMS® HSMs are located outdoors, there is a remote possibility that the ventilation air inlet and outlet openings could become blocked by debris from such unlikely events as floods and tornadoes. The NUHOMS® HSM system design features such as the perimeter security fence and redundant protected location of the air inlet and outlet openings reduces the probability of occurrence of such an accident. Nevertheless, for this conservative generic analysis, such an accident is postulated to occur and is analyzed.

During transfer under maximum ambient temperature and insolation, the loss of the sun shield and the liquid neutron shield in the TC represents the controlling transfer case.

It is determined in Section 3.3.6 that the HSM and DSC contain no flammable material and the concrete and steel used for their fabrication can withstand any credible fire accident condition. Fire parameters are dependent on the amount and type of fuel within the transporter and the fire accident condition shall be addressed within site-specific applications. Licensees are required to verify that loadings resulting from potential fires and explosions are acceptable in accordance with 10CFR72.212(b)(2). The hypothetical fire evaluation for the NUHOMS®-32PT system is included in Section M.4.6.3.

M.4.6.1 Blocked Vent Accident Evaluation

For the postulated blocked vent accident condition, the HSM ventilation inlet and outlet openings are assumed to be completely blocked for a 40-hour period concurrent with the extreme off-normal ambient condition of 117°F with insolation.

For conservatism, a transient thermal analysis is performed using the 3-D model developed in Section M.4.4.1, for heat load zoning configurations 1, 2, and 3. Heat load zoning configuration 3 envelopes the temperature results for heat load zoning configurations 1 and 2. When the inlet and outlet vents are blocked, the air surrounding the DSC in the HSM cavity is contained (trapped) in the HSM cavity. The temperature difference between the hot DSC surface and the surrounding cooler heat shield and concrete surfaces in the HSM cavity will result in closed cavity convection. This closed cavity convection in the HSM cavity is accounted for by calculating an effective conductivity of air. The HSM cavity is modeled as a combination of few separate enclosures as described below:

Enclosure 1 includes the HSM cavity within 0° to 90° sector limited by DSC shell surface, vertical and top horizontal heat shield surfaces. Enclosure 2 includes the HSM cavity within -90° to 0° sector limited by DSC shell, vertical heat shield and space under the bottom line of DSC shell surfaces. Enclosure 3 includes bottom of Enclosure 2 and inside surfaces of HSM side wall and floor. Enclosure 4 includes horizontal space limited by concrete roof surface and top horizontal heat shield surface. Enclosure 5 is vertical space limited by inside surface of concrete side wall and vertical heat shield. To be conservative, the closed cavity convection in Enclosure 3 is neglected and Enclosure 2 was assumed to be the average of Enclosure 1 and 3 (9.09 + 1)/2 = 5.045.

For zones of closed cavity convection to adjust a thermal conductivity of air k_{air} to account convection an empirical generalized formula was applied [4.12]:

$$\frac{k_{eff\ air}}{k_{air}} = C \cdot Ra^{n} \cdot \left(\frac{L}{\delta}\right)^{m}$$

where Ra - Raleigh number, L, δ- length and width of an enclosure, C, n, m - constants, to be defined by flow circumstances (Ra) and geometry (L/δ).

Iterative process is used to determine the mean temperatures used in air property calculations. The results are given below:

Enclosure in HSM Cavity	δ, in	L, in	$\overline{T}_{hot}$, °F	$\overline{T}_{cold}$, °F	Gr_{δ}	Pr	C	n	m	$k_{eff\ air}/k_{air}$
1	9.95	63	561	428	8.91e+6	0.68	0.4	0.2	0	9.09
4	2	40	432	319	1.55e+5	0.683	0.11	0.29	0	3.149
5	3	72	393	271	7.15e+5	0.685	0.197	0.25	-0.111	3.662

These effective conductivities are used in the ANSYS model to determine the transient DSC shell temperatures during blocked vent accident. These DSC shell temperatures are then used as boundary conditions to calculate the basket and fuel cladding temperatures during blocked vent transient.

The calculated temperature distribution within the hottest cross section is shown in Figure M.4-13 and the time history plot is shown in Figure M.4-15. Summaries of the calculated NUHOMS®-32PT DSC cladding and component temperatures are listed in Table M.4-13 and Table M.4-14, respectively.

M.4.6.2 Transfer Accident Evaluation

The postulated transfer accident event consists of transfer in the TC in a 117°F ambient environment with loss of the solar shield and the liquid neutron shielding. Heat load zoning configurations 1, 2 and 3 were evaluated. Heat load zoning configuration 1 bounded the results of configurations 2 and 3. The results for heat load zoning configuration 1 are shown in Table M.4-13.

M.4.6.3 Hypothetical Fire Accident Evaluation

For the postulated worst case fire accident, a 300 gallon diesel fire is simulated for a NUHOMS®-32PT DSC with a decay heat load of 24 kW during transfer in the TC. This bounds fire scenarios associated with loading operations and storage within the HSM due to the large thermal mass of the HSM and the HSM vent configuration which provides protection for the DSC and payload.

Steady-state, off-normal conditions are assumed prior to the fire, which consist of a 117°F ambient condition without solar shield in place on the TC but water filled neutron shield. The fire has a temperature of 1,475°F, and an emittance of 0.9 and a duration of 15 minutes based on the 300 gallon diesel fuel source and complete engulfment of the TC for the duration of the fire. The gap between lead shielding and structural shell of the transfer cask is conservatively closed for the

duration of the fire in the model. Subsequent to the fire, the TC is subjected to 117°F ambient conditions with maximum insolation. Note that these hypothetical fire parameters are very conservative.

The fire transient analysis presented is based on very conservative assumptions. It is assumed that liquid neutron shield (water) is present throughout the 15-minute fire transient even though it is expected to be lost and replaced with air very early in the fire transient. This assumption maximizes the heat input from the fire to the canister because of the high conductivity of water compared to air. To maximize the canister temperature during the post-fire transient, it is assumed that water in neutron shield cavity is lost at the beginning of post-fire transient and replaced by air as the heat flow is now from canister to the ambient. The gap between lead shielding and structural shell of the transfer cask is kept open for the post fire transient.

The gaps included in the thermal model of the 32PT DSC basket are summarized in Section M.4.4.1.1. These gaps are not removed for calculating the cladding temperatures during accident conditions. The canister shell temperatures change by a negligibly small amount (<2°F) during fire transient. This change is small during fire transient as the canister is protected due to the large thermal mass of the transfer cask. This shows that heat input from the fire to the canister is not significant. Since the canister shell temperature is almost unchanged, the cladding temperatures during 15-minute fire transient also are almost unchanged. Therefore, the assumption of not removing the gaps during fire transient has negligible impact on the cladding temperatures.

The calculated temperature response of selected components in the TC and DSC during the first 2,000 minutes of the fire accident is shown in Figure M.4-14. A summary of the calculated maximum fire transient temperatures for these components is listed in Table M.4-16. The calculated maximum fire transient DSC surface temperature is 545°F, which is less than the transfer accident case maximum DSC temperature of 591°F calculated in Section M.4.6.2. Therefore, the NUHOMS®-32PT DSC temperatures and pressures calculated for the transfer accident case bound the hypothetical fire accident case.

M.4.6.4 Fuel Cladding and Basket Materials

The short-term events are defined in Section M.4.1 for storage and transfer conditions. The blocked vent results are reported for 40 hours. The transfer accident case results are reported at steady state conditions. The results are reported for heat load zoning configuration 3 for blocked vent transient and heat load zoning configuration 1 for transfer accident in Table M.4-13. The maximum and minimum temperatures of the basket assembly are listed in Table M.4-14. The minimum temperatures reported for each component are not the minimum absolute component temperature in the entire basket. The minimum component temperatures reported in this table represents the minimum temperature for those components at the hottest radial cross-section.

M.4.6.5 Maximum Internal Pressures

The maximum accident pressure condition for the DSC occurs during the transfer accident case with the loss of the sun shield and liquid neutron shielding in the TC under extreme ambient temperature conditions of 117°F and maximum insolation. For this transfer accident condition, the average helium temperature is 703°F (1,163°R). In accordance with NUREG 1536, 100% of the fuel pins

are assumed to rupture during this event. During the blocked vent case, the average gas temperature is 623°F. However, since no DSC drop events can occur in conjunction with a blocked vent event, the maximum fraction of fuel pins that can be ruptured is limited.

A summary of the maximum accident operating pressures for the various 32PT DSC configurations are presented in Table M.4-15.

M.4.6.6 Evaluation of Cask Performance During Accident Conditions

The temperatures in the NUHOMS® HSM and TC are bounded by the existing analyses because of the same heat load for the NUHOMS®-24P DSC design. The NUHOMS®-32PT DSC shell and basket are evaluated for calculated pressures and temperatures in Section M.3.

The maximum fuel cladding temperature of 863°F is below the short-term limit of 1058°F (570°C). The accident pressure in the NUHOMS®-32PT DSC of 101.7 psig remains below the accident design pressure of 105 psig. It is concluded that the NUHOMS®-32PT system maintains confinement during the postulated accident condition.

M.4.7 Thermal Evaluation for Loading/Unloading Conditions

All fuel transfer operations occur when the NUHOMS®-32PT DSC and TC are in the spent fuel pool. The fuel is always submerged in free-flowing pool water permitting heat dissipation. After fuel loading is complete, the cask and DSC are removed from the pool and the DSC is drained, dried, backfilled with helium and sealed.

M.4.7.1 Maximum Fuel Cladding Temperatures During Vacuum Drying

The loading condition evaluated for the NUHOMS®-32PT DSC is the heatup of the DSC before its cavity is backfilled with helium. This typically occurs during the performance of the vacuum drying operation of the DSC cavity with the Cask in the vertical configuration inside the fuel handling building, and the annulus between the Cask and the DSC full of water.

The vacuum drying of the DSC generally does not reduce the pressure sufficiently to reduce the thermal conductivity of the water vapor and air in the DSC cavity [4.22] and [4.23]. Therefore, air is assumed during vacuum drying operations. Radiation in the gaps within the basket and rail components is conservatively neglected. Analyses are performed to determine the transient heat-up during the vacuum drying condition.

A transient thermal analysis is performed using the three-dimensional model developed in Section M.4.4.1, decay heat loads for heat load zoning configuration 1, 2, and 3 and a maximum DSC temperature of 215°F. The initial temperature of the DSC, basket and fuel is assumed to be 215°F, based on the boiling temperature of the fill water. Table M.4-17 and Table M.4-18 provide the maximum calculated temperatures for the fuel cladding and basket components, respectively, for all three configurations. Figure M.4-16 provides the maximum fuel cladding temperatures during the vacuum drying transient. The maximum cladding temperature reached during vacuum drying after 33 hours is 678°F, which is below the limit of 752°F [4.24].

M.4.7.2 Evaluation of Thermal Cycling of Fuel Cladding During Vacuum Drying, Helium Backfilling and Transfer Operations

ISG-11 also states that thermal cycling is to be minimized and imposes a limit of 65°C (118°F) on thermal cycling (reduction in fuel clad temperature from previous peak temperature). The basis for the limit is that as the cladding temperature is reduced more than 65°C the concentration of hydrogen available for hydride reorientation becomes significant.

After completion of vacuum drying step, the DSC is backfilled with helium, with the Cask in the same configuration as described above and the annulus between the Cask and DSC filled with water. This case results in the lowest steady state fuel cladding temperature of 578°F during the DSC drying/backfilling operations. Thus, the maximum temperature difference for the fuel cladding during this drying and backfilling operations is (678 – 578) = 100°F. This temperature difference meets the thermal cycling criteria specified by ISG-11 [4.24].

It is expected that with a lower DSC decay heat load, the vacuum drying operation may require a longer time duration to meet the limit of Technical Specification 1.2.2. An additional evaluation is

performed to determine the sensitivity of the thermal cycling analysis of fuel cladding temperatures when loading a DSC with a payload of up to 8.4 kW decay heat load. The Cask configuration for drying, backfilling and transfer operations is identical to that described above except for the DSC heat load. Figure M.4-16 provides the maximum fuel cladding temperatures during the vacuum drying transient for this case. The maximum cladding temperature reached during vacuum drying after 38 hours is 592°F, which is well below the limit of 752°F [4.24]. This 8.4 kW case results in the lowest steady state fuel cladding temperature of 492°F during the helium backfilling operations. Thus, the maximum temperature difference for the fuel cladding during this drying and backfilling operations is (592-492) = 100°F. The results demonstrate that with a vacuum drying time limit of 38 hours for a DSC with up to 8.4 kW heat load, the design meets the ISG-11 [4.24] maximum fuel cladding temperature limit of 752°F as well as the maximum fuel cladding temperature difference limit of 117°F.

M.4.7.3 Reflooding Evaluation

For unloading operations, the DSC will be filled with the spent fuel pool water through the siphon port. During this filling operation, the DSC vent port is maintained open with effluents routed to the plant's off-gas monitoring system. The NUHOMS®-32PT DSC operating procedures recommend that the DSC cavity atmosphere be sampled first before introducing any reflood water in the DSC cavity.

When the pool water is added to a DSC cavity containing hot fuel and basket components, some of the water will flash to steam causing internal cavity pressure to rise. This steam pressure is released through the vent port. The procedures also specify that the flow rate of the reflood water be controlled such that the internal pressure in the DSC cavity does not exceed 20 psig. This is assured by monitoring the maximum internal pressure in the DSC cavity during the reflood event. The reflood for the DSC is considered as a Service Level D event and the design pressure of the DSC is 105 psig. Therefore, there is sufficient margin in the DSC internal pressure during the reflooding event to assure that the DSC will not be over pressurized.

The maximum fuel cladding temperature during reflooding event is significantly less than the vacuum drying condition owing to the presence of water/steam in the DSC cavity. The analysis presented in Section M.4.7.2 shows that the maximum cladding temperature during vacuum drying after 33 hours is 678°F. Hence, the peak cladding temperature during the reflooding operation will be less than 678°F.

To evaluate the effects of the thermal loads on the fuel cladding during reflooding operations, a conservative assumption of high maximum fuel rod temperature of 750°F and a low quench water temperature of 50°F are used.

The material properties, corresponding to a temperature of 750°F, are used in the evaluation:

Modulus of Elasticity, E (psi) = 11.1 x10^6 [from Figure 4 of 4.13]
Coefficient of thermal expansion, α, (in/in/°F) = 3.73 x 10-6 [4.14]
Poison's Ratio, ν, = 0.38 [4.15]
Yield Stress (irradiated), Sy, = 50,500 psi [4.13]

The fuel cladding is evaluated as a hollow cylinder with an outer surface temperature of T (50°F), and the inner surface temperature of T+ΔT (750°F) using [4.16] equations. The maximum thermal stress in the fuel cladding due to the temperature gradient during reflooding is calculated as follows:

The maximum circumferential stress at the outer surface is given by:

$$\sigma_t = \frac{\Delta T * \alpha \cdot E}{2(1-\nu)\log_e(c/b)} * (1 - \frac{2 * b^2}{(c^2 - b^2)} * \log_e c/b)$$

The maximum circumferential stress at the inner surface is given by:

$$\sigma_t = \frac{\Delta T * \alpha \cdot E}{2(1-\nu)\log_e(c/b)} * (1 - \frac{2 * c^2}{(c^2 - b^2)} * \log_e c/b)$$

The maximum stresses are calculated as 22,420 psi (outer surface) and 24,325 psi (inner surface). Based on the results of the thermal stress analysis, these stresses in the cladding during reflood is much less than the yield stress of 50,500 psi [4.13]. Therefore, cladding integrity is maintained during reflood operations.

Therefore, no cladding damage is expected due to the reflood event. This is also substantiated by the operating experience gained with the loading and unloading of transportation packages like IF-300 [4.11] which show that fuel cladding integrity is maintained during these operations and fuel handling and retrieval is not impacted.

M.4.8 Determination of Minimum Effective Fuel Conductivity

In order to determine the bounding effective thermal conductivity of a fuel assembly for use in the thermal analysis of the NUHOMS®-32PT DSC, the fuel assembly with the lowest thermal conductivity at the design basis heat load is selected.

This section presents the methodology for the determination of axial and transverse effective thermal conductivity of spent fuel and the determination of the bounding fuel effective thermal conductivity. In addition, the methodology for calculation of effective specific heat and effective density of the fuel is also presented.

M.4.8.1 Determination of Bounding Effective Fuel Thermal Conductivity

M.4.8.1.1 Fuel Assemblies Evaluated

The fuel assemblies that are considered for storage in the NUHOMS®-32PT DSC are listed in Section M.2. The design data for each of the fuel assemblies are presented in Section M.2.

M.4.8.1.2 Summary of Thermal Properties of Materials

The thermal conductivity and specific heat values of Zircalloy, UO_2 pellets, and Helium are presented in Section M.4.2. The emissivity of Zircalloy is also presented in Section M.4.2.

M.4.8.1.3 Calculation of Fuel Axial Effective Thermal Conductivity

The axial fuel conductivity is assumed to be limited to the cladding conductivity weighted by its fractional area as required in NUREG 1536 [4.10].

$$K_{axl} = (K_{zirc})(A_{zirc}/A_{eff}) \qquad (1)$$

K_{zirc} = Conductivity of Zircaloy 4
A_{eff} = (8.70") x (8.70") = 75.69 in^2
A_{zirc} = Cross section area of Zircalloy cladding in the fuel assembly

Equation (1) is used to calculate axial effective conductivity for the fuel assembly types listed in Section M.2 The results are plotted in Figure M.4-19.

M.4.8.1.4 Calculation of Fuel Transverse Effective Thermal Conductivity

The transverse fuel effective conductivity is determined by creating a two-dimensional finite element model of the fuel assembly centered within a fuel compartment. The outer surfaces, representing the fuel compartment walls, are held at a constant temperature, and heat generating boundary condition is applied to the fuel pellets within the model. A maximum fuel assembly temperature is then determined. The isotropic effective thermal conductivity of a heat generating square, such as the fuel assembly, can be calculated as described in [4.27].

$$K_{eff} = 0.29468 \times \frac{Q'''}{a^2 (T_c - T_o)} \qquad (2)$$

where:

Q''' = heat load per unit volume of fuel assembly (Btu/hr-in^3),
a = half width of fuel compartment opening = 8.7 / 2 = 4.35",
Tc = Maximum Temperature of Fuel Assembly (°F),
To = Compartment Wall Temperature (°F).

with

$$Q''' = \frac{Q}{4a^2 L_a} \qquad (3)$$

where:

Q= decay heat load per assembly = 24 kW/32 = 0.75 kW/assembly, and
L_a = active fuel length

In determining the temperature dependent effective fuel conductivities, an average temperature, equal to $(T_c + T_o)/2$, is used for the fuel temperature.

2-D finite element models of each fuel assembly representing a quarter of the fuel assembly were modeled within ANSYS [4.9]. Plane 55 elements were used to model components such as the fuel pellets, fuel cladding, and the helium back fill gas. The gap between the fuel cladding and the fuel pellets is also included in the model.

Heat generated in the fuel pellets dissipates by conduction and radiation to the fuel compartment walls. Convection is not considered in the model. Radiation between the fuel rods, guide tubes, and basket walls was simulated using the radiation super-element processor (/AUX12). LINK32 elements were used for modeling of radiating surfaces in creating the radiation super-element and were unselected prior to the solution of the model. The compartment walls are not modeled as a solid entity. Only the LINK32 elements aligned with the outermost nodes of the model (not on symmetry lines) are given the emissivity of the compartment walls.

Emissivity of stainless steel was applied to the LINK elements on one compartment wall. The link elements on the other compartment wall were given the emissivity of 0.85 (aluminum with anodized or other processes). To eliminate the radiation heat transfer across the symmetry lines, the link elements on symmetry lines were given a very low emissivity (0.001). Although the symmetry boundaries result in the aluminum surfaces being not adjacent, as it would be in the actual compartment, the impact is negligible.

Since a quarter of fuel assembly is modeled in each case, the reaction solution after solving the 2D model is equal to the heat generated per unit length of the active fuel divided by four.

$$Q_{react} = \frac{Q}{4L_a} \qquad (4)$$

Substitution of equations (3) and (4) in equation (2) gives:

$$K_{eff} = 0.29468 \times \frac{Q_{react}}{(T_c - T_o)} \qquad (5)$$

Equation (5) is used to calculate the transverse effective fuel conductivity for each fuel assembly model.

The heat generating boundary conditions for each assembly is calculated as shown in equation 6.

$$dhl = \frac{Q/N}{n\left(\frac{\pi}{4} d_p^{\,2}\right) L_a} \qquad (6)$$

dhl = Heat generating boundary condition (Btu/min-in-°F)
Q = Total decay heat load = 24 kW = 1364.9 Btu/min
N = Number of assemblies =32
n = Number of fuel rods
d_p = Pellet outer diameter
L_a = Active fuel length

The models were run with a series of isothermal boundary conditions applied to the nodes representing the fuel compartment walls. The symmetry lines going through the center of the fuel assembly are kept at the adiabatic boundary conditions.

A finite element model for B&W 15x15 fuel assembly is shown in Figure M.4-18.

M.4.8.1.5 Results and Conclusion

Figure M.4-19 shows the calculated axial effective conductivities. As Figure M.4-19 shows, WE 14x14 has the minimum (bounding) axial conductivity. Backfill gas property does not have any effect on the axial effective fuel conductivity. Therefore, identical axial effective fuel conductivity values can be used for helium and vacuum conditions.

The calculated bounding axial effective conductivities are listed in the following table:

Temperature °F	k-axial (Btu/min-in-°F)
200	7.949E-04
300	8.387E-04
400	8.824E-04
500	9.189E-04
600	9.554E-04
800	1.036E-03

The calculated transverse conductivities are presented in Figure M.4-20 and Figure M.4-21 for helium and vacuum conditions, respectively. As shown in Figure M.4-20 and Figure M.4-21, WE

14x14 assembly has the (bounding) minimum transverse conductivity. The bounding transverse effective conductivity values are listed in the following table:

Temperature °F	k-transverse in Helium (Btu/min-in-°F)
138	2.894E-04
233	3.317E-04
328	3.968E-04
423	4.744E-04
519	5.668E-04
616	6.715E-04
714	7.879E-04
812	9.208E-04

Temperature °F	k-transverse in Vacuum (Btu/min-in-°F)
215	9.484E-05
288	1.246E-04
367	1.633E-04
452	2.119E-04
540	2.701E-04
632	3.373E-04
726	4.125E-04
822	4.949E-04

M.4.8.2 Calculation of Fuel Effective Specific Heat and Density

This section presents the calculation of the fuel effective specific heat and density used in the transient thermal analyses.

Volume average density and weight average specific heat are calculated to determine the effective density and specific heat for the fuel assembly.

The equations to determine the fuel effective density ρ_{eff} and specific heat $C_{p\ eff}$ are shown below.

$$\rho_{eff} = \frac{\sum \rho_i V_i}{V_{assembly}} = \frac{\rho_{UO2}\ V_{UO2} + \rho_{Zr4}\ V_{Zr4}}{4a^2 L_a}$$

$$C_{p,eff} = \frac{\sum \rho_i V_i C_{Pi}}{\sum \rho_i V_i} = \frac{\rho_{UO2}\ V_{UO2}\ C_{P,UO2} + \rho_{Zr4}\ V_{Zr4}\ C_{P,Zr4}}{\rho_{UO2}\ V_{UO2} + \rho_{Zr4}\ V_{Zr4}}$$

where:

ρ_i, $C_{p,i}$, V_i = density, specific heat, and volume of component,
L_a = active fuel length, and
a = half of compartment width.

The properties of Zircalloy-4 and UO_2 are provided in Section M.4.2

The calculated values of fuel effective specific heat and fuel effective density are summarized below:

Temperature °F	Fuel Effective Specific Heat (Btu/lbm-F)
80	0.0592
260	0.0654
692	0.0725
1502	0.0778

Fuel Effective Density (lbm/in3)	**0.1166**

M.4.9 Derivation of Effective Thermal Conductivity of Water Within the Neutron Shield of the OS197/OS197H Transfer Cask

This Section presents the derivation of effective thermal conductivity of water within the liquid neutron shield of the OS197/OS197H Transfer Cask.

The neutron shield of the OS197/OS197H transfer cask is a water filled jacket surrounding the cask's structural shell. Support ribs are used to support the 3/16" stainless steel panels that make up the outer skin of the neutron shield. The layout of the twenty-four (24) support ribs (i.e., Item 4) within the neutron shield is illustrated in the following figure.

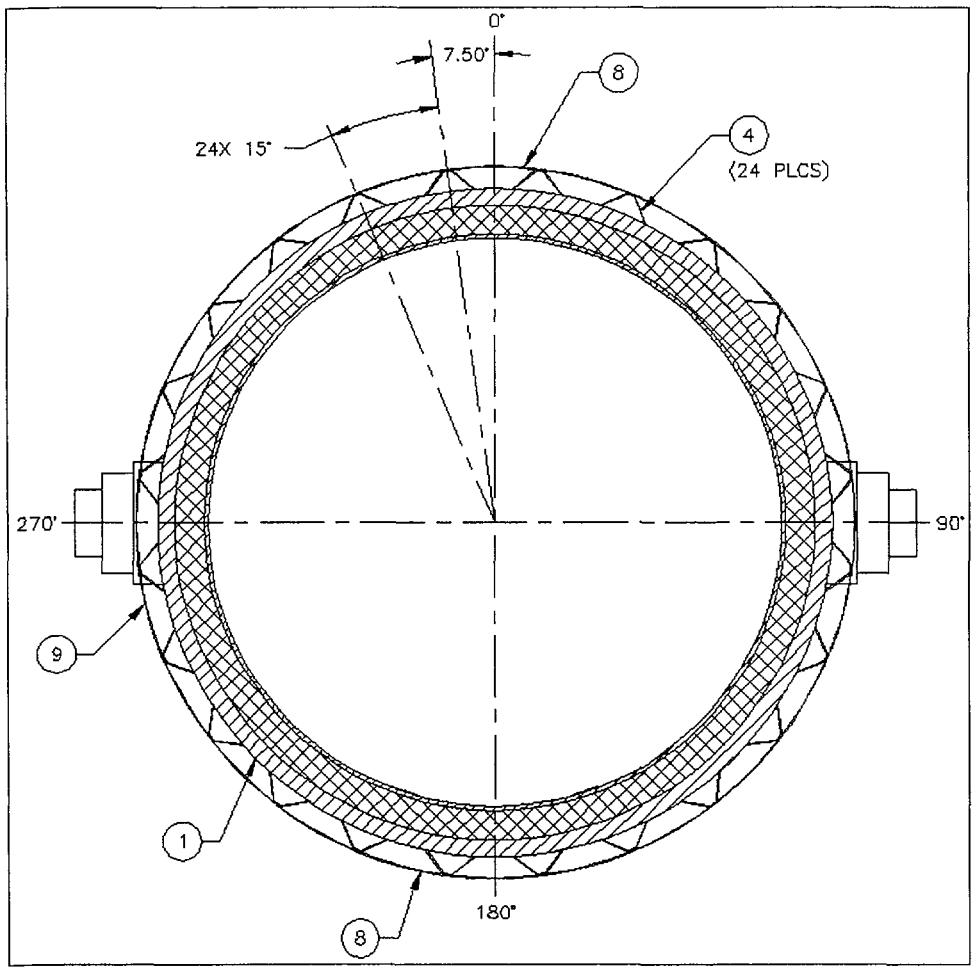

Cross-Section Through OS197/OS197H Cask

The presence of the support ribs act to divide up the void volume within the neutron shield into multiple enclosed regions. Heat transfer through the neutron shield is a combination of conduction and convection. Given the relatively large changes in the density of water with temperature, treating the water regions as a solid conductor material is grossly conservative from a heat transfer point of

view. Accordingly, a methodology based on established heat transfer principles is applied to determine the effective thermal conductivity within water-filled neutron shield for a transfer cask in a horizontal configuration.

No credit is taken for any flow through the drainage holes that exist in the ribs. Instead, credit is only taken for the convection that does occur as separate flow patterns within each region of the neutron shield.

A 15° segment of the cask circumference considered for the purposes of this analysis is presented in the following figure.

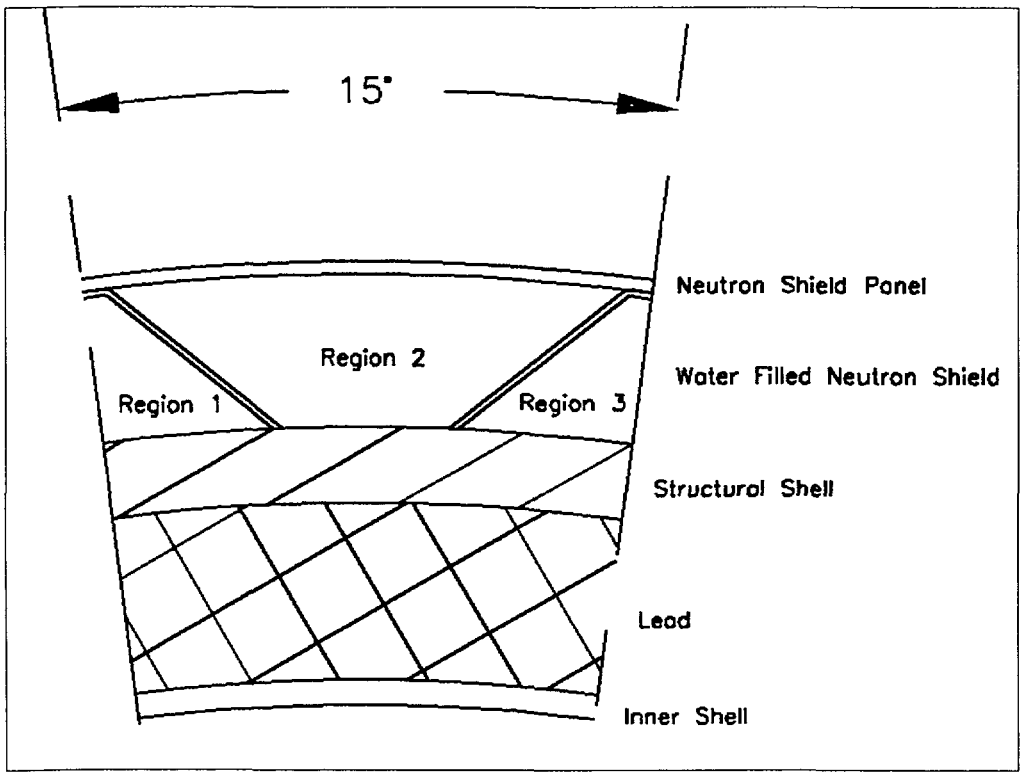

Modeling Layout of a 15° Segment of Cask Circumference

The symmetry planes that lie on either side of the modeled segment bisect the "hat" section of adjacent ribs. This modeling arrangement was selected for computational ease. Region 1 represents the enclosed region under one support rib, while Region 3 represents an identical region under the adjoining support rib. Region 2 represents the enclosed region between adjacent support ribs.

Each of these regions can be represented as enclosures with opposing parallel plates that are maintained at different temperatures. Heat transfer within such enclosures has been extensively studied and the presence of convective flow conclusively established for Rayleigh numbers (based on the separation distance between the parallel plates) in excess of 1000.

The Nusselt number, Nu_v, for a vertical enclosure is determined from Equations 126 to 129, page 6-53 of [4.22] for fluids with $Pr \approx 0.7$ and from Equations 130 and 131 for fluids with $Pr \geq 1.4$. Since the Pr of the water in the neutron shielding at the water temperatures expected under the transfer operation is approximately 1.4, Equations 126 to 129 are the appropriate set of equations to be used in calculating the Nusselt number. Equations 126 to 129 from [4.22] are as follows:

$$Nu_v = [Nu_{cl}, Nu_l, Nu_t]_{max}$$

where:

$$Nu_{cl} = \left[1 + \left\{\frac{0.0104\,Ra^{0.293}}{1 + (6310/Ra)^{1.36}}\right\}^3\right]^{0.3333}$$

$$Nu_l = 0.242\left(\frac{Ra * L}{H}\right)^{0.273}$$

$$Nu_t = 0.0606\,(Ra)^{0.3333}$$

$$Ra = \frac{g * \beta * (T_{hot} - T_{cold}) * L^3 * \mu * C_P}{\nu^2 \kappa}$$

where:

g = gravitational acceleration

β = coefficient of thermal expansion

T_{hot} = temperature of structural shell

T_{cold} = temperature of neutron shield skin

μ = dynamic viscosity

C_P = specific heat

L = width of the cavity

ν = kinematic viscosity

k = thermal conductance

For a horizontal cavity where the hot wall lies below the cold wall, the Nusselt number, Nu_h, is determined from Equations 114 to 117, page 6-46 of [4.22]. These equations are:

$$Nu_h = 1 + \left[1 - \frac{1708}{Ra}\right]^{\bullet} * \left[k_1 + 2\left(\frac{Ra^{\frac{1}{3}}}{k_2}\right)^{1-\ln\left(\frac{Ra^{\frac{1}{3}}}{k_2}\right)}\right] + \left[\left(\frac{Ra}{5830}\right)^{\frac{1}{3}} - 1\right]^{\bullet}$$

where:

$$k_1 = \frac{1.44}{1 + 0.018/Pr + 0.00136/Pr^2}$$

$$k_2 = 75 \exp(1.5\, Pr^{-0.5})$$

The brackets with a dot $[]^{\bullet}$ indicate that only positive terms are retained, otherwise the value within the brackets is to be set to zero.

The above equations can be used to estimate the Nusselt number at the top (i.e., circumferential position = 0 degrees) and the side (i.e., circumferential position = 90 degrees) of the cask. For other positions on the cask, scaling laws provided by Equations 134 to 139, page 6-58 of [4.22] are to be used.

For angles of $90° < \Theta \leq 180°$ (i.e., the bottom of the cask), the recommended scaling law is:

$$Nu_{\Theta} = 1 + (Nu_v - 1) * \sin\Theta$$

As seen, this equation will yield a Nusselt number = 1 (i.e., conduction only) for the bottom of the cask.

For angles of $45° < \Theta < 90°$, the recommended scaling law for an enclosure with $H/L \cong 2$ is:

$$Nu_{\Theta} = Nu_v (Ra * \sin\Theta)$$

While for angles of $0° < \Theta < 45°$, the recommended scaling law for an enclosure with $H/L \cong 2$ is:

$$Nu_{\Theta} = Nu_h * \left[\frac{Nu_v (Ra * \sin 45^o)}{Nu_h}\right]^{\frac{\Theta}{45}}$$

For the purposes of this calculation, H is assumed to be 7" and L is set equal to 3" or the thickness of the neutron shield. The choice of H=7 is based on the mean distance between the legs of the ribs. However, as seen from [4.22] the use of smaller values of H yields higher Nusselt numbers. Thus, the use of 7" yields conservative values of the Nusselt number.

To arrive at an effective thermal conductivity across the neutron shield, the thermal resistances for the heat transfer paths through Regions 1, 2, and 3 of the shield, as well as the heat conducted along the steel support ribs are computed and then summed assuming they represent parallel paths. The effective thermal conductivity across the neutron shield, k_{eff}, is then determined via:

$$\frac{1}{\frac{1}{R_{Region\,1}} + \frac{1}{R_{Region\,2}} + \frac{1}{R_{Region\,3}} + \frac{1}{R_{Ribs}}} = \frac{\ln\left(\frac{r_2}{r_1}\right)}{2 * \pi * Z * k_{effective}}$$

where:

k_{eff} = Effective thermal conductivity across the neutron shield,

$R_{Regioni}$ = Thermal Resistance of Region I,

r_2 = inside radius of neutron shield shell = 42.56",

r_1 = outside radius of structural shell = 39.56", and

Z = axial length of model section of the cask.

Since the Rayleigh number is a function of the temperature difference and the mean temperature within the neutron shield, an iterative process is used to arrive at a value for both temperature difference and the mean temperature that is required to balance the flow of heat across the neutron shield, assuming a decay heat loading of 24 kW.

The computed thermal resistances for each of the assumed thermal paths through the water-filled neutron shield, together with the computed effective thermal conductivity, are presented in the following table:

K_{eff} for OS197 Cask Neutron Shield (Water Filled) vs. Circumferential Position

Angle	Nu (Ra)	R Region 1	R Region 2	R Region 3	R Support Ribs	Total R	k effective, Btu/min-in-F
0	36.36	1.853	1.907	1.853	58.556	0.617	0.019
30	33.07	2.037	2.097	2.037	58.556	0.678	0.017
60	33.34	2.021	2.080	2.021	58.556	0.672	0.017
90	34.67	1.943	2.000	1.943	58.556	0.647	0.018
120	30.16	2.234	2.300	2.234	58.556	0.742	0.016
150	17.84	3.777	3.889	3.777	58.556	1.244	0.009
180	1.00	67.371	69.353	67.371	58.556	16.344	0.001

As expected, the presence of the convection within the shield will enhance the apparent thermal conductivity by a factor of 10 to 20 over that computed assuming the water acts as a solid material.

The computed thermal resistances for an air-filled neutron shield are presented in the following table:

K_{eff} for OS197 Cask Neutron Shield (Air Filled) vs. Circumferential Position

Angle	Nu (Ra)	R Region 1	R Region 2	R Region 3	R Support Ribs	Total R	k effective, Btu/min-in-F
0	6.98	187.650	193.169	187.650	58.556	30.239	0.000385
30	7.29	179.736	185.022	179.736	58.556	29.615	0.000393
60	7.88	166.434	171.329	166.434	58.556	28.500	0.000408
90	8.19	160.025	164.732	160.025	58.556	27.931	0.000417
120	7.23	181.356	186.690	181.356	58.556	29.745	0.000391
150	4.60	285.226	293.615	285.226	58.556	36.163	0.000322
180	1.00	1310.670	1349.219	1310.670	58.556	51.278	0.000227

As seen from the table, the lower Rayleigh numbers associated with an air filled neutron shield results in the presence of convection within the shield enhancing the apparent thermal conductivity by only a factor of approximately 2 over that computed assuming the air acts as a solid material.

The effective conductivity values interpolated from these tables are applied to the 24 segments (7.5 degrees each) along the neutron shield region of the transfer cask model described in Section M.4.4.1.5.

For each segment, the lowest k_{eff} value along the segment was applied.

M.4.10 References

4.1 Deleted.

4.2 Deleted.

4.3 Report, "Topical Report on Actinide-Only Burnup Credit for PWR Spent Nuclear Fuel Packages," Office of Civilian Radioactive Waste Management, DOE/RW-0472, Revision 2, September, 1998.

4.4 ASME Boiler and Pressure Vessel Code, Section II, Part D, Properties, 1998, including 2000 addenda.

4.5 Roshenow, W. M., J. P. Hartnett, and Y. I. Cho, *Handbook of Heat Transfer*, 3rd Edition, 1998.

4.6 Bolz, R. E., G. L. Tuve, *CRC Handbook of Tables for Applied Engineering Science*, 2nd Edition, 1973. Transfer, McGraw Hill, 1989.

4.7 Bucholz, J. A., *Scoping Design Analysis for Optimized Shipping Casks Containing 1-, 2-, 3-, 5-, 7-, or 10-Year old PWR Spent Fuel*, Oak Ridge National Laboratory, January, 1983, ORNL/CSD/TM-149.

4.8 Deleted.

4.9 ANSYS, Inc., ANSYS Engineering Analysis System User's Manual for ANSYS Revision 5.6, Houston, PA.

4.10 NRC NUREG-1536, *Standard Review Plan for Dry Cask Storage Systems,* January 1997.

4.11 Consolidated Safety Analysis Report for IF-300 Shipping Cask, CoC 9001.

4.12 J.P. Holman, Heat Transfer, McGraw Hill, 1989.

4.13 Chun, Ramsey; Witte, Monika; Schwartz, Martin, "Dynamic Impact Effects on Spent Fuel Assemblies," Lawrence Livermore National Laboratory, Report UCID-21246, October, 1987.

4.14 NUREG/CR-0497, "MATPRO-Version 11: "A Handbook of Materials Properties for Use in the Analysis of Light Water Reactor, Fuel Rod Behavior," EG&G, Inc. February, 1979.

4.15 Glasstone, S., Seasonske, A., "Nuclear Reactor Engineering," Third Edition, 1981.

4.16 Young, W.C., "Roark's Formulas for Stress and Strain," Sixth Edition, McGraw Hill.

4.17 Deleted.

4.18 Deleted.

4.19 Aluminum. Volume 1, Properties, Physical Metallurgy and Phase Diagrams, edited by Kent R. Van Horn, American Society for Metals, Metals Park, Ohio, 1967.

4.20 ASHRAE Handbook, 1981 Fundamentals, 4th Printing, 1983.

4.21 Deleted.

4.22 Rohsenow, Hartnett, "Handbook of Heat Transfer Fundamentals, " 2nd Edition, 1985.

4.23 Roth, A., "Vacuum Technology," 2nd Edition, 1982.

4.24 Interim Staff Guidance No. 11, Revision 2, "Cladding Considerations for the Transportation and Storage of Spent Fuel," July 30, 2002.

4.25 Calculation, "TN-24P Benchmarking Analysis Using ANSYS," Calculation No. NUH32PT.0408, Revision 0.

4.26 J. M. Creer, et al, "The TN-24 PWR Spent Fuel Storage Cask: Testing and Analyses," PNL Report, Report No. PNL-6054, 1987.

4.27 SAND90–2806, Sanders, T. L., et al., "A Method for Determining the Spent Fuel Contribution to Transport Cask Containment Requirements," TTC-1019, UC-820, November 1992.

4.28 Oak Ridge National Laboratory, RSIC Computer Code Collection, "SCALE, A Modular Code System for Performing Standardized Computer Analysis for Licensing Evaluation for Workstations and Personal Computers", NUREG/CR-0200, Rev. 6, ORNL/NUREG/CSD-2/V3/R6.

M.4.11 Example Input Files

M.4.11.1 Example ANSYS Input File for Applying Heat Generation

```
      /com apply heat generation to fuel regions
      /com select elements to apply heat generation
csys,0
cmsel,s,f_outer   ! select fuel elements
nsle,s,all
nsel,r,loc,z,act_end ,0
esln,r,0
esel,u,type,,7
bfedele,all,hgen

          /com read in z coordinates of burnup curve and values

*dim,z_fuel,,12
*dim,h_gen,,12
z_fuel(1)=act_end
h_gen(1)=0
z_fuel(2)= act_end +0.0278*act_fuel
h_gen(2)=0.652*heat_gen
z_fuel(3)= act_end +0.0833*act_fuel
h_gen(3)=0.967*heat_gen
z_fuel(4)= act_end +0.1389*act_fuel
h_gen(4)=1.074*heat_gen
z_fuel(5)= act_end +0.1944*act_fuel
h_gen(5)=1.103*heat_gen
z_fuel(6)= act_end +0.25*act_fuel
h_gen(6)=1.108*heat_gen
z_fuel(7)= act_end +0.3056*act_fuel
h_gen(7)=1.106*heat_gen
z_fuel(8)= act_end +0.3611*act_fuel
h_gen(8)=1.102*heat_gen
z_fuel(9)= act_end +0.4167*act_fuel
h_gen(9)=1.097*heat_gen
z_fuel(10)= act_end +0.4722*act_fuel
h_gen(10)=1.094*heat_gen
z_fuel(11)= act_end +0.5278*act_fuel
h_gen(11)=1.094*heat_gen
z_fuel(12)= act_end +0.5833*act_fuel
h_gen(12)=1.095*heat_gen

*get,emin,elem,0,num,min        ! get the minimum element #
*get,emax,elem,0,num,max        ! get the maximum element #
eln=0
*do,cnt,emin,emax,1
  *get,elnn,elem,eln,nxth       ! get next higher element number  than eln and
store in elnn
   eln=elnn
  *get,ei,elem,eln,node,1       ! get nodes which are attached to eln
  nzi=nz(ei)
  *get,ej,elem,eln,node,2       ! get nodes which are attached to eln
  nzj=nz(ej)
  *get,ek,elem,eln,node,3       ! get nodes which are attached to eln
```

```
nzk=nz(ek)
*get,el,elem,eln,node,4        ! get nodes which are attached to eln
nzl=nz(el)
*get,em,elem,eln,node,5        ! get nodes which are attached to eln
nzm=nz(em)
*get,en,elem,eln,node,6        ! get nodes which are attached to eln
nzn=nz(en)
*get,eo,elem,eln,node,7        ! get nodes which are attached to eln
nzo=nz(eo)
*get,ep,elem,eln,node,8        ! get nodes which are attached to eln
nzp=nz(ep)
n_z=(nzi+nzj+nzk+nzl+nzm+nzn+nzo+nzp)/8      ! find average z
*do,i,1,12,1
  *if,n_z,ge,z_fuel(i),then
    *if,n_z,lt,z_fuel(i+1),then
      z_diff=z_fuel(I+1)-z_fuel(I)
      gen_diff=h_gen(I+1)-h_gen(I)
      gen=(n_z-z_fuel(i))/(z_diff)*(gen_diff)+h_gen(i)
      bfe,eln,hgen,,gen
   *endif
  *endif
*enddo
*if,eln,eq,emax,exit
*enddo
```

M.4.11.2 Example ANSYS Input File for Solar Heat Flux Application

```
/com create radiation elements on outer surface of cask

type,9
real,9
mat,10

/com define space node
k,300,0,50,0
n,10000,0,50,0

esel,s,type,,1
esel,a,type,,2
esel,a,type,,3
esel,a,type,,4
esel,a,type,,5

nsle,s,all

esurf,10000

esel,s,type,,9
nsle,s,all
csys,1
nsel,r,loc,x,0,shell_od/2
nsel,a,node,,10000
esln,r,1
edele,all
csys,0

/com create surface elements for insolation

alls
csys,1
esel,s,type,,5
esel,a,type,,1
cmsel,s,a_nsp
cmsel,a,a_ns3
esla,r
type,6
esurf

csys,1
esel,s,type,,6
nsle,s,all
x1=cask_ir+inner_t+lead_t+struct_t
nsel,r,loc,x,x1-gy2,x1+gy2
esln,r,1
edele,all

/com delete elements on bottom half
esel,s,type,,6
nsle,s,all
x1=cask_ir+inner_t+lead_t+struct_t+ns3_t+nsp_t
```

```
nsel,r,loc,x,x1-gy2,x1+gy2
csys,0
nsel,r,loc,y,-100,0
esln,r,1
edele,all

csys,0
```

The ANSYS input file routine to apply insolation to the top outside surface of the cask is as follows:

```
/com 3rd load step, 100 deg F

/com load parameters

T_amb=100.
Insol=123/144/60
.
.
.
/com isolate insolation elements
csys,22
esel,s,type,,6
nsle,s,all
nsel,r,loc,x,cask_ir+inner_t+lead_t+struct_t+ns3_t+nsp_t
esln,r,1
sfedele,all,all,hflux
sfe,all,1,hflux,,insol
csys,0

alls
esel,u,type,,7
nsle,s,all

lswrite,3
```

Table M.4-1
Fuel Cladding Long-Term Storage Temperatures

Configuration No.	Maximum Temperature (°F)	Limit (°F)
1	634	752
2	619	
3	638	

Table M.4-2
Fuel Cladding Short-Term Normal Condition Maximum Temperatures

Operating Condition	Configuration 1 (°F)	Configuration 2 (°F)	Configuration 3 (°F)	Limit (°F)
0°F Storage	585	570	589	752
100°F Storage	655	640	658	
0°F Transfer	675	661	675	
100°F Transfer	720	705	720	

Table M.4-3
DSC Basket Assembly Maximum Normal Operating Component Temperatures; Configuration 1

Configuration	$T_{grid,max}$ (°F)	$T_{grid,min}$ (°F)	$T_{rail,max}$ (°F)	$T_{rail,min}$ (°F)	$T_{Al,max}$ (1) (°F)	$T_{DSC\ shell}$ (2) (°F)
DSC in HSM, 0°F	565	233	304	230	565	277
DSC in HSM, 100°F	638	316	395	312	638	374
DSC horizontal in cask, 0°F	659	344	418	340	659	390
DSC horizontal in cask, 100°F	705	405	471	402	705	445

(1) Includes aluminum and poison plates.

(2) Maximum temperature is at top of shell.

Table M.4-4
DSC Basket Assembly Maximum Normal Operating Component Temperatures; Configuration 2

Configuration	$T_{grid,max}$ (°F)	$T_{grid,min}$ (°F)	$T_{rail,max}$ (°F)	$T_{rail,min}$ (°F)	$T_{Al,max}$ (1) (°F)	$T_{DSC\ shell}$ (2) (°F)
DSC in HSM, 0°F	550	233	306	229	549	277
DSC in HSM, 100°F	623	316	397	311	623	374
DSC horizontal in cask, 0°F	644	342	420	339	644	390
DSC horizontal in cask, 100°F	691	406	473	401	691	445

(1) Includes aluminum and poison plates.

(2) Maximum temperature is at top of shell.

Table M.4-5
DSC Basket Assembly Maximum Normal Operating Component Temperatures; Configuration 3

Configuration	$T_{grid,max}$ (°F)	$T_{grid,min}$ (°F)	$T_{rail,max}$ (°F)	$T_{rail,min}$ (°F)	$T_{Al,max}$ (1) (°F)	$T_{DSC\ shell}$ (2) (°F)
DSC in HSM, 0°F	567	220	289	218	567	264
DSC in HSM, 100°F	639	304	381	301	639	361
DSC horizontal in cask, 0°F	657	327	400	323	657	374
DSC horizontal in cask, 100°F	704	390	456	387	704	431

(1) Includes aluminum and poison plates.

(2) Maximum temperature is at top of shell.

Table M.4-6
32PT DSC Initial Helium Fill Molar Quantities

DSC Configuration	Helium Fill (g-moles)
S100	110.8
S125	107.8
L100	115.6
L125	112.7

Table M.4-7
32PT DSC Maximum Normal Operating Condition Pressures

DSC Configuration	DSC Cavity Free Volume (in^3)	Helium Fill (g-moles)	Plenum Helium (g-moles)	BPRA Gas (g-moles)	Fission Products (g-moles)	Total Gas (g-moles)	Pressure (psig)	DSC Design Pressure (psig)
S100	226,141	110.74	1.75	0.00	2.60	115.11	6.31	15
S125	220,162	107.83	1.75	0.00	2.60	112.18	6.34	15
L100	236,094	115.62	1.75	0.359	2.60	120.34	6.35	15
L125	230,097	112.68	1.75	0.359	2.60	117.41	6.37	15

Table M.4-8
Off-Normal Event Fuel Cladding Maximum Temperatures

Operating Condition	Configuration 1 (°F)	Configuration 2 (°F)	Configuration 3 (°F)	Limit (°F)
-40°F Storage	558	542	562	1,058
117°F Storage	660	646	663	
117°F Transfer(1)	715	700	715	752

(1) Sunshade is used for ambient temperatures >100°F and ≤117°F.

Table M.4-9
Off-Normal Event DSC Basket Assembly Maximum Component Temperatures; Configuration 1

Configuration	$T_{grid,max}$ (°F)	$T_{grid,min}$ (°F)	$T_{rail,max}$ (°F)	$T_{rail,min}$ (°F)	$T_{Al,max}$ (1) (°F)	$T_{DSC\ shell}$ (2) (°F)
DSC in HSM, -40°F	536	200	266	197	536	237
DSC in HSM, 117°F	643	322	402	318	643	382
DSC horizontal in cask, -40°F(3)	-	-	-	-	-	-
DSC horizontal in cask with shade, 117°F	700	404	463	401	700	433

(1) Includes aluminum and poison plates.
(2) Maximum temperature is at top of shell.
(3) Not evaluated for cask with liquid neutron shield (OS197/OS197H). Per Technical Specification 1.2.13 transfer operations outside the fuel handling building at basket temperatures (assumed conservatively equal to ambient temperature) below 0°F are not permitted.

Table M.4-10
Off-Normal Event DSC Basket Assembly Maximum Component Temperatures; Configuration 2

Configuration	$T_{grid,max}$ (°F)	$T_{grid,min}$ (°F)	$T_{rail,max}$ (°F)	$T_{rail,min}$ (°F)	$T_{Al,max}$ (1) (°F)	$T_{DSC\ shell}$ (2) (°F)
DSC in HSM, -40°F	520	200	268	196	520	237
DSC in HSM, 117°F	629	322	404	317	628	382
DSC horizontal in cask, -40°F(3)	-	-	-	-	-	-
DSC horizontal in cask with shade, 117°F	686	405	464	400	686	433

(1) Includes aluminum and poison plates.
(2) Maximum temperature is at top of shell.
(3) Not evaluated for cask with liquid neutron shield (OS197/OS197H). Per Technical Specification 1.2.13 transfer operations outside the fuel handling building at basket temperatures (assumed conservatively equal to ambient temperature) below 0°F are not permitted.

Table M.4-11
Off-Normal Event DSC Basket Assembly Maximum Component Temperatures; Configuration 3

Configuration	$T_{grid,max}$ (°F)	$T_{grid,min}$ (°F)	$T_{rail,max}$ (°F)	$T_{rail,min}$ (°F)	$T_{Al,max}$ (1) (°F)	$T_{DSC\ shell}$ (2) (°F)
DSC in HSM, -40°F	538	187	252	185	538	224
DSC in HSM, 117°F	645	310	388	307	644	368
DSC horizontal in cask, -40°F(3)	-	-	-	-	-	-
DSC horizontal in cask with shade, 117°F	699	389	447	386	698	418

(1) Includes aluminum and poison plates.

(2) Maximum temperature is at top of shell.

(3) Not evaluated for cask with liquid neutron shield (OS197/OS197H). Per Technical Specification 1.2.13 transfer operations outside the fuel handling building at basket temperatures (assumed conservatively equal to ambient temperature) below 0°F are not permitted..

Table M.4-12
32PT DSC Maximum Off-Normal Operating Condition Pressures

	DSC Cavity Free Volume (in3)	Helium Fill (g-moles)	Plenum Helium (g-moles)	BPRA Gas (g-moles)	Fission Products (g-moles)	Total Gas (g-moles)	Pressure (psig)	DSC Design Pressure (psig)
S100	226,142	110.76	17.50	0.00	26.02	154.28	13.36	20
S125	220,163	107.83	17.50	0.00	26.02	151.35	13.57	20
L100	236,095	115.63	17.50	3.59	26.02	162.74	13.66	20
L125	230,097	112.68	17.50	3.59	26.02	159.81	13.87	20

Table M.4-13
Accident Fuel Cladding Maximum Temperatures

Operating Condition	Temperature (°F)	Limit (°F)
DSC in HSM blocked vent at 40 hours, 117°F – Configuration 3	788	1,058
Post accident transfer 117°F (loss of sunshade, loss of neutron shield) – Configuration 1	863	1,058

Table M.4-14
DSC Basket Assembly Maximum Accident Condition Component Temperatures;

Configuration	$T_{grid,max}$ (°F)	$T_{grid,min}$ (°F)	$T_{rail,max}$ (°F)	$T_{rail,min}$ (°F)	$T_{Al,max}$ (1) (°F)	$T_{DSC\ shell}$ (2) (°F)
DSC in HSM blocked vent at 40 hours, 117°F – Configuration 3	774	479	582	476	774	574
Post accident transfer 117°F (loss of sunshade, loss of neutron shield) – Configuration 1	852	611	631	609	852	600

(1) Includes aluminum and poison plates.

(2) Maximum temperature is at top of shell.

Table M.4-15
32PT DSC Maximum Accident Condition Pressures

	DSC Cavity Free Volume (in3)	Helium Fill (g-moles)	Plenum Helium (g-moles)	BPRA Gas (g-moles)	Fission Products (g-moles)	Total Gas (g-moles)	Pressure (psig)	DSC Design Pressure (psig)
S100	226,142	110.76	175.04	0.00	260.17	545.95	95.96	105
S125	220,163	107.83	175.04	0.00	260.17	543.03	98.25	105
L100	236,095	115.63	175.04	35.9	260.17	586.74	99.40	105
L125	230,097	112.69	175.04	35.9	260.17	583.80	101.68	105

Table M.4-16
Maximum Component Temperatures for the Hypothetical Fire Accident Case for the NUHOMS®-32PT DSC in the TC

Component	Maximum Temperature (°F)	Allowable Range (°F)
DSC Shell	545	*
Cask Lead Shielding	485	621

* The components perform their intended safety function within the operating range.

Table M.4-17
Vacuum Drying Fuel Cladding Maximum Temperatures

Operating Condition	Configuration 1 (°F)	Configuration 2 (°F)	Configuration 3 (°F)	Limit (°F)
Vacuum Drying, 33 hours	663	645	678	752

Table M.4-18
DSC Basket Assembly Maximum Component Temperatures During Vacuum Drying at 33 hours(2)

Condition/Configuration	$T_{grid,max}$ (°F)	$T_{grid,min}$ (°F)	$T_{rail,max}$ (°F)	$T_{rail,min}$ (°F)	$T_{Al,max}$ (°F)(1)
Vacuum Drying/Configuration 1	645	324	345	314	644
Vacuum Drying/Configuration 2	626	326	352	314	626
Vacuum Drying/Configuration 3	656	314	335	306	656

(1) Includes aluminum and poison plates.

(2) Temperatures correspond to 35 hours into vacuum drying which is conservative for 33 hour case.

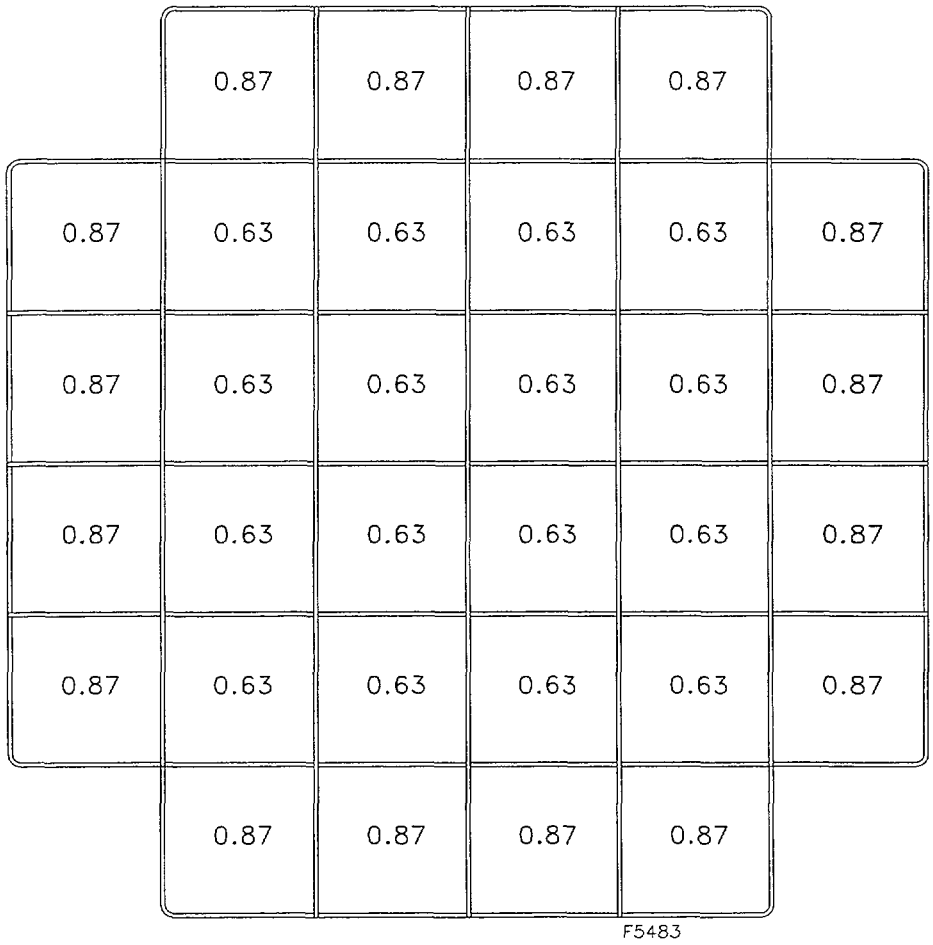

Figure M.4-1
Heat Load Zoning Configuration 1, Maximum Decay Heat for Various Assemblies

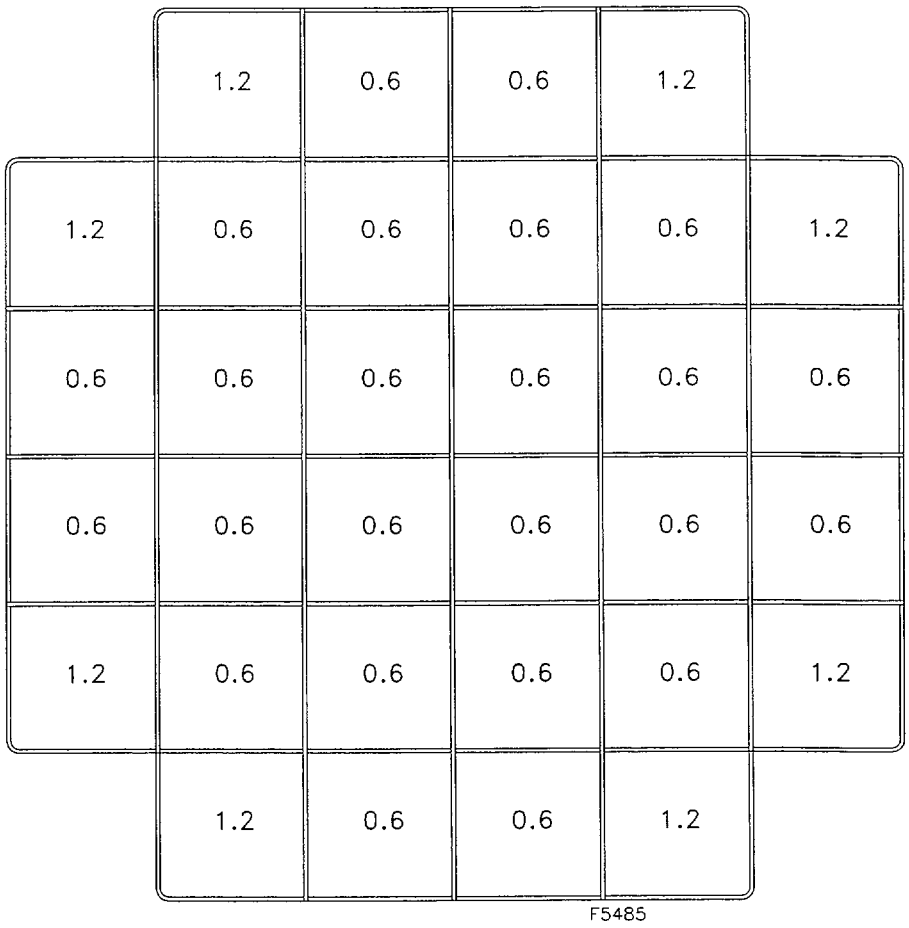

Figure M.4-2
Heat Load Zoning Configuration 2, Maximum Decay Heat for Various Assemblies

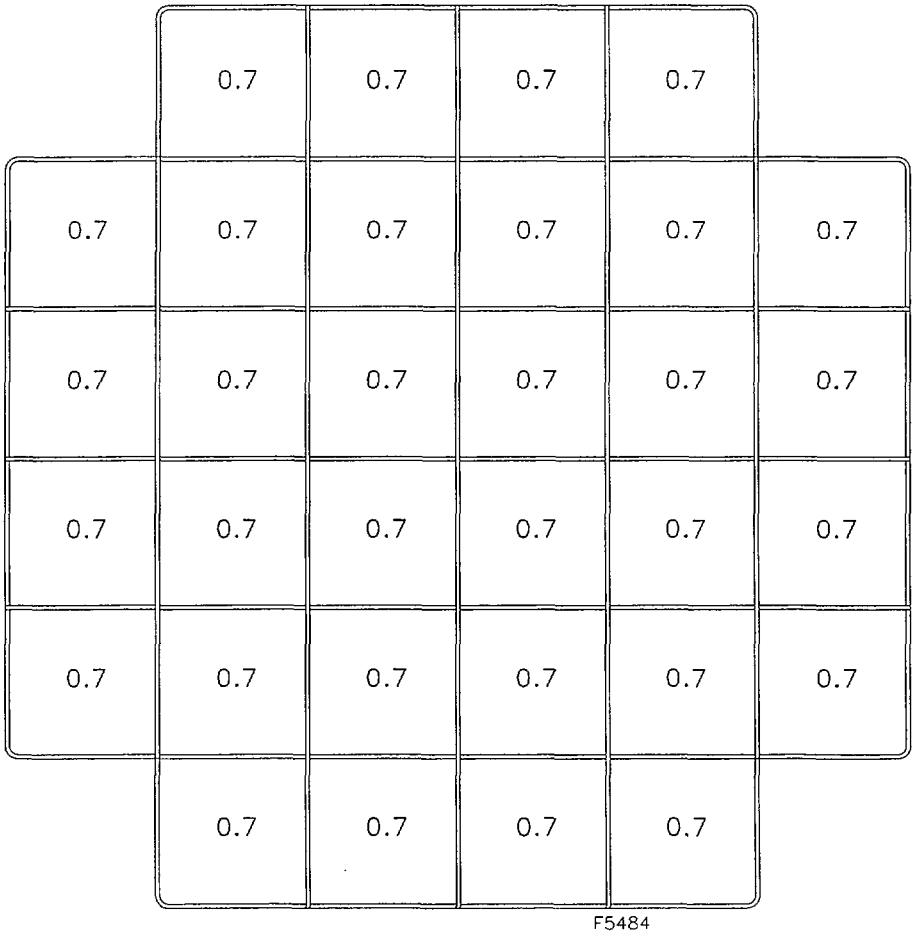

Figure M.4-3
Heat Load Zoning Configuration 3, Maximum Decay Heat for Various Assemblies

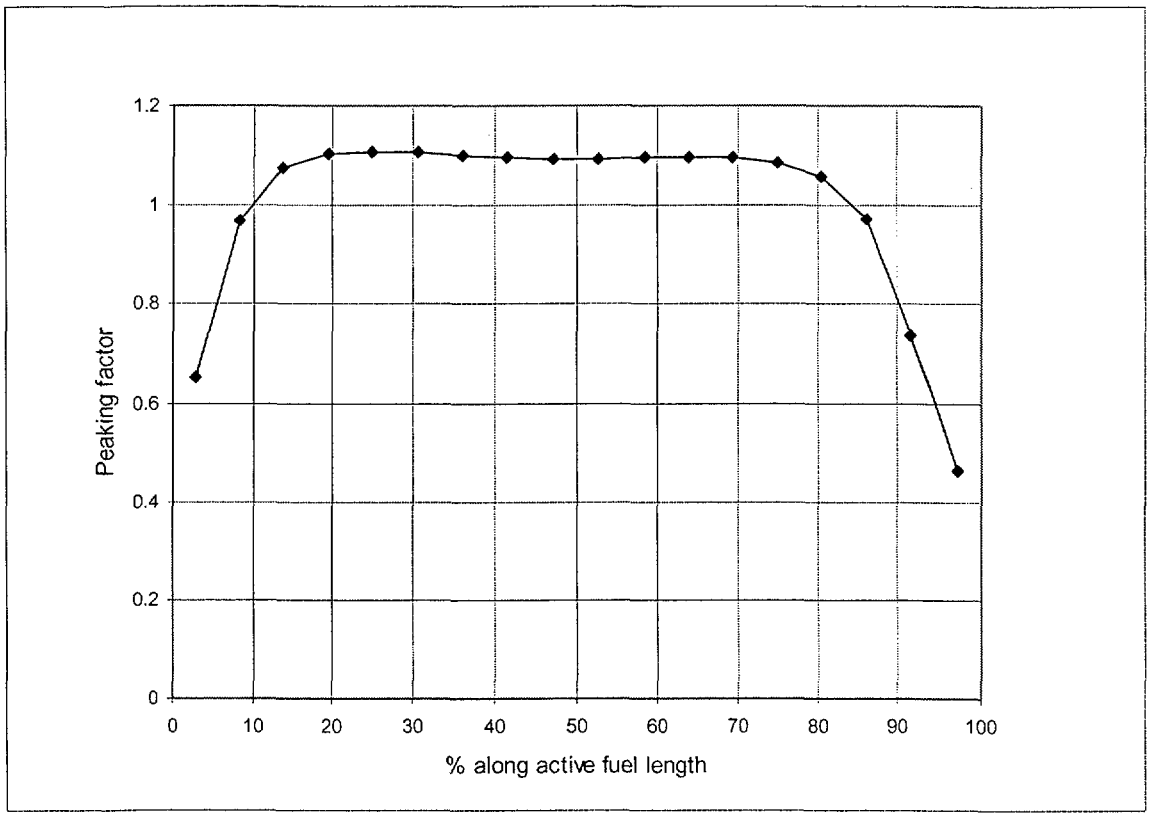

Figure M.4-4
Axial Heat Profile for PWR Fuel

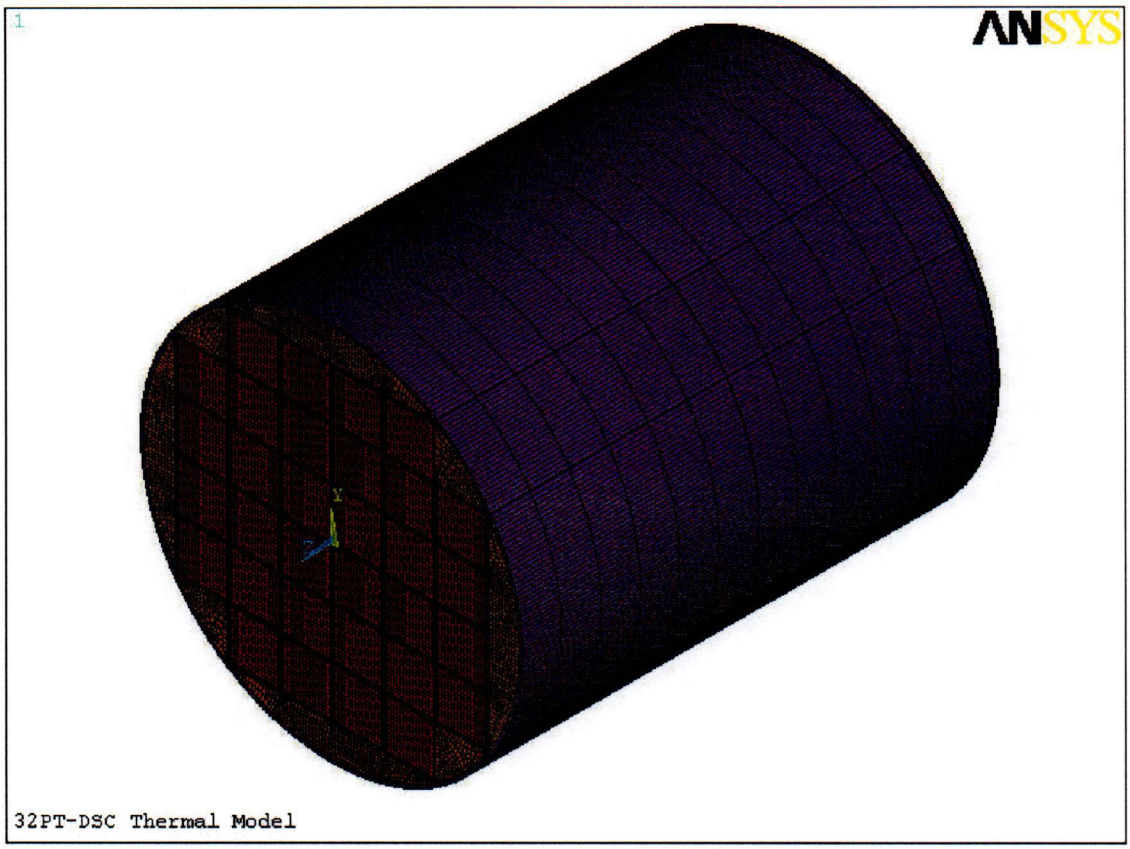

Figure M.4-5
32PT-DSC Thermal ANSYS Model, Isometric View

C06

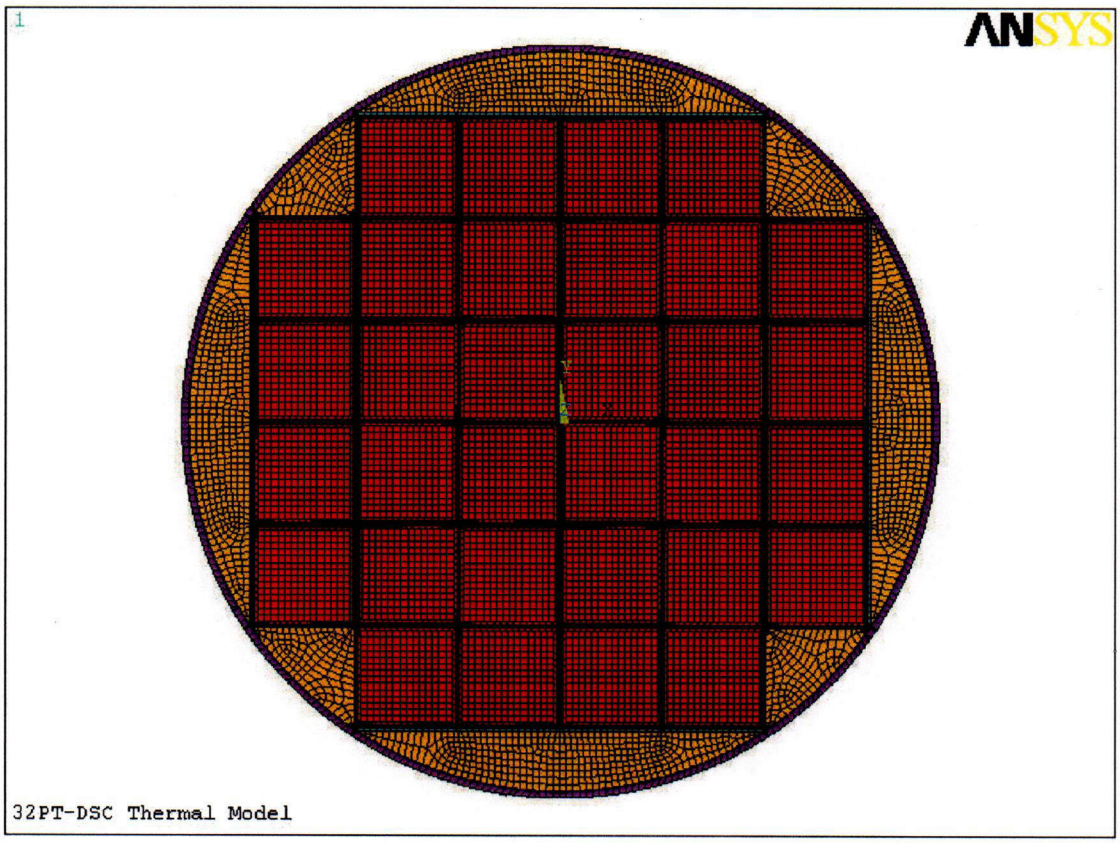

Figure M.4-6
32PT DSC Thermal ANSYS Model, Cross-Section View

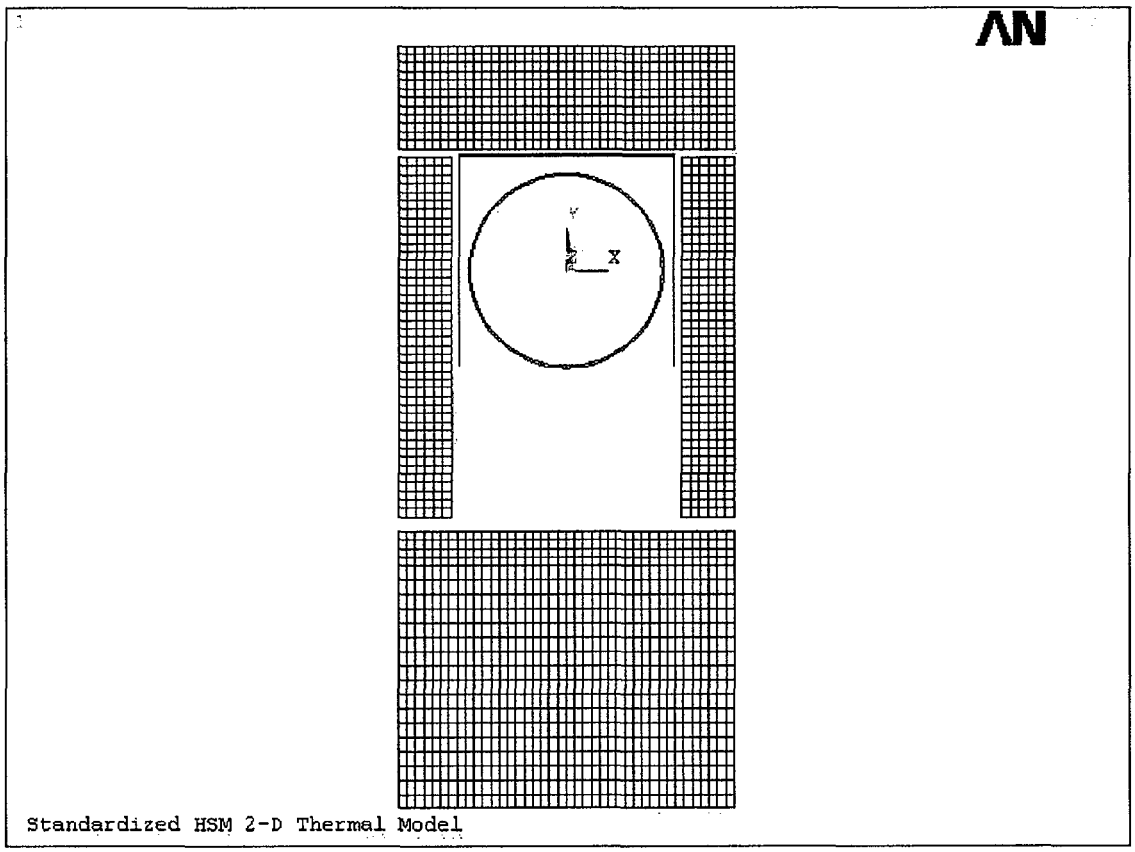

Figure M.4-7
Thermal Model of DSC in HSM

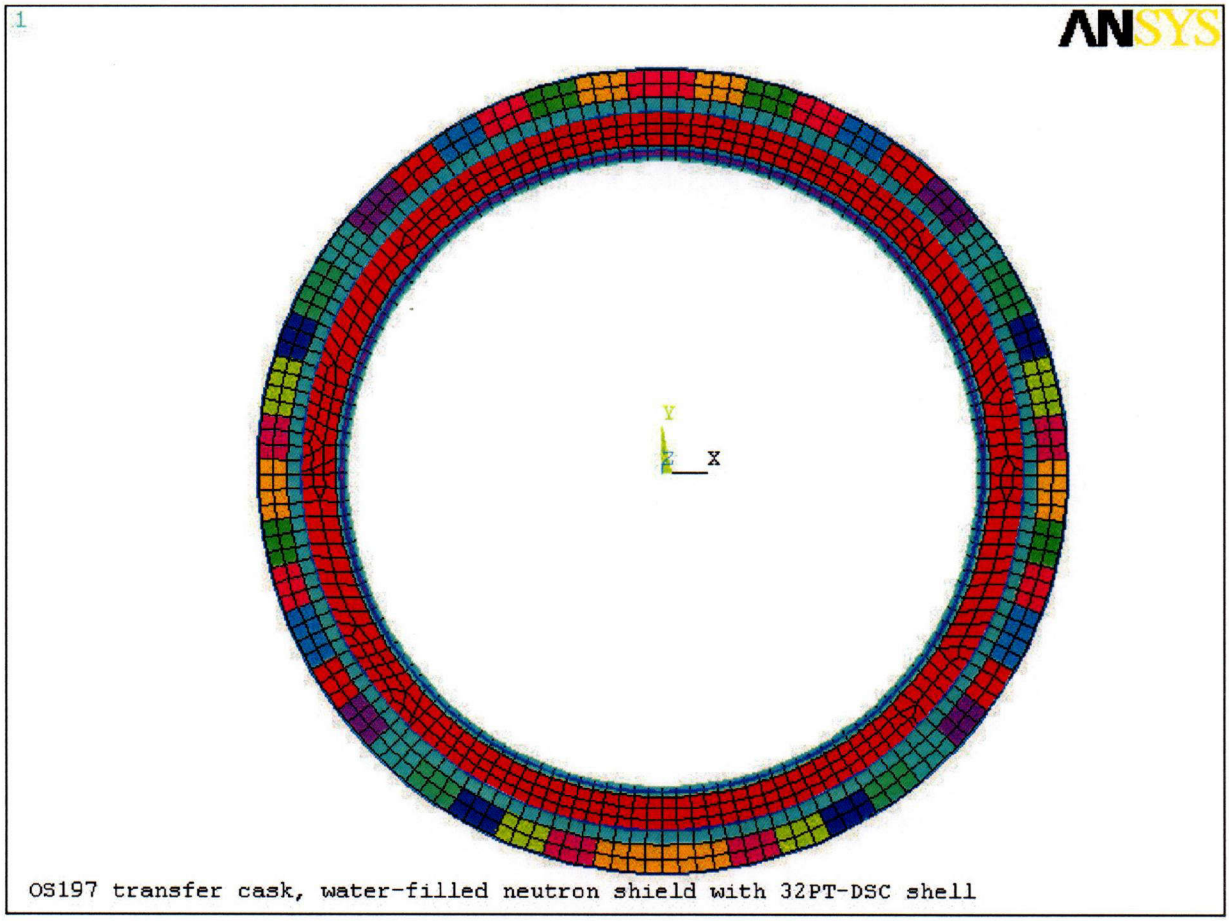

Figure M.4-8
Thermal Model of TC

C08

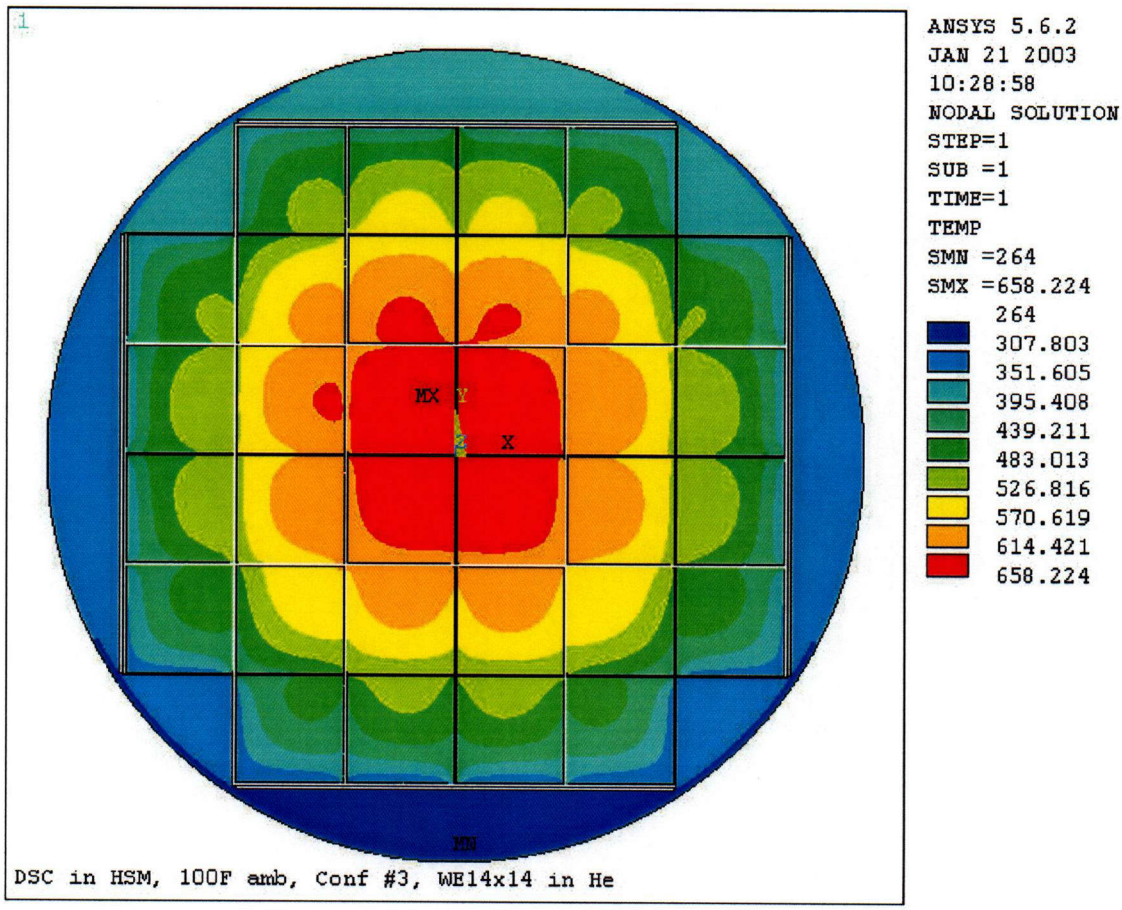

Figure M.4-9
Results for 100°F Storage Case With Heat Load Zoning Configuration 3

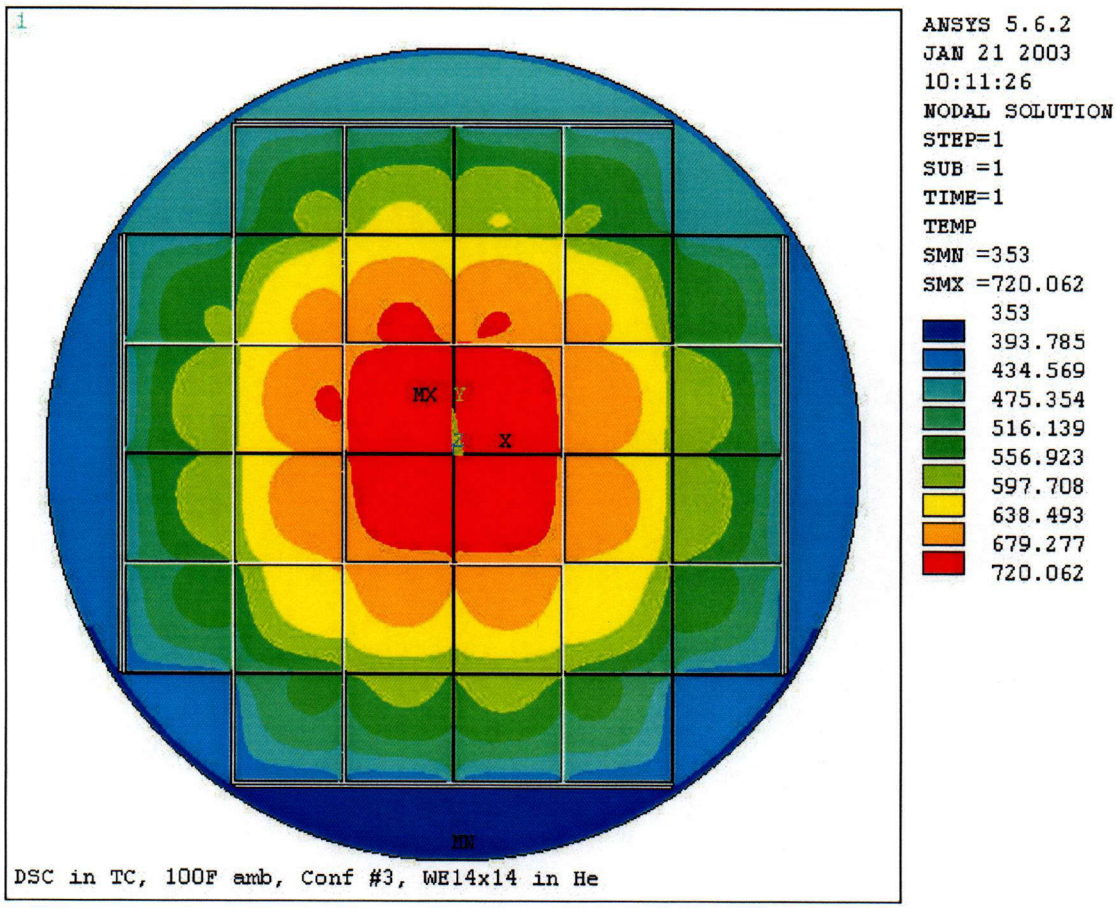

Figure M.4-10
Results for 100°F Transfer Case With Heat Load Zoning Configuration 3

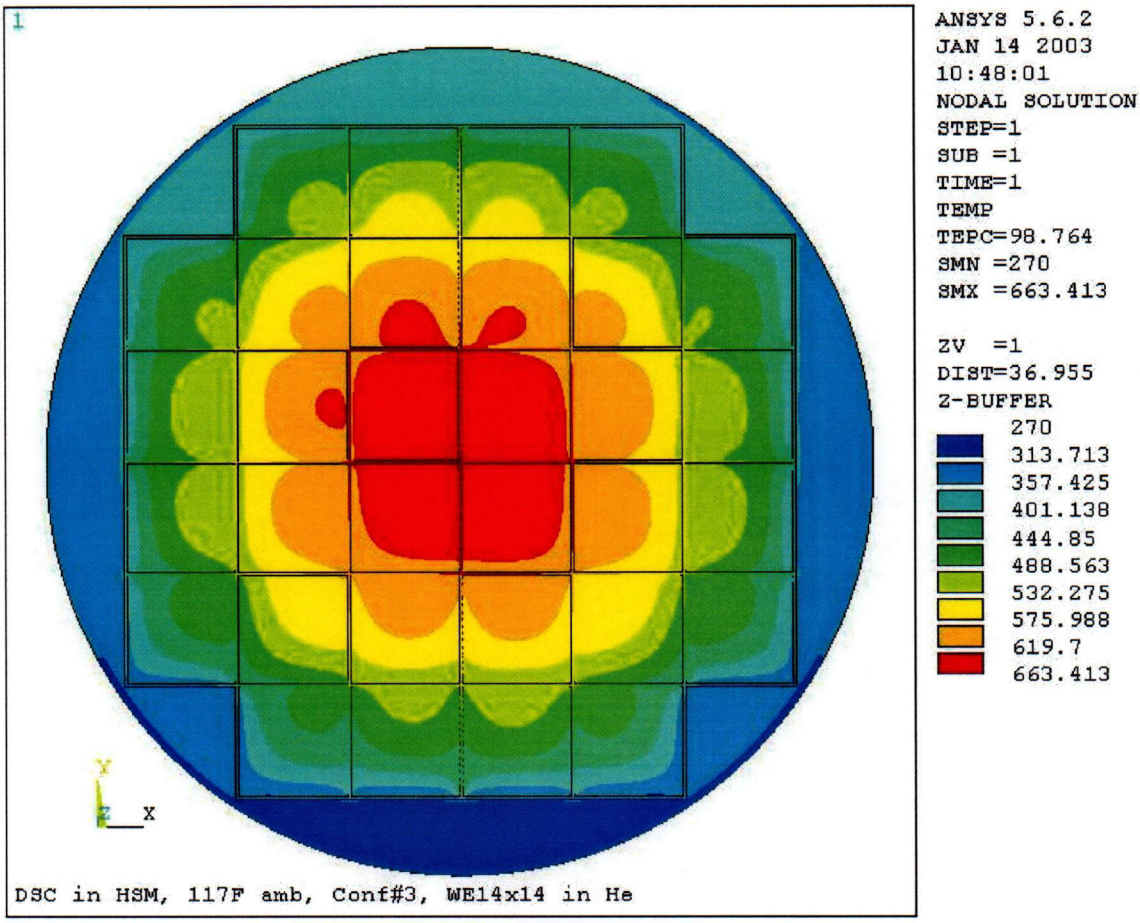

Figure M.4-11
Results for 117°F Storage Case With Heat Load Zoning Configuration 3

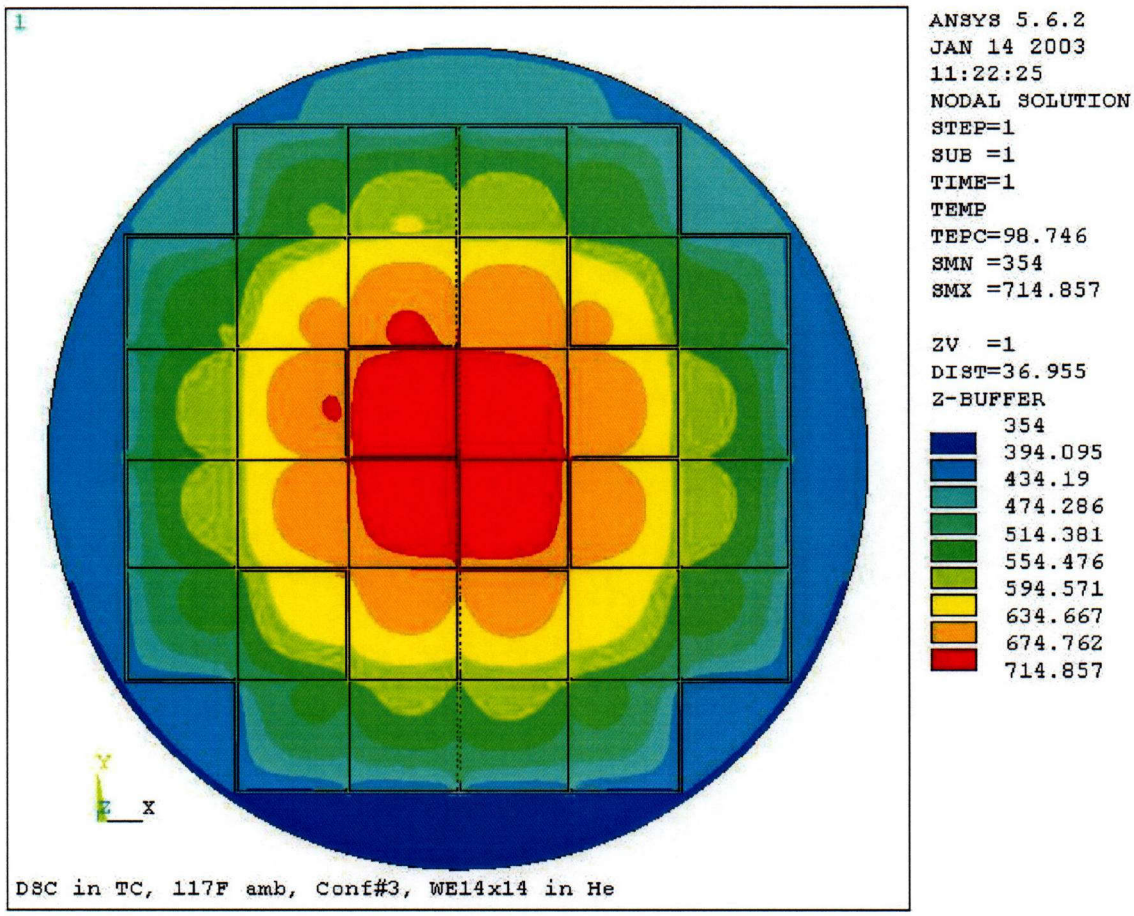

Figure M.4-12
Results for 117°F Transfer Case With Heat Load Zoning Configuration 3

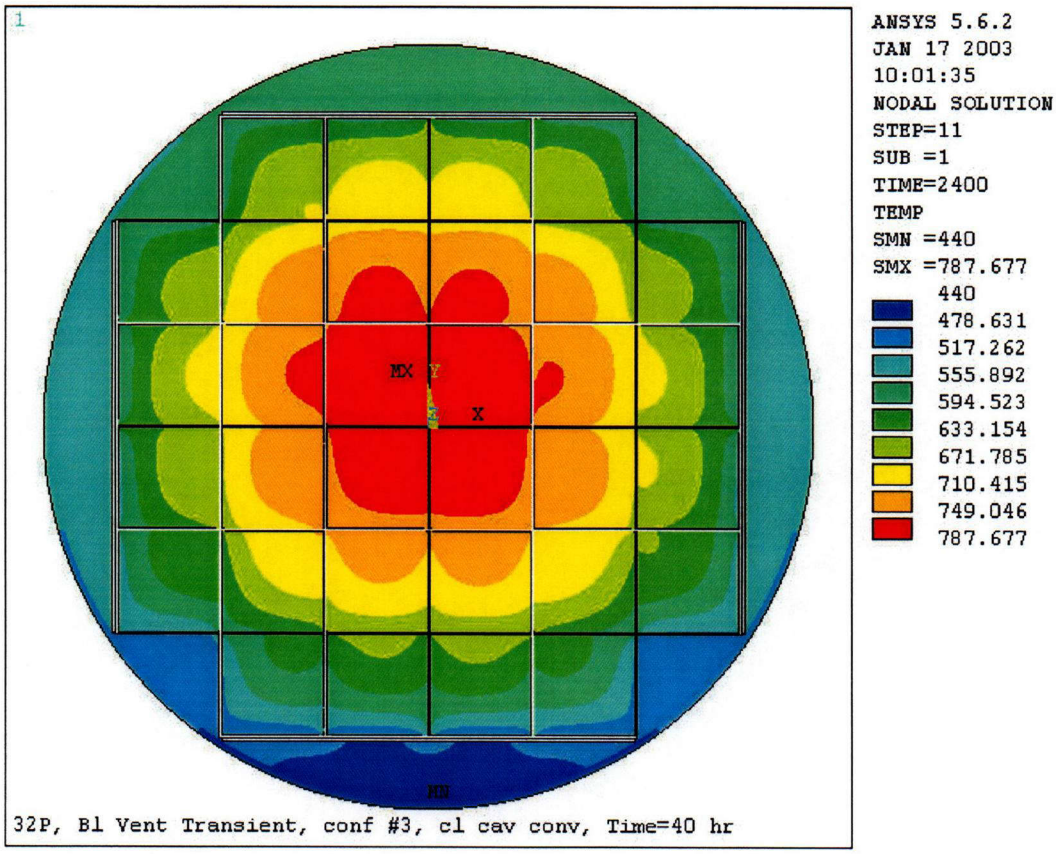

Figure M.4-13
Results for Blocked Vent Case With Heat Load Zoning Configuration 3 at 40 Hours

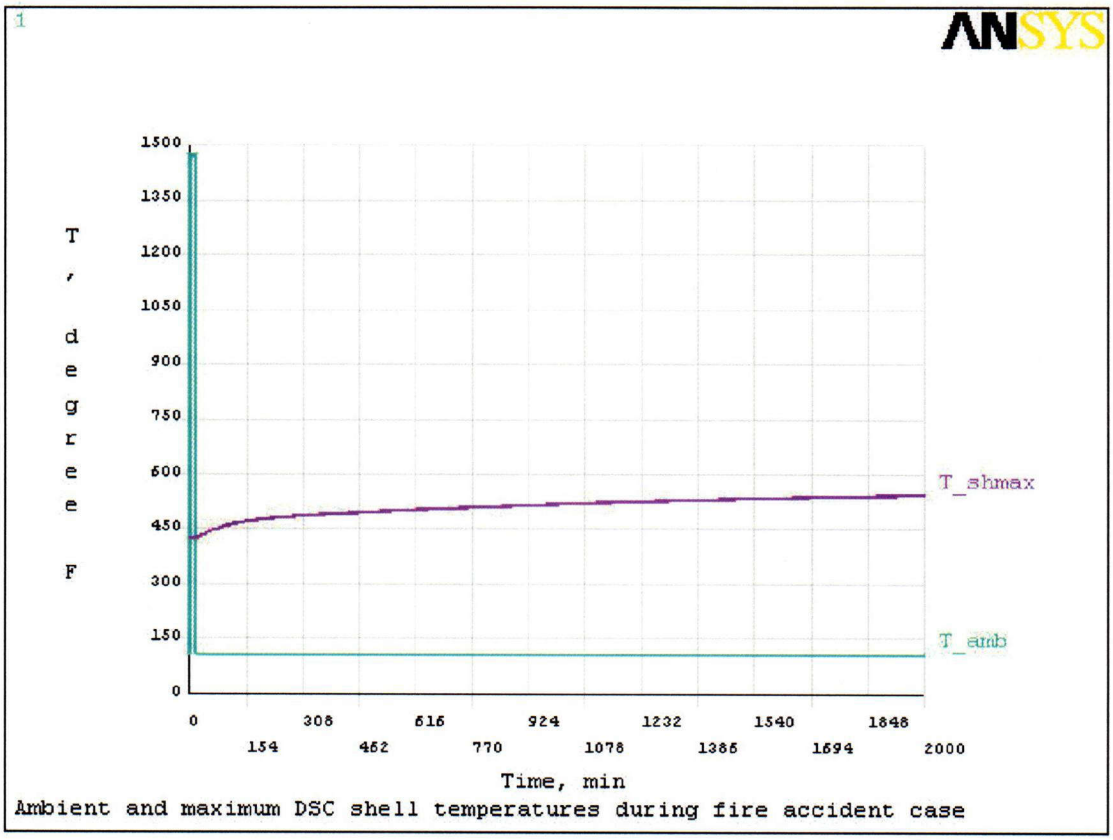

Figure M.4-14
NUHOMS®-32PT DSC and TC Temperature Response to 15 Minute Fire Accident Conditions

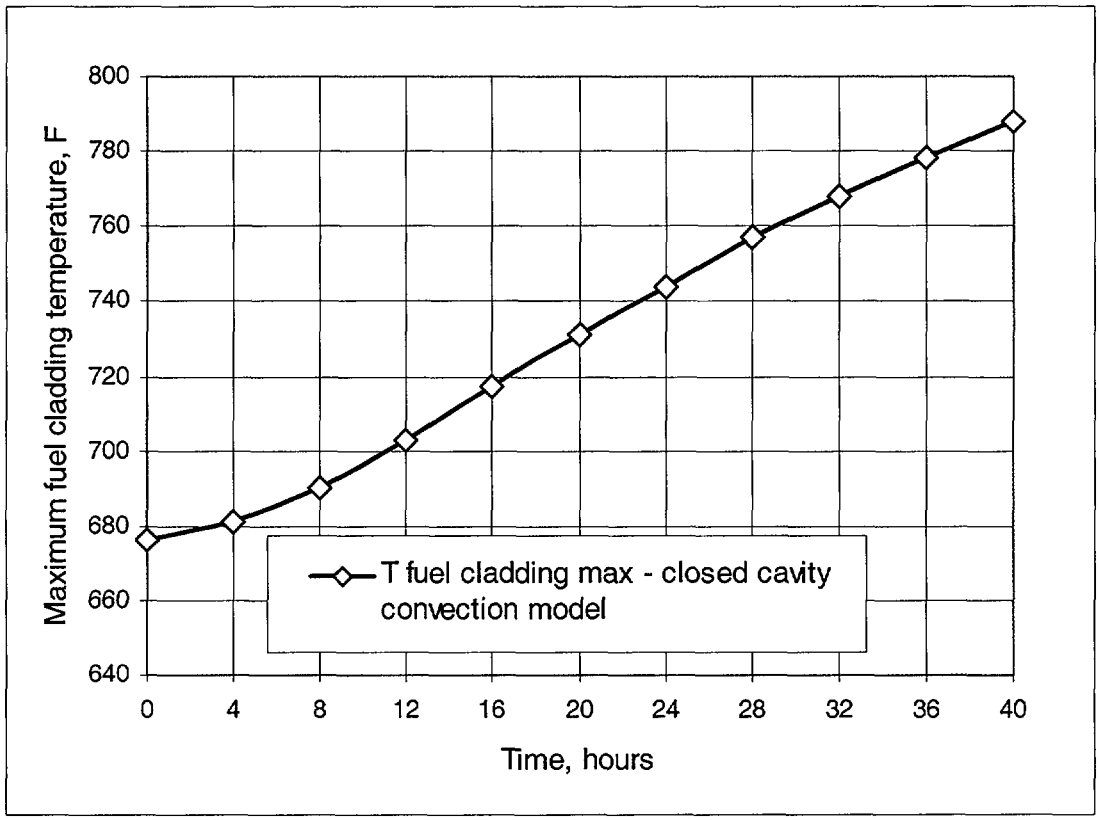

Figure M.4-15
Time-History Profile of the Maximum Fuel Cladding Temperature during Blocked Vent Case, Configuration #3

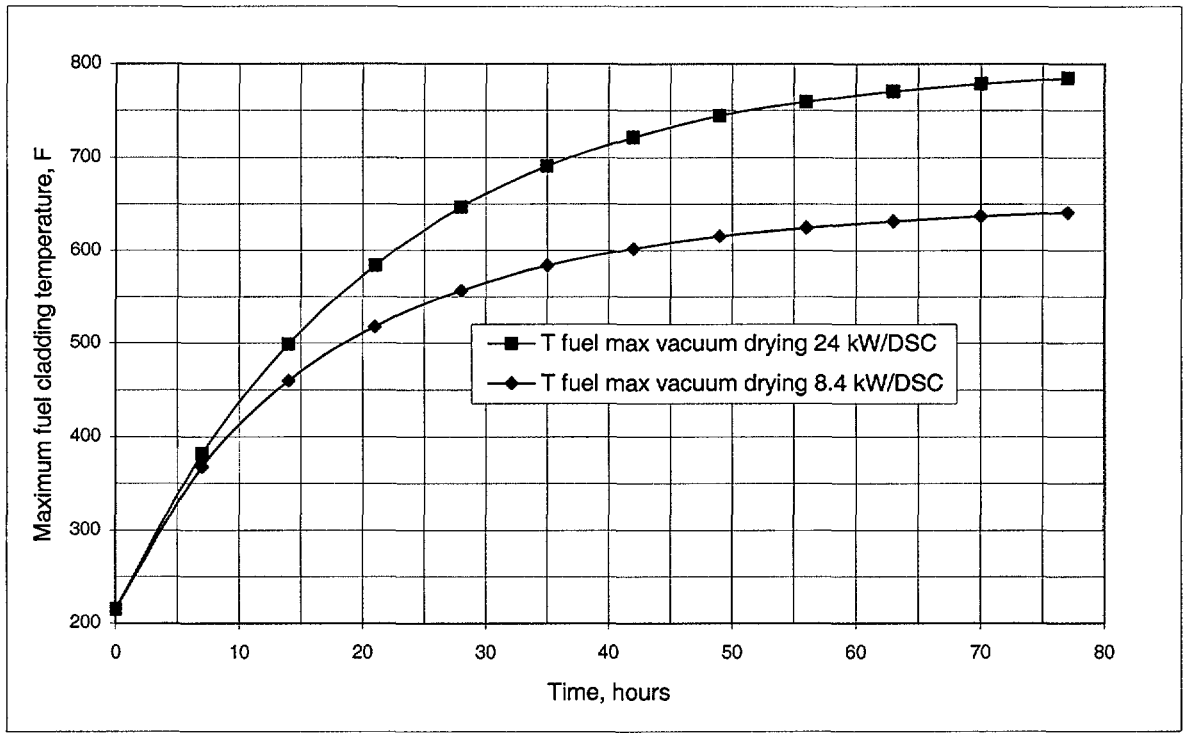

Figure M.4-16
Maximum Fuel Temperature during Vacuum Drying with Heat Load Zoning Configuration 3

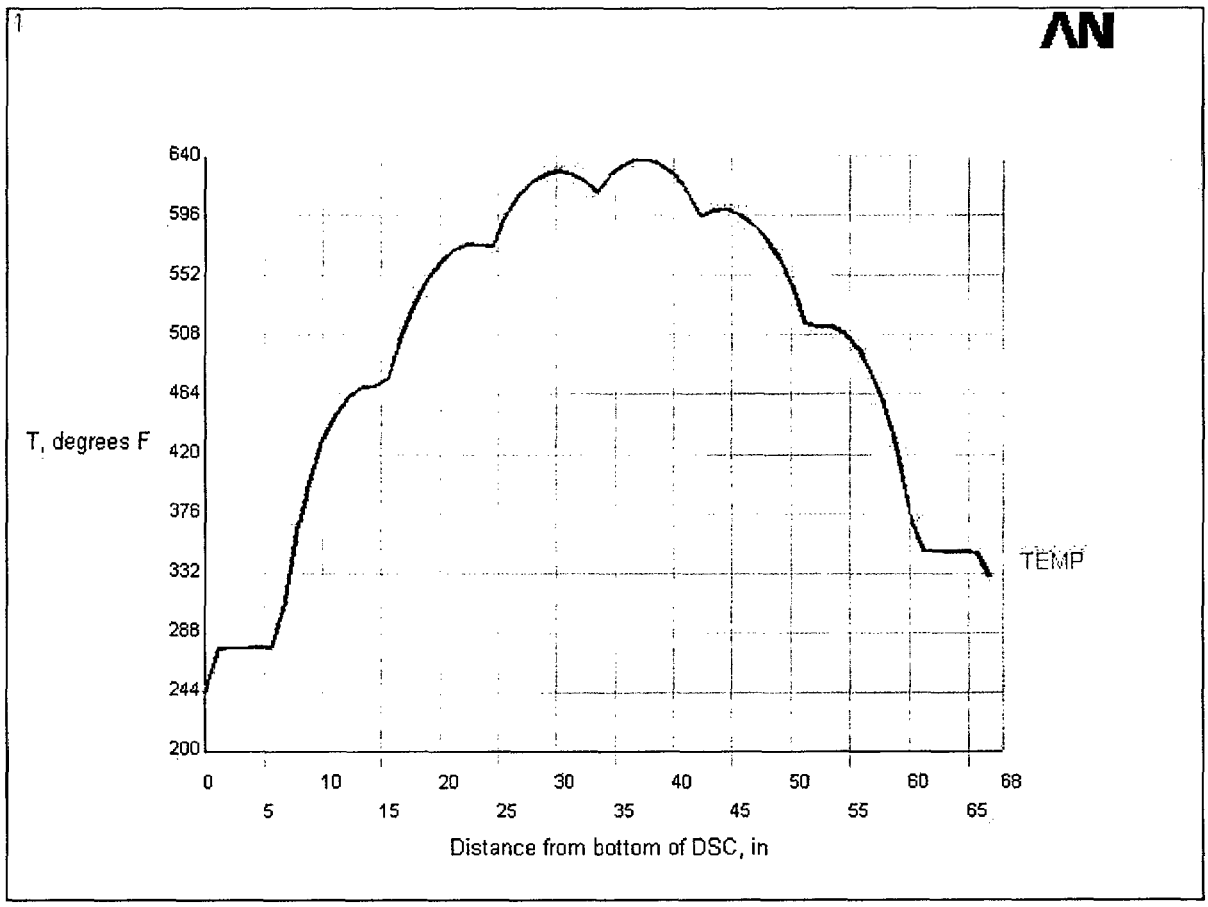

Figure M.4-17
Temperature Distribution from Bottom to Top of DSC at Cross-Section with Highest Temperatures, 70°F HSM Storage Case (Configuration 3)

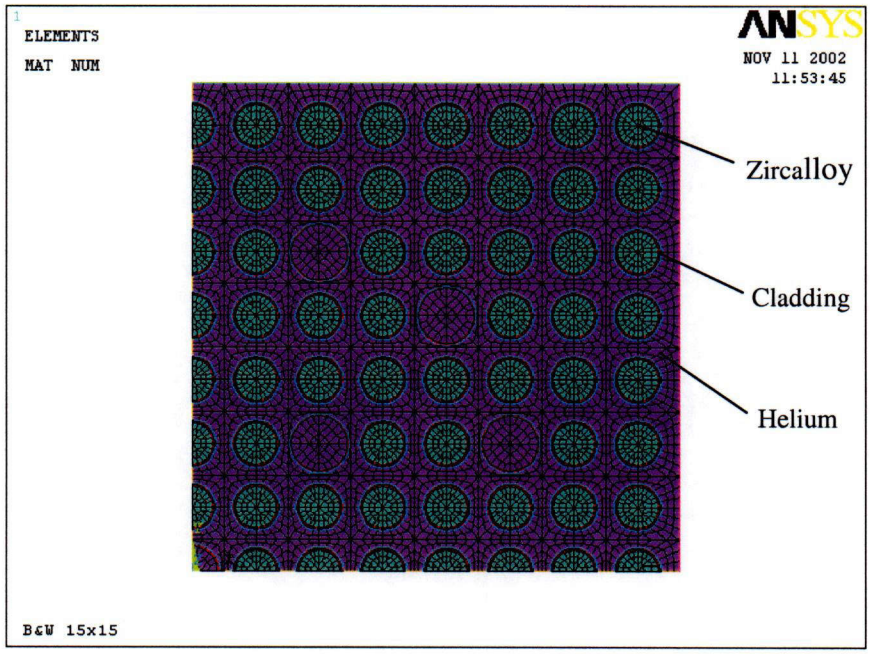

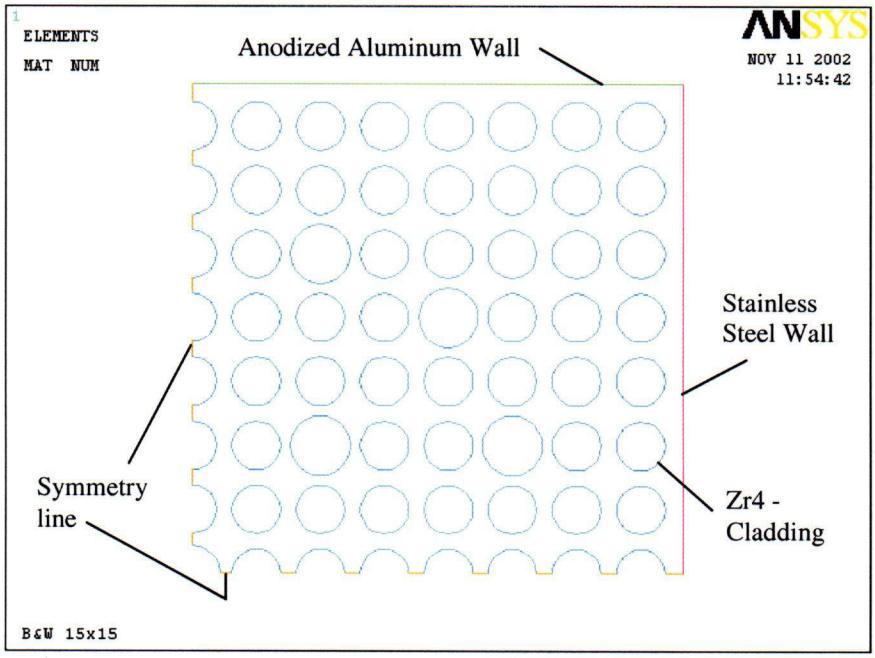

Figure M.4-18
Finite Element Model of B&W 15x15 Fuel Assembly

C15

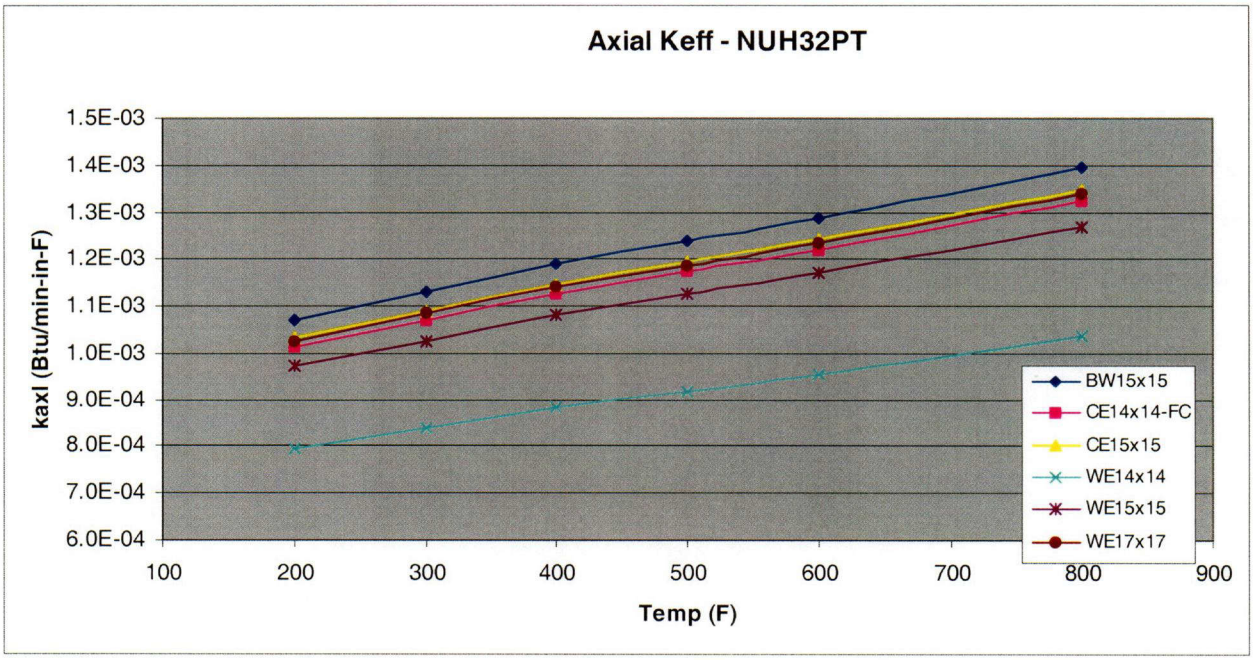

Figure M.4-19
Fuel Axial Effective Conductivity

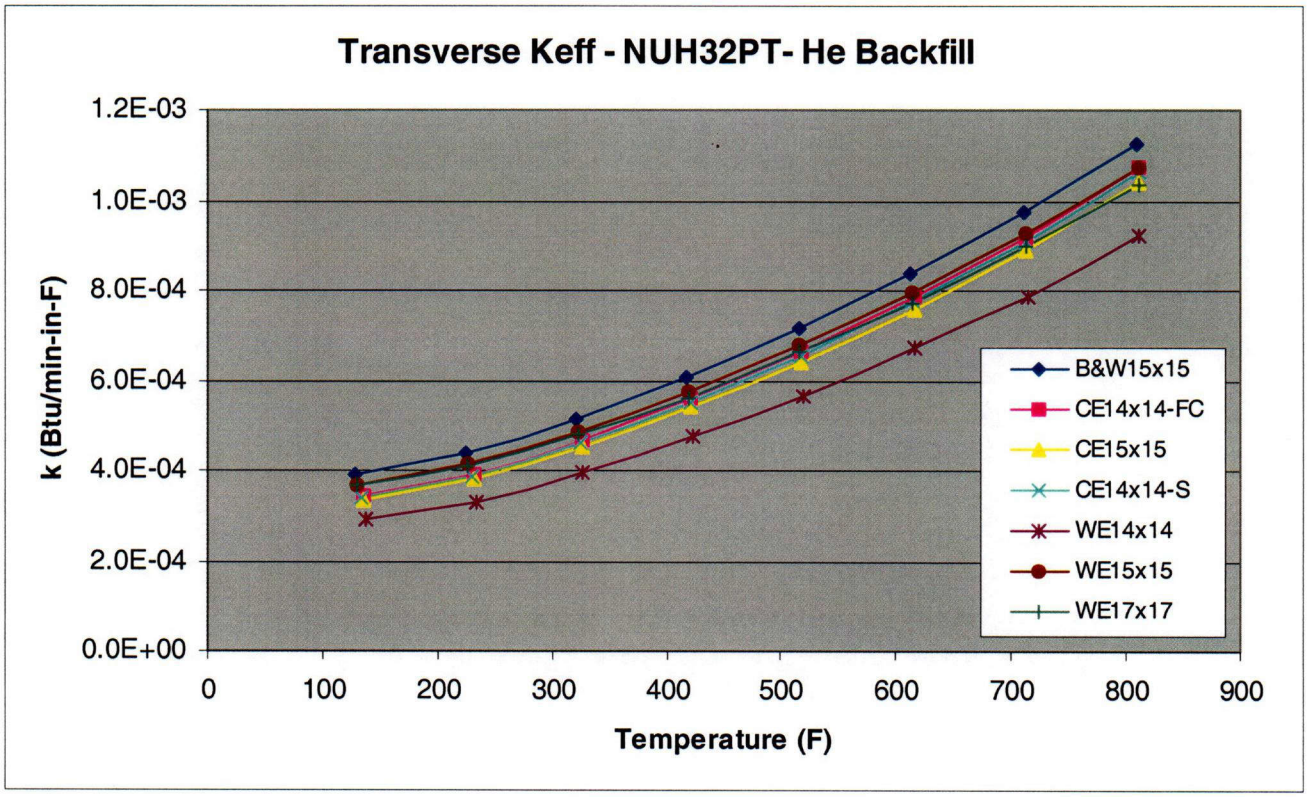

Figure M.4-20
Fuel Transverse Effective Conductivity in Helium

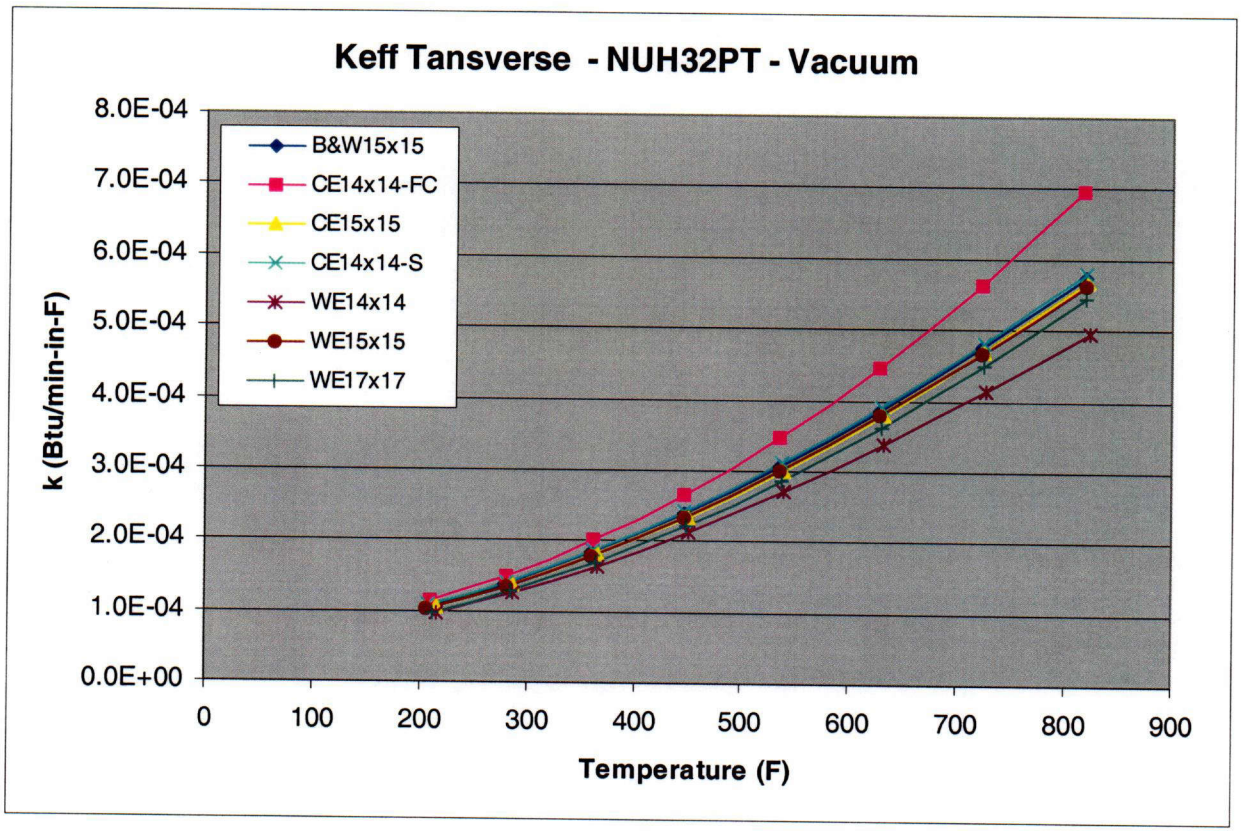

Figure M.4-21
Fuel Transverse Effective Conductivity in Vacuum